Universität Rostock

Traditio et Innovatio

Development and characterization of hydrogels and their use in in-vitro studies of drug-coated balloons

Dissertation

to obtain the academic degree

„Doktor der Naturwissenschaften“ (Dr. rer. nat.)

submitted at the

Mathematisch-Naturwissenschaftlichen Fakultät

an der Universität Rostock

submitted by

Dipl.-Chem. Jenny Bandomir

born on March 11th 1985 in Wismar

Rostock, 23.07.2014

urn:nbn:de:gbv:28-diss2015-0225-2

The present work was conducted during the period of time September 2010 till July 2014 under the supervisor of Professor Dr. Udo Kragl in the Institute for Chemistry at the University of Rostock.

Referees:

1st Referee: Prof. Dr. Udo Kragl

2nd Referee: Prof. Dr. Detlef Behrend

Thesis submission: July 23rd, 2014

PhD Defense: October 14th, 2014

Abstract

Development and characterization of hydrogels and their use in *in-vitro* studies of drug-coated balloons

Jenny Bandomir

This thesis summarizes the development and characterization of novel hydrogels based on polymerized ionic liquids. Next to the thermal properties of these materials, the mechanical characterization by tensile and compression tests was mainly performed using various parameters influencing the stability. In addition, a comparison with well-known hydrogels was made. These materials were used as artificial vessel model to carry out balloon dilations. By use of a flow-through cell, an artificial vessel wall could be generated. The drug release of drug-coated balloon catheters as the first and important phase was characterized in detail. The drug delivery as well as the transfer into the vessel wall was investigated for different hydrogels and compared to each other.

Diese Arbeit befasst sich mit der Entwicklung und Charakterisierung von neuartigen Hydrogelen auf Basis von polymerisierten ionischen Flüssigkeiten. Neben den thermischen Eigenschaften dieser Materialien wurde im Hauptteil dieser Arbeit die mechanische Charakterisierung durch Zug- und Druckversuche vorgenommen, wobei verschiedene Einflussparameter auf die Stabilität untersucht wurden. Außerdem erfolgte ein Vergleich mit bereits bekannten Hydrogelen. Die Materialien wurden als künstliches Gewebemodell eingesetzt, um Ballondilatationen vorzunehmen. Mit Hilfe einer Durchflusszelle konnte eine Gefäßwand künstlich erzeugt werden. Die Wirkstoffverteilung von beschichteten Ballonkathetern konnte in der ersten wichtigen Phase der Freisetzung charakterisiert werden. Die Wirkstoffabgabe sowie der Transport in die Gefäßwand wurden für verschiedene Hydrogele untersucht und miteinander verglichen.

Acknowledgement

Writing a PhD thesis takes many kinds of support. Therefore, I would like to express my gratitude to those who made it possible.

First, I want to thank Prof. Dr. Udo Kragl for making me part of this group and providing me this interesting research project. You gave me the opportunity to pursue my own ideas.

A huge thank you goes to the REMEDIS project employees Prof. Dr. Katrin Sternberg, Dr. Svea Petersen, Sebastian Kaule, Jana Unger and André Schulz. Thanks for your support and the great cooperation within the project. It was nice to work with you all.

Special thanks are directed towards Satomi Taguchi for introduction to work with ionic liquids. Together, we achieved a lot in your short research stay in Rostock.

For the warm and welcoming atmosphere I want to thank the entire working group of Prof. Kragl. In our coffee breaks we always had a funny atmosphere. I will miss it.

Without the analytical measurements these work would not have been possible. Hence, I want to thank Dr. Dirk Michalik, Brigitte Goronzi, Petra Duncker and Angela Weihs. Also, I want to thank Fabian Reiß for all Raman measurements.

My parents I also want to express my gratitude for their support and their faith in me.

Finally, all my friends I have to acknowledge for the time outside the “Chemistry building”. Especially Diana, Steffi, Janine and Christina I want to thank for the last difficult time in my life. Thank you for always being there for me.

“ Eine wissenschaftliche Entdeckung ist nie die Arbeit von nur einer Person.” – Louis Pasteur

Table of Contents

Index of Figures

Index of Tables

List of Abbreviation

AAILs	amino acid ionic liquids
ACN	acetonitrile
APS	ammonium persulfate
ASTM	a standard anatomic model
ATRP	atom transfer radical polymerization
Bis	bisacrylamide (*N,N′*-methylenebisacrylamide)
BTHC	butyryl-tri-hexyl citrate
Cetpyrsal	cetylpyridinium salicylate
CL	cross-linker
DAPT	dual antiplatelet therapy
DCB	drug-coated balloon catheters
DCM	dichloromethane
DEB	drug-eluting balloon catheters
DES	drug-eluting stents
DMSO	dimethyl sulfoxide
EGTA	ethylene glycol-bis (*β*-aminoethyl ether)-*N,N,N′,N′*-tetraacetic acid
et al.	et alii, et aliae or et alia
EtOAc	ethyl acetate
G	guluronic acid
GC	gas chromatography
GOx	glucose oxidase
HA	hyaluronic acid
HPLC	high pressure liquid chromatography
Im	imidazolium
ID	inner diameter
IL	ionic liquid
IPN	interpenetrating polymer network
LCST	lower critical solution temperature
M	mannuronic acid
M_W	molecular weight
n. a.	not available
n. d.	not determinable
OTW	over-the wire (PTX-coated balloon)
PAA	poly(acrylic acid)

PAAm	poly(acryl amide)
PEG	poly(ethylene glycol)
PEO	poly(ethylene oxide)
PHEMA	poly(hydroxyethyl methacrylate)
PILs	polymerized (polymeric) ionic liquids
PLA	poly(lactic acid)
PLGA	poly(lactic-co-glycolic acid)
PNIPAAm	poly(N-isopropyl acrylamide)
PTCA	percutaneous transluminal coronary angioplasty
PTX	paclitaxel
PVA	poly(vinyl alcohol)
PVP	poly(vinyl pyrollidone)
RAFT	reversible addition-fragmentation polymerization
RE	rapid exchange
TEMED	N,N,N´,N´-tetramethylenediamine
TFSI	bis(trifluoromethylsulfonyl)imide
THF	tetrahydrofuran
vs.	versus
WC	water content

1. Introduction

1.1 Definition and classification of hydrogels

Back to 1960, the pioneering work of Wichterle and Lim introduced hydrophilic hydrogels for biological uses [Wichterle *et al.* 1960]. During the past decades, hydrogels have gained tremendous interest, reflected in the increasing number of published reports on hydrogels up to now (about 42,200 in March 2014). Hydrogels are water-swollen, three-dimensional cross-linked polymeric networks containing (1) covalent bonds generated by the reaction of single or multiple monomers, (2) physical cross-links due to chain entanglements, (3) association bonds including hydrogen bonds or strong van der Waals interactions between chains, or (4) crystallites that bring together two or more macromolecular chains [Peppas *et al.* 2000; Van Vlierberghe *et al.* 2011]. The networks are insoluble due to the presence of chemical or physical cross-links. The hydrogel materials are usually discussed based on different classifications [Bindu *et al.* 2012; Kopecek *et al.* 2012; Ahmed 2013]:

(1) Classification based on source;
(2) Classification according to polymeric composition;
(3) Classification based on configuration;
(4) Classification based on type of cross-linking;
(5) Classification based on physical appearance;
(6) Classification according to network charge.

Hydrogels (**1**) can be categorized into two groups based on their natural or synthetic origins [Gibas *et al.* 2010; Singh *et al.* 2010; Vermonden *et al.* 2012]. The most widely researched natural polymers as hydrogels origin are proteins (*e.g.* collagen, gelatin, fibrin) and polysaccharides (*e.g.* chitosan, hyaluronic acid (HA), alginate, agarose, dextran) [Lee *et al.* 2001; Hoffman 2002; Peppas *et al.* 2006; Vermonden *et al.* 2012; Zhao *et al.* 2013; Kim *et al.* 2014a]. On the other hand, hydrogels with a well-defined structure and tailored characteristics such as enhanced mechanical properties can be designed by synthetic polymers. The most common synthetic polymers can be generated from derivatives of poly(vinyl alcohol) (PVA), poly(ethylene glycol) (PEG), poly(vinyl pyrollidone) (PVP), poly(ethylene oxide) (PEO), poly(hydroxyethyl methacrylate) (PHEMA), poly(acryl amide) (PAAm), poly(N-isopropyl

acrylamide) (PNIPAAm) and poly(lactic acid) (PLA) [Peppas *et al.* 2000; Hoffman 2002; Langer *et al.* 2003; Peppas *et al.* 2006; Kopecek *et al.* 2007; Gulrez *et al.* 2011].

The formation of hydrogels (**2**) can be classified by polymer composition [Ahmed 2013]:

(a) Homo-polymeric hydrogels consist of a single type of monomer, which is a basic structural unit of the polymer network. Homopolymer networks exhibit a cross-linked skeletal structure depending on the monomer natures as well as polymerization techniques [Das 2013].
(b) Co-polymeric hydrogels consist of two or more different monomers with at least one hydrophilic component [Das 2013]. The arrangement in the hydrogel can be in a random, block or alternating configuration along the chain of the polymer network.
(c) Interpenetrating polymer networks (IPN) are generated of two independent cross-linked synthetic and/or natural polymer components, contained in a network form [Kopecek *et al.* 2007; Matricardi *et al.* 2013; Naficy *et al.* 2013]. Semi-interpenetrating networks (semi-IPN) are produced by synthesizing a hydrophilic polymer matrix around an entrapped water soluble polymer. An alternative route is to prepare the network by selectively cross-linking of one polymer in a polymer blend [Chan *et al.* 2012; Dinu *et al.* 2013].

Another classification of hydrogels (**3**) is based on the configuration. Here, the physical structure and the chemical composition are important, (a) amorphous (non-crystalline), (b) semi-crystalline and (c) crystalline hydrogels.

The type of cross-linking in hydrogels can be classified (**4**) into two categories: chemical or physical nature of the cross-link junctions [Hoffman 2002; Ottenbrite *et al.* 2010; Gulrez *et al.* 2011; Zhao *et al.* 2013]. Comparing to hydrogels cross-linked by chemical bonds, physical hydrogels hold together by non-covalent junctions, such as van der Waals, coulombic, dipole-dipole, hydrophobic and hydrogen bonding interactions [Kopecek *et al.* 2007; Hennink *et al.* 2012; Seiffert *et al.* 2012].

Hydrogels (**5**) appearance as film, matrix or microsphere regulated by the technique of the polymerization participated in the preparation process. The last hydrogel classification (**6**) is according to the network electrical charge. Hydrogels may be classified into four groups based on how electrical charges are present on the cross-linked chains:

(a) neutral (nonionic)
(b) ionic (anionic or cationic)
(c) ampholytic (containing both acidic and basic groups)
(d) zwitterionic (containing both anionic and cationic groups in each repeating unit).

1.2 Swelling behavior of hydrogels

Hydrogels can be characterized by their degree of swelling [Ottenbrite *et al.* 2010]. The swelling behavior of hydrogels is an important factor deciding their applications especially in pharmaceutical, biomedical, ophthalmology and tissue engineering [Ottenbrite *et al.* 2010; Patel *et al.* 2011]. Usually, the driving force for the absorption or swelling process is from a balancing of three forces of electrostatic, osmotic and entropy-favored dissolution of polymer in water [Omidian *et al.* 2008].

The final water content of hydrogels depends on kinetic as well as thermodynamic parameters [Peppas 2004; Omidian *et al.* 2008; Ganji *et al.* 2010; Patel *et al.* 2011]. The water accommodated by a hydrogel is classified into four types as shown Figure 1-1 [Ottenbrite *et al.* 2010].

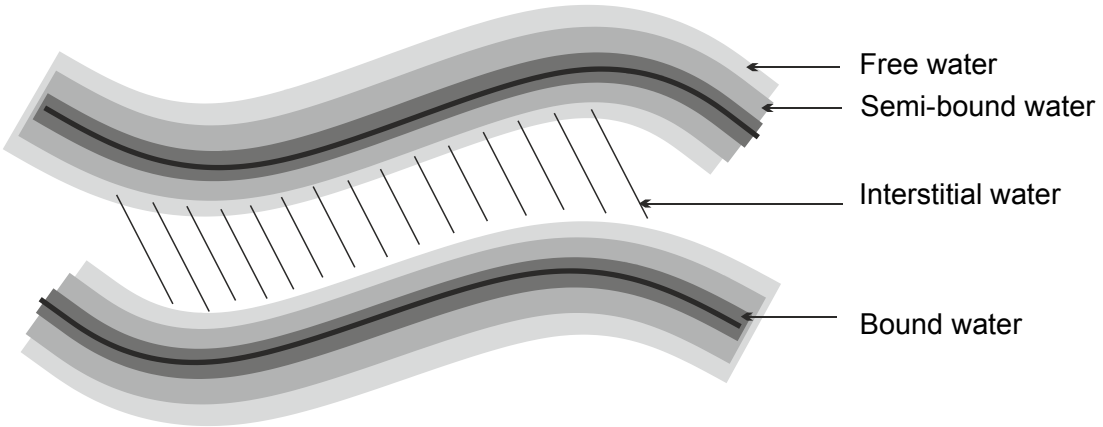

Figure 1-1 Different types of water in hydrogels (adapted from [Ottenbrite *et al.* 2010])

Free water is in the outermost layer of the hydrogel and can be easily removed from the network. The interstitial water is not attached to the hydrogels network, but between the hydrated polymers chains physically trapped. However, the bound water is directly attached to the polymer chain through hydration of functional groups or ions. The bound water can only be separated at very high temperatures due to the fact that this water remains as an integral part of the hydrogels structure. There exist a type of water with intermediate properties of a bound water and free water which is called semi-bound water [Ottenbrite *et al.* 2010]. All types of water in a hydrogel can be analyzed and characterized with differential scanning calorimeter measurements.

The water absorption of hydrogels depends on many factors such as cross-link density (the most important factor), nature of the solution, hydrogels structure (porous or poreless), network parameters and drying techniques. It should be noted that the magnitude of the cross-link density determines the swelling properties of a given hydrogel. The swelling behavior can be seen as a diffusion process followed by a relaxation process depending on the cross-link density as shown in Figure 1-2 [Ottenbrite *et al.* 2010]. Highly cross-linked hydrogel networks show faster swelling compared to their slightly cross-linked counterparts because of the structure of the hydrogel like a metal mesh [Omidian *et al.* 2008].

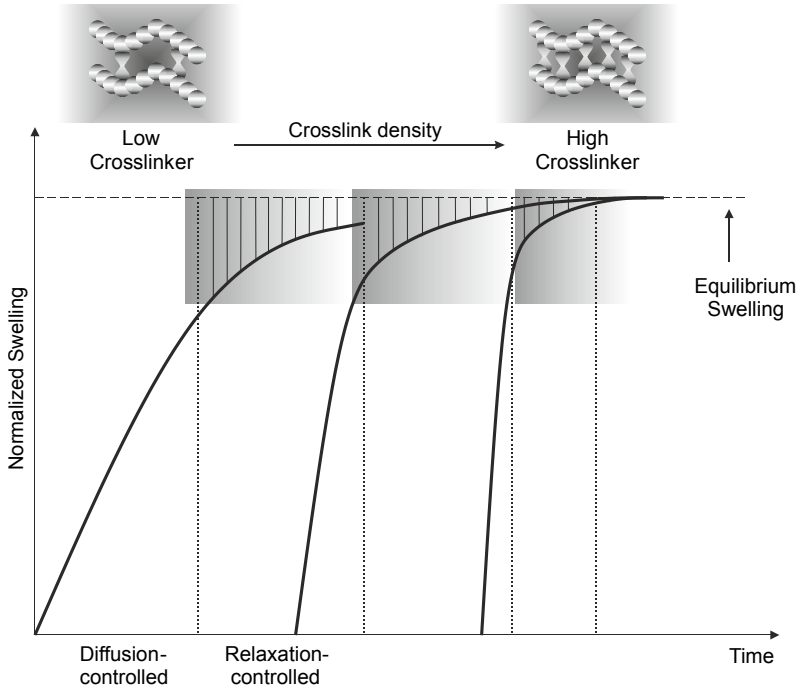

Figure 1-2 Swelling kinetics of hydrogels depending on the cross-link density (adapted from [Ottenbrite *et al.* 2010])

Water diffusion into the network structure is rate-determining at the beginning of the swelling from the hydrogel. This depends on the molecular weight and temperature of the solvent, as well as the extent of porosity within the hydrogel structure. The second hydrogel swelling step is relaxation-controlled - how fast the polymer chains can relax, which is a slower process. However, the absorption mechanism in highly cross-linked hydrogels potentially changes toward a single diffusion process. Highly cross-linked hydrogels acts like a metal mesh, which permits a constant amount of water to pass through continuously [Ottenbrite *et al.* 2010].

Omidian and Park reported that the swelling process of a hydrogel was controlled by three major elements: the cross-linker content, the ionic content and the hydrophilic content [Omidian *et al.* 2008]. The cross-linker content is already mentioned and discussed. Now the other two elements will be introduced in the following paragraphs.

Ionic content of the system and the surrounding: Swellable hydrogel networks can be classified into two groups: ionic and non-ionic. At a certain amount of elastic forces, swelling of the ionic hydrogels will be a more entropy-favored process compared to their non-ionic counterparts. As the number of ions within the hydrogel network increases, more and more osmotic and electrostatic forces will be induced. Changing the nature of the environment (water) can control the entropy-driven swelling process of the hydrogel. The addition of ions to the environment limits the swelling capacity of an ionic hydrogel [Omidian *et al.* 2008].

Hydrophilic content: The hydrophilic content of the hydrogel will influence the intermolecular forces responsible for the diffusion as well as the swelling of the network. As hydrophilicity of the hydrogel increases, the interaction between water and hydrogel will increase too, and thus the water diffusion is facilitated whereby a greater swelling of the hydrogel results [Omidian *et al.* 2008].

A comparison of general features of different hydrogel structures is shown in Table 1-1.

Table 1-1 Comparison between different types of hydrogel network (adapted from [Omidian *et al.* 2008])

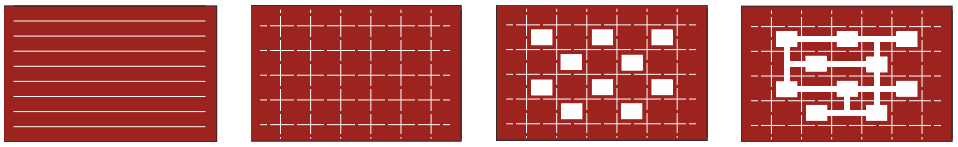

Hydrogel type	Non-cross-linked	Poreless cross-linked	Porous cross-linked	Superporous cross-linked
Porosity	Poreless	Nanoporous	Macroporous	Interconnected macroporous
Intermolecular forces	High	Low	Lower	Lowest
Chain packing	Tight	Loose	Looser	Loosest
Water diffusion	Slow	Fast	Very fast	Ultra-fast
Timed swelling capacity	Low	High	High	High
Resistance to water permeation	High	Low	Low	Very low
Swelling rate	Slow	Fast	Very fast	Ultra-fast

In contrast to the swelling behavior, desorption in hydrogels depends on more factors. The desorption process is diffusion-controlled and takes place at a slow or fast rate. The wetter the surrounding environment is, the slower the desorption process. De-swelling in hydrogels is related to the mechanical properties of hydrogels [Ottenbrite *et al.* 2010]. For the evaluation of the de-swelling of the hydrogel, the weight reduction can be measured over time. Depending on the environment (temperature and pressure) and the porosity of the hydrogel, the de-swelling behavior may range from a linear to an exponential trend.

1.3 Selected hydrogels and their applications

In this following section, the commonly used hydrogels will be discussed. Calcium alginate as the hydrogel of choice regarding to their tissue-like behavior within *in-vitro* studies will be presented [Neubert *et al.* 2008]. Otherwise, polyacrylamide (PAAm) as covalently cross-linked networks, and polymerized ionic liquids (PILs) as novel hydrogel materials, will be introduced. The application of hydrogels as vessel model in *in-vitro* studies of DCBs is connected with unique properties of the material like long-term stability, flexibility and permeability. In dependency of the properties of the hydrogels they can be used for different applications which are described in this chapter.

1.3.1 Calcium alginate

Alginate is used for many biomedical applications [Van Vlierberghe *et al.* 2011] due to its low toxicity, biocompatibility, mild gelation by addition of divalent cations such as Ca^{2+} and low costs [Gombotz *et al.* 1998; Kuo *et al.* 2001; Lee *et al.* 2012]. Alginic acid as a natural anionic polymer is a polysaccharide consisting of blocks of mannuronic (M) and guluronic acids (G) in various arrangements along the polymer chain [Becker *et al.* 2001; Kuo *et al.* 2001]. Commercial alginates are extracted from brown algae including *Laminaria hyperborea*, *Macrocystis pyrifera* and *Ascophyllum nodosum* [Gombotz *et al.* 1998]. In all of these algae, alginate is the main polysaccharide and presents up to 40% of the dry matter. The alginate extraction procedure from algae is shown in Figure 1-3.

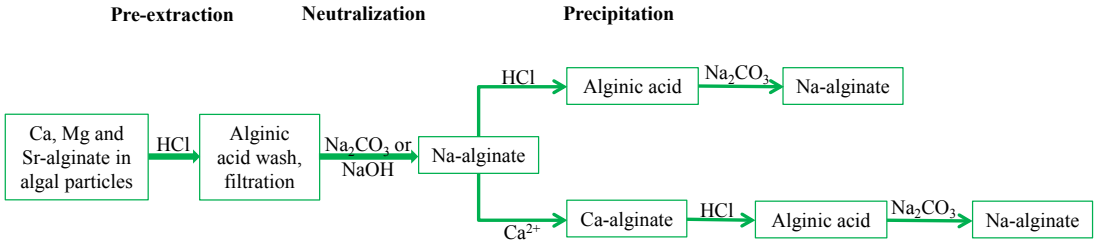

Figure 1-3 Alginate extraction procedure from algae (adapted from [Pawar *et al.* 2012])

Sodium alginate chelates with divalent cations such as Ca^{2+} to form hydrogels. The gelation is driven by the interactions between G-block monomers which associate to form tightly held junctions in the presence of Ca^{2+} cations [Rees *et al.* 1977; Pawar *et al.* 2012]. Resulting gel structures can be described by the so-called egg-box model (Figure 1-4) [Rees *et al.* 1977; Draget *et al.* 2005]. In this context, alginates are attracted to follow different divalent cations with decreasing affinity: Pb > Cu > Cd > Ba > Sr > Ca > Co, Ni, Zn >Mn [Morch *et al.* 2006]. Additional to G-blocks, MG blocks also participate, while forming weak junctions [Donati *et al.* 2005].

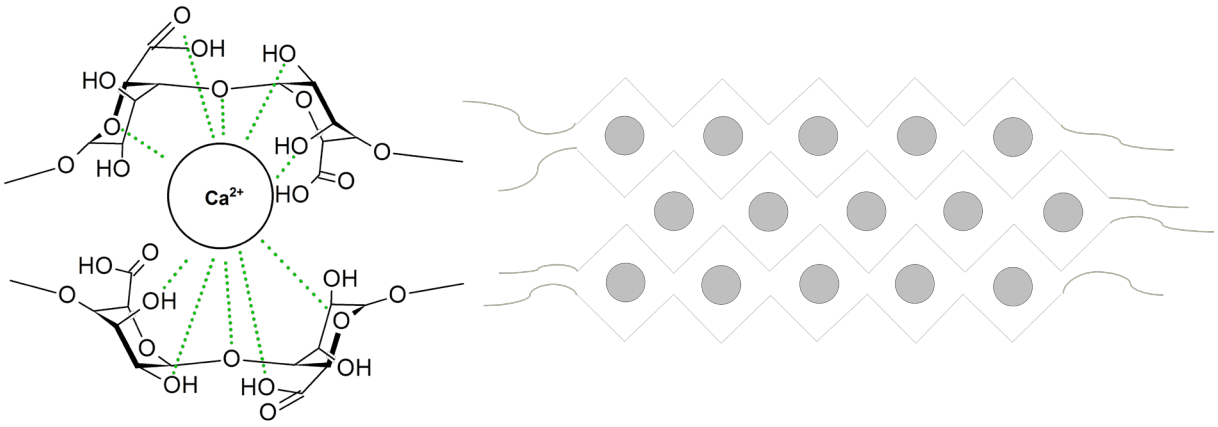

Figure 1-4 *left*: GG/GG junctions; *right*: resulting egg-box model of calcium alginate hydrogels (adapted from [Draget *et al.* 2005])

There are two methods to perform calcium cross-linked alginate networks. The diffusion method is the first one, wherein cross-linking ions diffuse into the alginate solution from an outside reservoir. Calcium chloride ($CaCl_2$) is one of the most used agents for the first method. However, the gelation process is too rapid, and can be poorly controlled due to the high solubility of $CaCl_2$ in aqueous solutions [Skjåk-Bræk *et al.* 1989; Draget *et al.* 2005; Lee *et al.* 2012]. The internal setting is the second method, where the ion source is situated within the alginate solution and a controlled trigger (solubility of the ion source or pH) sets off the release of cross-linking ions into the solution. Calcium sulfate ($CaSO_4$) can slow down the gelation rate attributed to their low solubility in water.

Ionic alginate hydrogels are known to have limited long-term stability *in-vivo* and *in-vitro*. In physiological media, stabilizing divalent cations are exchanged by monovalent cations such as Na^+ followed by an uncontrolled rupture and dissolution of the hydrogel matrix [Thu *et al.* 1996]. Degradation of calcium alginate hydrogels can also occur if the calcium ions are removed by using a chelating agent such as ethylene glycol-bis (*β*-aminoethyl ether)-*N,N,N′,N′*-tetraacetic acid (EGTA), lactate, citrate or phosphate [Gombotz *et al.* 1998]. Chemical cross-linking is an alternative to overcome this drawback. Some research groups reported covalently cross-linked alginate hydrogels [Grasselli *et al.* 1993; Lee *et al.* 2004; Jeon *et al.* 2009; Krebs *et al.* 2009; Jeon *et al.* 2010; Zhao *et al.* 2010; Andersen *et al.* 2012]. Alginate gels are extremely interesting to be applied in the biomedical field. An overview of the biomedical applications of alginates is given in Table 1-2 [Van Vlierberghe *et al.* 2011].

Alginate has been proven as biocompatible, biodegradable, non-toxic, mucoadhesive and non-immunogenic substance [Becker *et al.* 2001; Sushmitha *et al.* 2010; Mazur *et al.* 2014]. Alginate can form strong complexes with polycations including chitosan and synthetic polymers. These formed complexes do not dissolve in the presence of Ca^{2+} chelators [Gombotz *et al.* 1998].

Table 1-2 Overview of biomedical applications of alginate (adapted from [Van Vlierberghe *et al.* 2011])

Type of polymer	Application
alginate, alginate-*cis*-aconityl-daunomycin, calcium alginate/silk fibroin, hyaluronic acid/alginate, PLGA/calcium alginate	drug delivery
alginate/elastin/PEG, angiogenic factors/alginate	blood vessel
alginate microbeads, alginate/gelatin/hydroxyapatite, oxidized alginate/gelatin/tricalcium phosphate, chitosan/alginate, alginate/poly(lactic-*co*-glycolic acid)/calcium phosphate, collagen/alginate/nanohydroxyapatite	bone
sodium alginate, chitosan/alginate, gelatin/alginate	bone marrow
alginate/fibrin, agarose/alginate/gelatin, chitsosan/alginate/hyaluronate, PLGA/alginate, transforming growth factor-β(1) loaded alginate	cartilage
injectable alginate, gelatin/alginate	heart
alginate/chitosan	ligament
macroporous alginate, alginate/galactosylated chitosan, sodium alginate	liver
chitosan/calcium polyphosphate	meniscus
gelatin/alginate	skin
alginate	spinal cord
alginate/chitosan	tendon

Degradation can also be caused by enzymes, *e.g.* alginate lyase (EC 4.2.2.X) which degrade alginate to produce oligosaccharides [Wong *et al.* 2000; Zhang *et al.* 2006; Li *et al.* 2011c]. Mechanical properties as well as the degradation of alginate can be regulated depending on the cross-linkers. Several covalent cross-linking methods have been used in regard of enhancing mechanical and degradation characteristics [Lee *et al.* 2000]. Moreover, other kinds of modification are reported to prepare alginate derivates with different characteristics, *e.g.* acetylation, phosphorylation, sulfation or hydrophobic modification [Pawar *et al.* 2012; Wu *et al.* 2013].

Alginates, as a kind of natural polymer, exhibits promising characteristics, but they show rather disadvantageous results in long-term stability. Due to this fact, other polymer networks

have been investigated and researched. In the following section, polyacrylamide, as synthetic material, will be introduced.

1.3.2 Polyacrylamide (PAAm)

Polyacrylamide (PAAm) is one of the best characterized hydrogels [Darnell *et al.* 2013; Oyen 2014]. The monomer acrylamide is polymerized in aqueous solution in the presence of small amounts of the cross-linker, *N,N′*-methylenebisacrylamide (Bis or bisacrylamide), resulting in a polymer network (Figure 1-5). This polymerization reaction occurs via a free-radical mechanism. Ammonium persulfate (APS) is utilized as an initiator and TEMED (N,N,N′,N′-tetramethylenediamine) is used to catalyze the polymerization [Feng *et al.* 1988; Walker 1996]. The acrylamide monomer is toxic [Exon 2006].

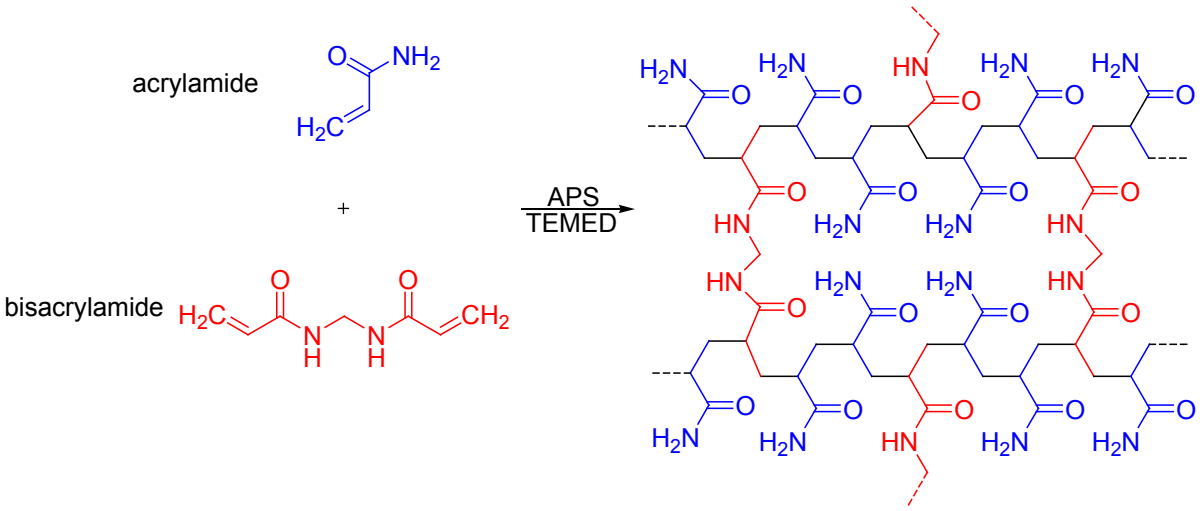

Figure 1-5 Polymerization reaction of acrylamide and bisacrylamide to form a hydrogel

The advantage of synthetic polymers is the variation of monomer to cross-linker ratio whereby different hydrogel characteristics can be realized, *e.g.* water content, mechanical and thermal properties, swelling behavior and permeability [Tse *et al.* 2010; Li *et al.* 2011a; Liu *et al.* 2013; Naficy *et al.* 2013]. Properties of hydrogels can also be tuned by the synthesis temperature [Dinu *et al.* 2007; Dinu *et al.* 2013].

There are two key parameters used to determine the nature of the PAAm hydrogel: (1) T is the total polymer concentration (in %) that included both, the monomer and the cross-linker; (2) C is the cross-linker concentration (in %). Usually, the polymer concentration %T is only calculated based on the monomer, because the cross-linker is typically present in a much smaller amount. The cross-linker concentration %C is calculated from the ratio of

bisacrylamide to monomer. There exists a complex relationship between pore size and both, T and C [Oyen 2014]. When %T is fixed, the pore size decreases with increasing %C until a critical point. Then, a larger %C causes a more open or macroporous structure due to polymer chains agglomerating [Lira *et al.* 2009; Oyen 2014]. In this case, the cross-link density is too high. In the other case, when %C is fixed, the pore size decreases with increasing %T [Lira *et al.* 2009; Oyen 2014]. Therefore, the mechanical behavior of PAAm hydrogels depends on polymer as well as cross-linker content. Cross-linking is used to enhance the mechanical properties of materials. Generally, an increase of the cross-link density results in stiffer hydrogel materials, consequently lower extensibility [Kong *et al.* 2003; Hao *et al.* 2013]. PAAm hydrogels can be tailored to range the elastic moduli from 0.2 MPa to over 1 MPa, which corresponds with applications in cartilage treatment [Kleemann *et al.* 2005; Kiviranta *et al.* 2008; Li *et al.* 2011a].

Besides the good mechanical performance PAAm hydrogels are characterized by high water content, transparency, long-term stability as well as homogeneity. Furthermore, PAAm hydrogels demonstrated non-toxicity and biocompatibility [Gin *et al.* 1990]. The high cohesive and adhesive properties favor PAAm hydrogels as a competent material in tissue engineering [Bajpai *et al.* 1991; Li *et al.* 2011d; Bait *et al.* 2013]. PAAm hydrogels also offer broad applications in different technological areas, *e.g.* as materials for contact lenses and protein separation, matrices for cell-encapsulation, and devices for controlled release of proteins and drugs [Hennink *et al.* 2012; Darnell *et al.* 2013; Dinu *et al.* 2013; Malana *et al.* 2014]. The PAAm hydrogels are widely used in ophthalmic operations, food packaging as well as water purification. These hydrogels have also been used in plastic and aesthetic surgery for more than 20 years [Christensen *et al.* 2003].

It is possible to synthesize alginate/polyacrylamide hydrogels. Yang *et al*. reported that these hydrogels exhibit exceptional mechanical properties. They synthesized strengthened alginate/polyacrylamide hydrogels using various multivalent cations [Yang *et al.* 2013]. Sun *et al*. also reported extremely stretchable and tough hydrogels by mixing alginate and polyacrylamide hydrogels [Sun *et al.* 2012a]. The working group of Mooney investigated the biocompatibility and maintenance of mechanical properties of alginate/polyacrylamide hydrogels in cell culture and *in-vivo* conditions [Darnell *et al.* 2013]. The obtained results suggest the valuable further exploration of extremely tough alginate/polyacrylamide IPN hydrogels as biomaterials [Darnell *et al.* 2013].

1.4 Polymerized (polymeric) ionic liquids (PILs)

1.4.1 Definition and types of polymerizable IL monomers

100 years ago, the first ionic liquid ethylammonium nitrate with a melting point of 13-14 °C was described by Paul Walden [Walden 1914]. Polymerized ionic liquids (PILs), also called poly(ionic liquids)s, refer to a subclass of polyelectrolytes and were pioneered by Ohno and co-workers in 1998 [Ohno et al. 1998; Mecerreyes 2011]. PILs are described as "*polymers which contain at least one ionic center, similar by composition to the structure of commonly used ILs as a covalently bonded part of their constitutional repeating (monomer) unit*" [Torriero *et al.* 2011]. The initial research of PILs can be dated back to 1970´s when the free radical polymerization of cationic vinyl monomers was investigated [Hoover 1970; Yuan *et al.* 2011a].

Reviews of first-generation PILs have been reported by various research groups in this field [Green *et al.* 2009a; Green *et al.* 2009b; Lu *et al.* 2009; Mecerreyes 2011; Yuan *et al.* 2011a; Yuan *et al.* 2013]. These reviews presented synthesis and chemistry of PILs, including physico-chemical properties and applications. PILs have gained tremendous interest in the fields of polymer chemistry as well as material science, not only because of the combination of ILs with unique characteristics (*e.g.* ionic conductivity, thermal stability, tuneable solution properties and chemical stability), but also a matter of achieving new properties and functions [Mecerreyes 2011; Yuan *et al.* 2011a]. The major advantages for such polymeric forms (instead of an IL) are the enhanced mechanical stability, improved processability, flexibility and durability in applications as practical materials [Kadokawa ; Shaplov *et al.* 2011b; Yuan *et al.* 2011a; Frank-Finney *et al.* 2013].

The polymerization of IL monomers is another strategy to prepare ionic gels, consisting of two basic routes: (1) direct polymerization of IL monomers, (2) chemical modification of existing polymers [Lu *et al.* 2009; Yuan *et al.* 2011a]. The IL monomers used in free radical polymerizations have a polymerizable unit in the cation and/or anion. In the following a variety of polymerizable IL systems such as (1) polycation-type ILs, (2) polyanion-type ILs, (3) copolymer and (4) poly(zwitterion)-type ILs will be introduced.

(1) Polymerizable cation-type ILs

Imidazolium is the most popular cation which has been included into polymer backbones obtained from vinyl [Ohno *et al.* 1998; Marcilla *et al.* 2004], styrenic [Tang *et al.* 2005a; Kadokawa *et al.* 2008] and (meth)acryloyl monomers [Cardiano *et al.* 2008; Pohako-Esko *et al.* 2013] (Scheme 1-1). To a minor extent, polymers bearing other types of cations such as pyridinium, tetraalkyl ammonium, guanidinium, piperidinium or pyrrolidinium have also been synthesized [Mecerreyes 2011; Yuan *et al.* 2011a].

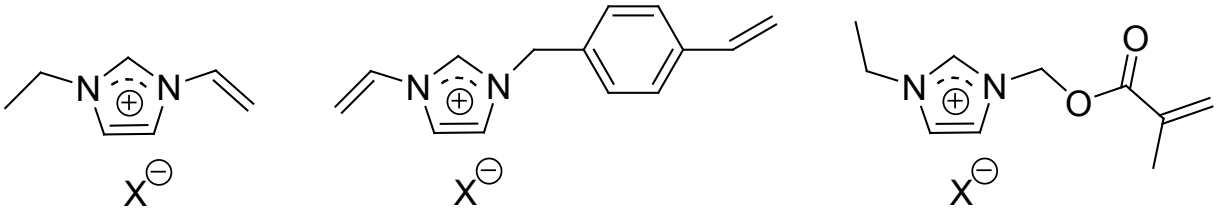

Scheme 1-1 Examples for polymerizable cation-type ILs: imidazolium-IL with vinyl- (*left*), styrene- (*center*) and methacrylate functions (*right*)

N-vinylimidazolium-based ionic liquids are synthesized via a simple one-step quaternization reaction of N-vinylimidazole with a halo-alkane compound [Marcilla *et al.* 2004; Hu *et al.* 2010; Green *et al.* 2011; Pinaud *et al.* 2011; Yang *et al.* 2011]. The structural variables in this monomer family are the alkyl chain length as well as the anion. Anion exchange is another method to modify the IL family. By replacing the halide with anions such as $[PF_6]^-$ or $[TFSI]^-$ (bis(trifluoromethylsulfonyl)imide), the IL monomers become more hydrophobic [Yuan *et al.* 2011a]. It is also possible to perform anion exchange reaction with silver salts, *e.g.* silver nitrate, silver acetate and silver lactate. However, sometimes the complete removal of the by-product becomes problematic, and silver salts are expensive [Harjani *et al.* 2009; Xu *et al.* 2009].

Styrene is the precursor to polystyrene and several copolymers. IL monomers with a styryl group have been studied by Gin and Noble [Bara *et al.* 2008a; Bara *et al.* 2008b]. The IL monomers can be synthesized by reacting, for example 4-chloromethyl styrene with imidazole through a quaternization reaction. Kaneko and co-workers published an easy method for the preparation of composites composed of cellulose and a polystyrene-type polymeric ionic liquid [Kadokawa *et al.* 2008].

(Meth)acryloyl-based IL monomers can be obtained in a two-step synthesis. First, a (meth)acryloyl group is introduced by usage of a hydroxyl-containing halo-alkane with (meth)acryloyl chloride resulting in the formation of the corresponding ester. In the next step, the obtained product reacts with N-alkyl imidazole and the quaternization reaction yields the (meth)acryloyl-based IL monomers [Yuan *et al.* 2011a]. Last year, Mäeorg and co-workers reported a new method for synthesis of methacrylate-type polymerizable ILs [Pohako-Esko *et al.* 2013].

Recently, a number of polymerizable cationic IL monomers (illustrated in Scheme 1-2) have been introduced [Yuan *et al.* 2011a]. In the literature are reported further polymerizable cationic IL monomers [Yoshizawa *et al.* 2002; Vygodskii *et al.* 2007; Green *et al.* 2009a; Lu *et al.* 2009; Shaplov *et al.* 2009; Mecerreyes 2011; Shaplov *et al.* 2011b; Moreno *et al.* 2012; Shaplov *et al.* 2012; Choi *et al.* 2013; Jeremias *et al.* 2013; Rahman *et al.* 2013; Adzima *et al.* 2014; Li *et al.* 2014; Tang *et al.* 2014; Zhang *et al.* 2014].

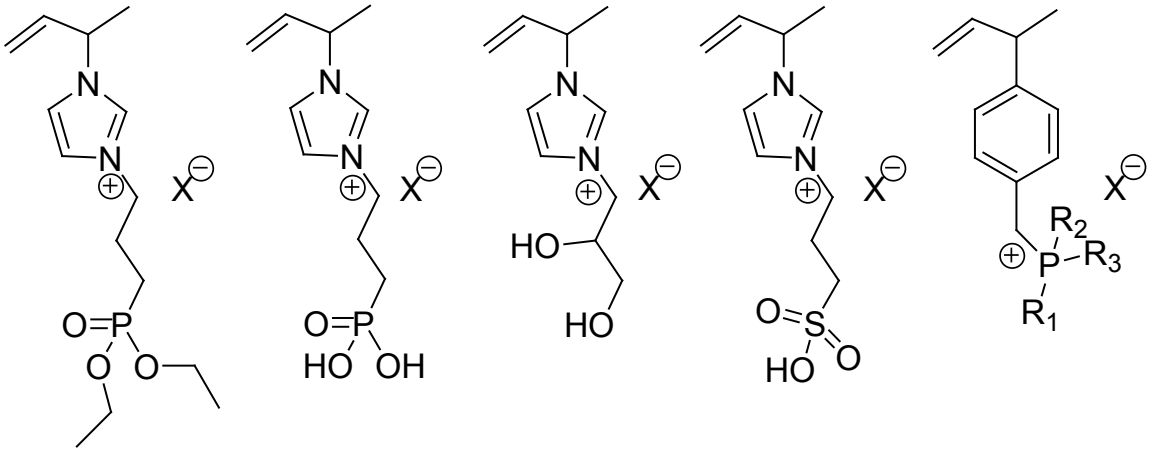

Scheme 1-2 Several selected structures of polymerizable cationic IL monomers [Yuan *et al.* 2013]

The anion X is universally, *e.g.* it can be halides or in case of phosphorous-type cationic IL also $[NTf_2]^-$ or $[N(CN)_2]^-$ are possible counterparts. With sulphur-type cationic IL also $[HSO_4]^-$ as anion is possible.

(2) Polymerizable anion-type ILs

The number of polymerizable anionic IL monomers has been much smaller than that for the cationic ones. It is possibly because of the difficulty of synthesizing anionic-type IL monomers [Mecerreyes 2011]. A few examples are shown in Scheme 1-3.

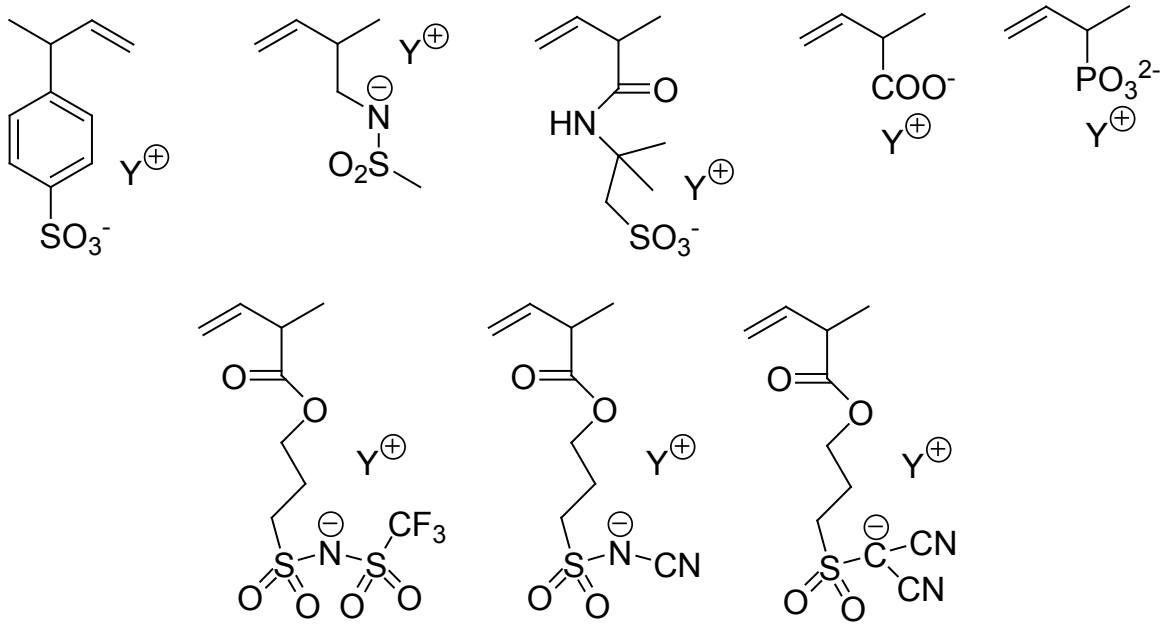

Scheme 1-3 Several selected structures of polymerizable anionic IL monomers with Y^+ (tetraalkylammonium or alkyl-imidazolium type counter-cations) [Mecerreyes 2011; Shaplov *et al.* 2011a; Yuan *et al.* 2013]

Again, PILs based on anionic IL monomers are synthesized by conventional radical polymerization reaction. Thus, PILs have backbones such as poly(styrene sulfonate), poly(acryl acid), poly(phosphonic acid) or poly(acrylamido)-2-methylpropane sulfonate [Yoshizawa *et al.* 2002; Ohno *et al.* 2004; Washiro *et al.* 2004; Mecerreyes 2011; Shaplov *et al.* 2011a].

Shaplov *et al*. reported that the anionic PILs, compared to their cationic counterpart, presented relatively higher ionic conductivities [Shaplov *et al.* 2011a].

(3) PIL block copolymers

In a homopolymer of PILs, each repeating unit results from an ionic liquid monomer. In the literature are described various imidazolium-based PIL block copolymers [Grubjesic *et al.* 2009; Shaplov *et al.* 2011b; Yuan *et al.* 2011a; Yuan *et al.* 2013]. The atom transfer radical polymerization (ATRP) as well as reversible addition-fragmentation polymerization (RAFT) is useful for synthesizing PIL block copolymers [Mori *et al.* 2009; Yuan *et al.* 2011b; Yuan *et al.* 2013]. Zhang *et al*. studied the kinetics of the copolymerization of 1-vinyl-3-ethylimidazolium bromide with acrylonitril under various conditions. The obtained copolymers were characterized and can be used in the preparation of precursor fibers and carbon fibers [Zhang *et al.* 2009]. Kou and co-workers reported that the synthesized copolymers (1-vinyl-3-alkylimidazolium halide with N-vinyl-2-pyrrolidone) are capable of acting as soluble bi-functional stabilizers for IL media. The obtained copolymers were highly soluble in 1-butyl-3-methylimidazolium [BMIm] ILs, and they synthesized active rhodium nanoparticles in the presence of the copolymers dissolved in [BMIm][BF_4] [Mu *et al.* 2005]. Chen et al. published in their study the effect of random copolymer composition on the ion conduction [Chen *et al.* 2009]. Synthesized imidazolium-based PIL block copolymers reported in the literature are shown in Scheme 1-4.

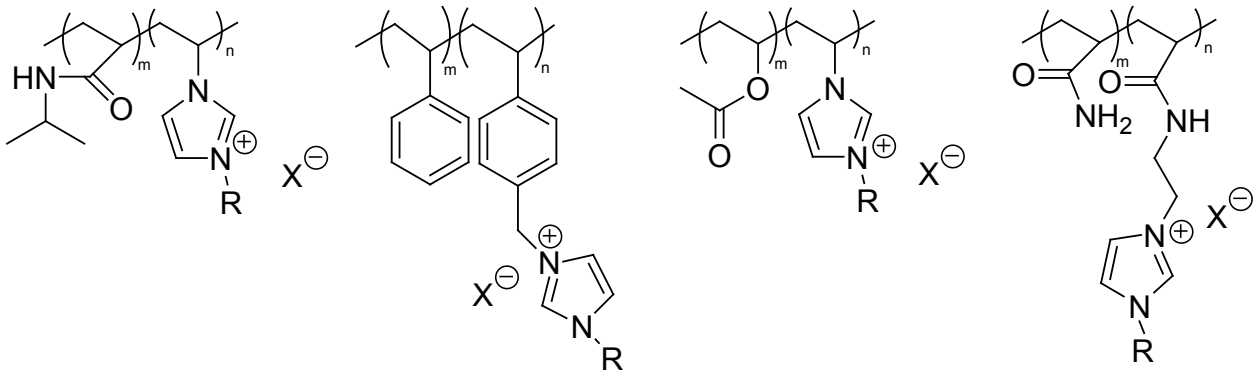

Scheme 1-4 Imidazolium-based PIL block copolymers described in the literature [Yuan *et al.* 2013]

Mecerreyes and co-workers used *N,N′*-methylenebisacrylamide as cross-linker to achieve polymeric ionic liquid microgel particles [Marcilla *et al.* 2006b]. In a second step, the halide anion (bromide) was exchanged in water with different anions, and swelling studies of the PIL microgels in various organic solvents were investigated. In the literature are known further cross-linkers, *e.g*. polyethylene glycol diacrylate [Rahman *et al.* 2013], di(ethylene glycol) divinyl ether and tri(ethylene glycol) divinyl ether [Washiro *et al.* 2004].

(4) Polymerizable zwitterionic-type ILs

Some examples of polymerizable zwitterionic-type ionic liquids are described and reported in the scientific literatures [Yoshizawa *et al.* 2001; Pinaud *et al.* 2011; Taguchi *et al.* 2011; Ueda *et al.* 2011; Taguchi *et al.* 2012; Soll *et al.* 2013]. In this case, the monomer has both anion and cation covalently bonded in the backbone. In Scheme 1-5 are illustrated selected polymerizable zwitterionic-type monomers [Mecerreyes 2011].

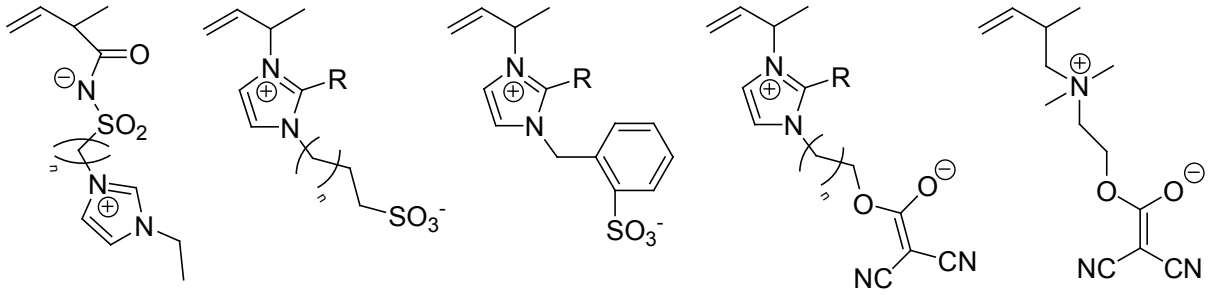

Scheme 1-5 Chemical structures of polymerizable zwitterionic-type monomers [Mecerreyes 2011]

The monomers are solid salts with high melting points in some cases. The PILs having imidazolium or tetraalkylammonium cations together with sulphonate, or trifluoromethanesulfamide or alkoxydicyanoethenolates anions in the same monomer can be synthesized by radical polymerization. In the literature these polymers are described as new PIL structures [Mecerreyes 2011].

1.4.2 Applications of PILs

Polymeric ionic liquids with unique and fascinating properties have attracted growing interest in the last few years. PILs refer to a special type of polyelectrolytes [Yuan *et al.* 2011c]. The use of PILs as polymer electrolytes is well reported in the scientific literature [Green *et al.* 2009b; Mecerreyes 2011; Yuan *et al.* 2011a; Yuan *et al.* 2013]. They are of interest for energy conversion and storage devices, such as fuel cells [Lin *et al.* 2010], lithium batteries [Park *et al.* 2013; Li *et al.* 2014; Yin *et al.* 2014], supercapacitors [Kim *et al.* 2010; Pandey *et al.* 2012; Jeremias *et al.* 2013] and dye sensitized solar cells [Sun *et al.* 2012b]. PILs possess unique physiochemical properties such as high ionic conductivity [Marcilla *et al.* 2006a; Ye *et al.* 2012], high thermal and electrochemical stability and tuneable properties via anion exchange [Marcilla *et al.* 2004; Carrasco *et al.* 2011; Merle *et al.* 2013; Rahman *et al.* 2013]. Elabd and co-workers reported many research results from PILs with regard to ionic conductivity and potential applications [Chen *et al.* 2009; Green *et al.* 2011; Weber *et al.* 2011; Ye *et al.* 2011; Salas-de la Cruz *et al.* 2012; Ye *et al.* 2012; Ye *et al.* 2013].

Currently, the ability of PILs in catalysis focuses on their use as a (co)catalyst, catalyst support as well as catalyst precursor. Wang and co-workers have investigated a few PILs [Xiong *et al.* 2011; Xiong *et al.* 2012a; Xiong *et al.* 2012b] and synthesized cross-linked PIL nanoparticles because they are easy to recycle and they can provide a large active surface area. The high activity and selectivity of these cross-linked nanoparticle catalysts were used for the cycloaddition of various epoxides with CO_2 [Xiong *et al.* 2011; Xiong *et al.* 2012b]. Dyson and co-workers reported the synthesis of imidazolium-based PILs and also their use as heterogeneous catalysts for the cycloaddition of CO_2 with epoxides [Ghazali-Esfahani *et al.* 2013]. Furthermore, PILs have been tested for a number of reactions. Liu *et al*. reported the transesterification reaction of tripalmitin with methanol catalyzed by ionic liquids on superhydrophobic mesoporous polymers [Liu *et al.* 2012]. Another research group reported and synthesized cross-linked PILs as high loaded dual acidic organocatalyst [Pourjavadi *et al.* 2012]. The obtained heterogeneous catalyst is used for the synthesis of dihydropyrimidines under mild reaction conditions with high yields. Mecerreyes *et al*. synthesized a microgel based on PILs with paramagnetic anions, *e.g*. tetrachloroferrate (III). This microgel was used as a reusable catalyst for Friedel-Crafts alkylation [Doebbelin *et al.* 2011]. PILs can stabilize catalytically active metal and metal oxide nanoparticles. For example, Kou and co-workers published the stabilization of rhodium nanoparticles by a copolymer of N-vinyl-2-pyrrolidone

and 1-butyl-3-vinylimidazolium bromide in 1-butyl-3-methylimidazolium tetrafluoroborate IL solvent [Mu *et al.* 2005]. The long lifetime nanocluster catalysts were used for benzene hydrogenation. Also, PIL microspheres/Pt nanoparticle hybrids were developed and evaluated for the electrocatalytic oxidation of methanol as well as oxidation of benzyl alcohol [Yang *et al.* 2011]. A further possibility is the functionalization of carbon nanotubes by an ionic liquid polymer [Wu *et al.* 2009]. Structured semifluorinated polymer ionic liquids for the preparation of metal nanoparticle were synthesized by Mülhaupt and co-workers [Schadt *et al.* 2013]. Removing ionic liquids from IL/polymer composites is an easy way to synthesize porous polymers. Some research groups have been prepared porous PIL materials [Snedden *et al.* 2003; Yan *et al.* 2006; Yan *et al.* 2007; Huang *et al.* 2010; Zhao *et al.* 2012]. The pore size of the porous PIL materials can be tuned by adjusting the cross-linker content. More cross-linker agent resulted in a smaller pore size of the porous polymer [Yan *et al.* 2007]. The usage of porous PIL particles is an emerging research area in the biotechnology. For example, peroxidase (HRP) was encapsulated in a PIL microparticle, and it showed a 2-fold higher activity than the enzyme encapsulated in a polyacrylamide microparticle [Nakashima *et al.* 2009]. Also, the enzyme glucose oxidase (GOx) was immobilized in PIL microparticles and evaluated as a possible glucose sensor [Lopez *et al.* 2006].

In the field of separation science, PILs also show unique properties and they are used in solid-phase microextraction as sorbent coatings [Zhao *et al.* 2008; Wanigasekara *et al.* 2010; Meng *et al.* 2011; Ho *et al.* 2013; Zhang *et al.* 2014]. Anderson and co-workers developed selective coatings based on polymeric ionic liquids for the extraction of esters [Zhao *et al.* 2008] as well as for polar compounds [Meng *et al.* 2011]. Polymeric imidazolium ionic liquids were used as stationary phases in gas chromatography (GC) [Hsieh *et al.* 2007; Hsieh *et al.* 2008; Gonzalez-Alvarez *et al.* 2012; Ho *et al.* 2013], HPLC [Qiu *et al.* 2010] and as coating of capillary electrophoresis [Li *et al.* 2010; Li *et al.* 2011b; Zhou *et al.* 2011; Tang *et al.* 2014]

PILs have been approved as hopeful sorbents for CO_2 since they showed high CO_2 absorption capacity [Tang *et al.* 2005a; Tang *et al.* 2005b; Tang *et al.* 2009; Xiong *et al.* 2012a; Soll *et al.* 2013]. Shen and co-workers investigated structure effects on the CO_2 sorption. Poly(ionic liquid)s with varied structures including different cations (*e.g.* tetraalkylammonium, imidazolium), anions (*e.g.* tetrafluoroborate, hexafluorophosphate) and backbones was used. The tetraalkylammonium-based PILs exhibited higher CO_2 sorption capacities than the imidazolium-based PILs. An ammonium cation with a short alkyl group, an tetrafluoroborate

anion and polystyrene backbone were found to favor CO_2 sorption in PILs [Tang *et al.* 2009]. Bara *et al*. reported an improved CO_2 selectivity in polymerized room-temperature ionic liquid gas separation membranes through the incorporation of polar substituents [Bara *et al.* 2008a].

For polymeric ionic liquid (hydro)gels there are only a few published reports in the scientific literatures [Gu *et al.* 2011; Frank-Finney *et al.* 2013; Ziolkowski *et al.* 2013; Gallagher *et al.* 2014; Kasahara *et al.* 2014]. Ziolkowski and Diamond reported the first thermo-responsive poly(ionic liquid)-based hydrogels in 2013. Two monomeric ILs have been photo-polymerized with different cross-linkers of varying length. The result was that only hydrogels with a long chain cross-linker allow the material to swell in water without cracking and disintegrating. They investigated interesting properties of these hydrogels, *e.g*. the lower critical solution temperature (LCST) [Ziolkowski *et al.* 2013]. Further investigations of these group was swelling and shrinking properties of thermo-responsive poly(ionic liquid) hydrogels with an embedded linear polymer *N*-isopropylacrylamide [Gallagher *et al.* 2014]. The synthesized semi-interpenetrating hydrogels were found to have improved shrinking and re-swelling characteristics. Matsuyama and co-workers prepared for the first time novel polymer gels containing amino acid ionic liquids (AAILs). The ion-gel films containing AAILs were produced by free radical polymerization of vinyl monomers [Kasahara *et al.* 2014].

1.5 Drug-coated balloons (DCB)

In the last few years the use of percutaneous, catheter-based vascular devices to medicate the symptoms of cardiovascular disease has emerged as a therapeutic standard to drug eluting stents (DES) [Babcock *et al.* 2013; Lupi *et al.* 2013]. Drug-coated balloon catheters (DCB) have been exhibited to be effective in the prevention of restenosis [Scheller *et al.* 2004; Scheller *et al.* 2006]. The used drug should possess specific chemical characteristics, mechanism of action as well as pharmacokinetics to be quickly absorbed by the vessel wall. Commonly, the used drug is paclitaxel (PTX), a cytotoxic agent [Krokidis *et al.* 2013]. This drug was determined as the primary drug for DCB due to its rapid uptake as well as extended retention [Waksman *et al.* 2009]. The cytotoxic, anti-proliferative effect of DES on the vessel wall has been widely investigated [Narbute *et al.* 2011; Krokidis *et al.* 2013]. Preclinical data with DCB have exhibited that 3 $\mu g/mm^2$ is the efficacious dose to obtain an effective, long-term, antiproliferative effect on the vessel wall [Posa *et al.* 2010; Krokidis *et al.* 2013]. Drug delivery during angioplasty depends mainly on the drug dose, transfer system, inflation time, release pattern and appropriate balloon coating [Krokidis *et al.* 2013]. Preclinical and clinical data are reported in the literatures [Scheller *et al.* 2006; Cortese *et al.* 2012; Loh *et al.* 2012; Lupi *et al.* 2013]. Different balloon coating technologies are described in the literatures [Waksman *et al.* 2009; Kelsch *et al.* 2011; Cortese *et al.* 2012; Loh *et al.* 2012; Kleber *et al.* 2013; Krokidis *et al.* 2013]. In addition to pure PTX balloon catheters, different drug formulations with additives are commercially available, listed in Table 1-3. The drug paclitaxel is lipophilic, a property that vastly limits its transfer into the vessel wall during the short inflation time. A carrier can be used to enable the transfer of the hydrophobic drug paclitaxel into the vessel wall without increasing early loss of the drug on the way to the target lesion [Afari *et al.* 2012; Krokidis *et al.* 2013]. Hydrophilic additives allow higher tissue concentrations of PTX [Heilmann *et al.* 2010].

The Paccocath technology, introduced by Scheller, with paclitaxel embedded in hydrophilic iopromide coating increases the solubility and the drug transfer to the vessel wall [Scheller *et al.* 2006]. About 80% of the drug is retained during the balloon delivery to the target lesion, and 10-15% of the drug is transferred to the vessel wall during 60s balloon expansion [Waksman *et al.* 2009]. This coating is stable during ethylene oxide sterilization. Drug delivery is also achieved through the FreePac technology, which uses a natural excipient urea as carrier. This hydrophilic coating technology enhances the drug absorption and release

[Krokidis *et al.* 2013]. The DIOR paclitaxel-eluting coronary balloon catheter utilizes the Shellac® coating technology composed of aleuritic and shellolic acid, as well as paclitaxel. Posa *et al*. reported the safety and efficacy of DEB in their preclinical model (porcine coronary arteries). Using the DIOR coating effective tissue concentrations were achieved after balloon expansion times of 30 s [Posa *et al.* 2010]. DIOR uses folded balloon technology, whereby Waksman *et al*. published a full drug release up to 60 s [Waksman *et al.* 2009]. During balloon inflation, the blood flow in the vessel is interrupted and therefore expansion can only be maintained up to one minute. A novel balloon coating method based on cetylpyridinium salicylate as additive is reported by Petersen *et al*. [Petersen *et al.* 2013a].

Table 1-3 Commercially available DCBs (adapted from [Krokidis *et al.* 2013])

DCB	Company	Paclitaxel content	Coating technology	Delivery Diameter Length
ELUTAX©	Aachen-Resonance® GmbH, Aachen, Germany	3 µg/mm²	Matrix of pure paclitaxel without additives	0.014″ RE 2.5-4 mm 10-27 mm
PANTERA LUX™	Biotronik GmbH, Berlin, Germany	3 µg/mm²	Paclitaxel and butyryl-tri-hexyl citrate (BTHC)	0.014″ RE 2-4 mm 20-30 mm
SeQuent Please®	B. Braun Melsungen AG, Melsungen, Germany	3 µg/mm²	Paccocath® technology (excipient: iopromide)	0.014″ OTW 2.5-4 mm 10-30 mm
DIOR®	Eurocor AG, GmbH, Bonn, Germany	3 µg/mm²	Excipient: Shellac (aleuritic and shellolic acid)	0.014″ RE 2-4 mm 20-40 mm
FREEWAY®	Eurocor AG, GmbH, Bonn, Germany	3 µg/mm²	Excipient: Shellac (aleuritic and shellolic acid)	0.014″ OTW 2-4 mm 40-150 mm
IN.PACT Admiral™	Medtronic Inc., Frauenfeld, Switzerland	3 µg/mm²	FreePac™ hydrophilic coating (excipient: urea)	0.035″ OTW 4-7 mm 40-120 mm
IN.PACT Pacific™	Medtronic Inc., Frauenfeld, Switzerland	3 µg/mm²	FreePac™ hydrophilic coating (excipient: urea)	0.018″ OTW 3-7 mm 40-120 mm
MOXY™	Lutonix Inc., Maple Grove, MN	2 µg/mm²	Proprietary hydrophilic nonpolymeric carrier	0.018″-0.035″ N/A

OTW: over-the wire PTX-coated balloon; RE: rapid exchange

A major advance from drug-coated balloons compared to drug-eluting stents (DES) is the rapid drug elution (see Table 1-4). Currently, PTX-eluting stents elute the drug in about one month, while DCBs elute about 80% of the drug during balloon expansion [Cortese *et al.* 2012]. After 12-24 h the drug concentration in the vessel wall is low [Scheller *et al.* 2004; Page *et al.* 2007]. Calculated curves for PTX tissue concentration as function of time are provided in the literature. Within the first hour, the concentration decreases dramatically

[Ruebben *et al.* 2010; Afari *et al.* 2012]. The use of DCB is very attractive, especially for lesions whose healing is expected to be fast.

Table 1-4 Drug-coated balloons vs. drug-eluting stents (adapted from [Waksman *et al.* 2009])

	DCB	DES
Platform of drug delivery	Balloon	Stent scaffolding
Retention	Embedded imprinted	Polymer based
Drug dose	High: 300-600 µg	Low: < 100-200 µg
Release kinetics	Fast	Slow and controlled
Distribution	Balloon surface homogeneous distribution	Strut-based vascular penetration
Advantages	Larger surface area Less drug localization in the vessel wall Accessible to complex lesions and long segments May not require prolonged DAPT	Mechanical support Abluminal trapping Less drug spillage into the circulation Proven efficacy in many indications No acute recoil tackled dissection

DAPT: dual antiplatelet therapy

There are some properties of DCB that are deciding for ensuring an effective drug delivery to the target site, including (1) the degree of early loss of the drug during the insertion; (2) its stability during production, handling and storage; (3) the homogeneity of distribution along the balloon surface; (4) the ability to release during balloon expansion; (5) the amount of particulate material released to the distal circulation and (6) the drug transfer efficiency to the vessel wall [Scheller 2011]. One drawback of DIOR-I was the low drug transfer of only 20-25% into the vessel wall after 60 s inflation times [Posa *et al.* 2010; Belkacemi *et al.* 2011]. Next to the composition of the drug coating are important factors the duration of delivery time as well as the size of the balloon catheter.

2. Objectives of the work

Within the REMEDIS subproject is the task of developing a new coating of a balloon catheter. Commonly, the balloons were only coated with the drug paclitaxel to minimize the restenosis. However, the drug loss during insertion of the balloon is very high due to the fact that the needle-like crystals of the drug can easily drop off. The novel homogeneous coating of the balloon catheter with an ionic liquid as additive should be evaluated. One objective of this work is to develop and establish an *in-vitro* vessel model to carry out balloon dilations. Hydrogels can be used as materials to simulate an artificial vessel wall. Often, calcium alginate is utilized as vessel model for *in-vitro* investigation of balloon catheters and stents. However, alginate is a natural polysaccharide and does not show long-term stability. Therefore, it is the aim of this work to produce novel hydrogel materials, which should be characterized in respect to mechanical and thermal behavior. A comparison of these novel hydrogels with polyacrylamide hydrogels of covalent-type cross-linking and alginate-based hydrogels of ionic-type cross-linking is also an objective of this work. Furthermore, different hydrogels may used as models for a vessel wall. Generally speaking, the main objective is an *in-vitro* study of drug-coated balloons with an ionic liquid as additive to determine the distribution of paclitaxel after simulated use in a flow-through cell using different hydrogels. The local drug delivery after balloon dilation in the first minute is determined in a vessel-simulating flow-through cell by a simulated blood stream. By using different hydrogels, a comparison and an assessment can be made. Scheme 2-1 illustrated all objectives of these work.

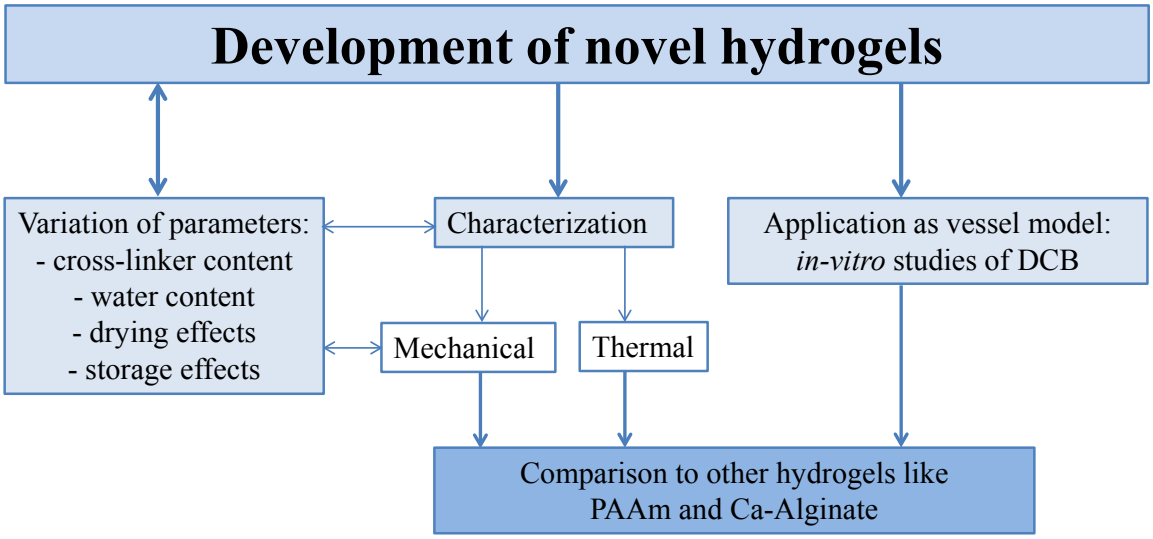

Scheme 2-1 Objectives of the work

3. Materials and methods

This chapter describes the used methods to understand all preparation procedures. Next to the synthesis of various ILs the hydrogel preparations as well as the mechanical and thermal characterization are explained. The application of hydrogel materials as vessel models in studies of drug-coated balloons is also described in detail.

3.1 Synthesis of various ILs and their analytic

Chemicals: 1-Vinylimidazole (≥ 99%; Aldrich), ethyl bromide (≥ 99%; Merck), *n*-butyl chloride (≥ 99%; Merck), *n*-butyl bromide (> 98%; Merck) and silver acetate (99%, Sigma-Aldrich) were used as received. Ammonium peroxydisulphate (≥ 98%, APS), tetramethylethylenediamine (TEMED, 99%), Rotiphorese® Gel 30 (acrylamide/bisacrylamide, 37.5:1) and Rotiphorese® Gel B (2% bisacrylamide) were obtained from Carl Roth and used as received. Sodium alginate (Fagron, solid) was applied as 3% (w) alginate sol in de-ionized water. Calcium sulphate dihydrat (≥ 99%; Merck) and trisodium phosphate decahydrate (≥ 99%; VEB Berlin Chemie) were used as received.

NMR: ^{1}H and ^{13}C spectra were recorded on a Bruker AVANCE 250 (250 MHz), AVANCE 300 (300 MHz) spectrometer and were referenced externally. DMSO-d_6 (≥ 99.9%; Aldrich) was used as received. IR: Nicolet 380 FT-IR with a Smart Orbit ATR device was used. CHN analyses: Analysator Flash EA 1112 from Thermo Quest, or C/H/N/S-Mikroanalysator TruSpec-932 from Leco was used. DSC: DSC 823e from Mettler-Toledo (Heating-rate 5 °C/min) was used.

Synthesis of vinyl imidazolium halides (1-3)

1-Vinyl-3-ethyl-imidazolium bromide (**1,** [VEIm][Br]), 1-vinyl-3-butyl-imidazolium bromide (**2,** [VBIm][Br]) and 1-vinyl-3-butyl-imidazolium chloride (**3,** [VBIm][Cl]) were prepared by quarternization of 1-vinylimidazole according to published procedures [Marcilla *et al.* 2004; Hu *et al.* 2010; Green *et al.* 2011; Pinaud *et al.* 2011].

[VEIm][Br] (**1**): ^{1}H NMR (250 MHz, DMSO-d_6, δ): 9.64 (s, 1H, N=C<u>*H*</u>–N), 8.24 (s, 1H, N–C<u>*H*</u>=CH–N), 7.98 (s, 1H, N–CH=C<u>*H*</u>–N), 7.32 (dd, J = 15.68 Hz, J = 8.75 Hz, 1H, N–C<u>*H*</u>=CH_2), 5.98 (dd, J = 15.61 Hz, J = 2.36 Hz, 1H, N–CH=C<u>*H*</u>$_2$), 5.41 (dd, J = 8.75 Hz,

J = 2.29 Hz, 1H, N–CH=C$\underline{H_2}$), 4.24 (q, J = 7.41 Hz, 2H, *ethyl-α*-C$\underline{H_2}$), 1.45 (t, J = 7.33 Hz, 3H, *ethyl-β*-C$\underline{H_3}$). ^{13}C NMR (250 MHz, DMSO-d_6, δ): 135.07 (N=$\underline{C}$H–N), 128.04 (N–$\underline{C}$H=CH–N), 122.93 (N–$\underline{C}$H=CH$_2$), 119.10 (N–CH=$\underline{C}$H–N), 108.44 (N–CH=$\underline{C}$H$_2$), 44.57 (*ethyl-α*-$\underline{C}$H$_2$), 14.74 (*ethyl-β*-$\underline{C}$H$_3$). IR (ATR): ν = 3132 (w), 3093 (m), 3072 (s), 3055 (s), 2991 (m), 2980 (m), 2908 (w), 2870 (w), 1660 (s), 1645 (m), 1581 (s), 1545 (s), 1520 (w), 1504 (w), 1495 (w), 1456 (m), 1417 (w), 1375 (m), 1346 (m), 1331 (s), 1302 (m), 1279 (w), 1257 (m), 1184 (s), 1167 (vs), 1136 (m), 1115 (m), 1095 (m), 1047 (m), 1032 (w), 1011 (w), 978 (s), 959 (m), 926 (s), 889 (m), 852 (s), 783 (s), 717 (m), 690 (m), 658 (w), 635 (m), 617 (s), 596 cm^{-1} (vs). Yield: 90.4%. Mp. (onset) 87.7 °C; (peak) 99.2 °C (DSC). Anal. calcd. for $C_7H_{11}N_2Br$: C 41.40, H 5.46, N 13.79; found: C 41.56, H 5.55, N 13.81.

[VBIm][Br] (**2**): ^{1}H NMR (300 MHz, DMSO-d_6, δ): 9.64 (s, 1H, N=C$\underline{H}$–N), 8.24 (s, 1H, N–C$\underline{H}$=CH–N), 7.97 (s, 1H, N–CH=C$\underline{H}$–N), 7.32 (dd, J = 15.58 Hz, J = 8.78 Hz, 1H, N–C$\underline{H}$=CH$_2$), 5.98 (dd, J = 15.67 Hz, J = 2.46 Hz, 1H, N–CH=C$\underline{H_2}$), 5.42 (dd, J = 8.69 Hz, J = 2.27 Hz, 1H, N–CH=C$\underline{H_2}$), 4.21 (t, J = 7.27 Hz, 2H, *butyl-α*-C$\underline{H_2}$), 1.81 (q, 2H, *butyl-β*-C$\underline{H_2}$), 1.28 (sxt, 2H, *butyl-γ*-C$\underline{H_2}$), 0.89 (t, 3H, *butyl-δ*-C$\underline{H_3}$). ^{13}C NMR (300 MHz, DMSO-d_6, δ): 135.29 (N=$\underline{C}$H–N), 128.85 (N–$\underline{C}$H=CH–N), 123.22 (N–$\underline{C}$H=CH$_2$), 119.14 (N–CH=$\underline{C}$H–N), 108.59 (N–CH=$\underline{C}$H$_2$), 48.89 (*butyl-α*-$\underline{C}$H$_2$), 31.02 (*butyl-β*-$\underline{C}$H$_2$), 18.75 (*butyl-γ*-$\underline{C}$H$_2$), 13.26 (*butyl-δ*-$\underline{C}$H$_3$). IR (ATR): ν = 3107 (w), 3090 (m), 3039 (s), 2980 (m), 2968 (m), 2955 (m), 2928 (m), 2872 (m), 2847 (w), 1705 (w), 1684 (w), 1651 (m), 1566 (s), 1539 (s), 1514 (w), 1495 (m), 1466 (m), 1456 (m), 1433 (m), 1414 (m), 1385 (w), 1365 (m), 1338 (w), 1321 (w), 1308 (w), 1290 (w), 1273 (w), 1230 (w), 1159 (vs), 1132 (m), 1115 (m), 1086 (m), 1049 (w), 1022 (w), 1007 (m), 982 (s), 941 (w), 926 (s), 881 (s), 804 (s), 739 (s), 723 (m), 681 (w), 662 (s), 635 (m), 604 (s), 532 cm^{-1} (w). Yield: 49.3%. Mp. (onset) 80.0 °C; (peak) 81.9 °C (DSC). Anal. calcd. for $C_9H_{15}N_2Br$: C 46.77, H 6.54, N 12.12; found: C 46.75, H 6.59, N 11.95.

[VBIm][Cl] (**3**): ^{1}H NMR (250 MHz, DMSO-d_6, δ): = 9.85 (s, 1H, N=C$\underline{H}$–N), 8.29 (s, 1H, N–C$\underline{H}$=CH-N), 7.99 (s, 1H, N–CH=C$\underline{H}$–N), 7.36 (dd, J = 15.68 Hz, J = 8.75 Hz, 1H, N–C$\underline{H}$=CH$_2$), 6.03 (dd, J = 15.61 Hz, J = 2.36 Hz, 1H, N–CH=C$\underline{H_2}$), 5.41 (dd, J = 8.75 Hz, J = 2.29 Hz, 1H, N–CH=C$\underline{H_2}$), 4.22 (t, J = 7.17 Hz, 2H, *butyl-α*-C$\underline{H_2}$), 1.81 (q, 2H, *butyl-β*-

C$\underline{H_2}$), 1.28 (sxt, 2H, *butyl-γ*-C$\underline{H_2}$), 0.90 (t, 3H, *butyl-δ*-C$\underline{H_3}$). ^{13}C NMR (250 MHz, DMSO-d_6, *δ*): 135.47 (N=$\underline{C}$H–N), 128.89 (N–$\underline{C}$H=CH–N), 123.22 (N–$\underline{C}$H=CH$_2$), 119.18 (N–CH=$\underline{C}$H–N), 108.51 (N–CH=$\underline{C}$H$_2$), 48.86 (*butyl-α*-$\underline{C}$H$_2$), 31.04 (*butyl-β*-$\underline{C}$H$_2$), 18.77 (*butyl-γ*-$\underline{C}$H$_2$), 13.26 (*butyl-δ*-$\underline{C}$H$_3$). IR (ATR): ν = 3109 (w), 3090 (m), 3030 (vs), 2976 (s), 2958 (s), 2931 (s), 2874 (m), 2848 (m), 1714 (w), 1651 (m), 1645 (m), 1566 (s), 1541 (s), 1504 (w), 1495 (w), 1462 (m), 1456 (m), 1435 (m), 1416 (m), 1367 (m), 1340 (m), 1323 (w), 1308 (w), 1292 (m), 1275 (m), 1161 (vs), 1134 (s), 1115 (m), 1053 (m), 993 (s), 955 (m), 924 (s), 981 (s), 818 (s), 768 (m), 741 (s), 723 (m), 683 (m), 663 (s), 658 (s), 638 (m), 621 (m), 608 (vs), 536 cm^{-1} (m). Yield: 34.7%. Mp. (onset) 112.7 °C; (peak) 114.3 °C (DSC). Anal. calcd. for $C_9H_{15}N_2Cl$: C 57.90, H 8.10, N 15.01; found: C 58.12, H 7.94, N 15.15.

Synthesis of 1-vinyl-3-ethyl-imidazolium acetate, [VEIm][Ac] (4)

IL **4** was prepared by using anion exchange reaction of **1**, different from the published synthesis of acetate containing ILs [Xu *et al.* 2009]. To a solution of 2.5 g **1** (12.3 mmol) in 30 mL methanol an equimolar amount of silver acetate (12.3 mmol, 2.055 g) in 30 mL methanol was added. The reaction mixture was allowed to stir for 10 min in the dark and precipitated silver bromide was filtered off. The IL was extracted with chloroform and filtered to remove residual silver salt. Finally $CHCl_3$ was evaporated at reduced pressure to obtain 2.23 g of **4** (99.1% yield).

[VEIm][Ac] (**4**): ^{1}H NMR (300 MHz, DMSO-d_6, *δ*): 10.49 (s, 1H, N=C$\underline{H}$–N), 8.30 (s, 1H, N–C$\underline{H}$=CH-N), 8.00 (s, 1H, N–CH=C$\underline{H}$–N), 7.45 (dd, J = 15.67 Hz, J = 8.88 Hz, 1H, N–C$\underline{H}$=CH$_2$), 6.05 (dd, J = 15.67 Hz, J = 2.27 Hz, 1H, N–CH=C$\underline{H_2}$), 5.35 (dd, J = 8.69 Hz, J = 2.27 Hz, 1H, N–CH=C$\underline{H_2}$), 4.26 (q, J = 7.30 Hz, 2H, *ethyl-α*-C$\underline{H_2}$), 1.59 (s, 3H, CO–C$\underline{H_3}$), 1.44 (t, J = 7.27 Hz, 3H, *ethyl-β*-C$\underline{H_3}$). ^{13}C NMR (250 MHz, DMSO-d_6, *δ*): 173.14 ($\underline{C}$=O), 136.51 (N=$\underline{C}$H–N), 129.13 (N–$\underline{C}$H=CH–N), 122.83 (N–$\underline{C}$H=CH$_2$), 119.02 (N–CH=$\underline{C}$H-N), 108.05 (N–CH=$\underline{C}$H$_2$), 44.39 (*ethyl-α*-$\underline{C}$H$_2$), 26.17 (CO–$\underline{C}$H$_3$), 14.82 (*ethyl-β*-$\underline{C}$H$_3$). IR (ATR): ν = 3051 (m), 2982 (m), 1653 (m), 1564 (vs), 1547 (vs), 1466 (m), 1448 (m), 1423 (m), 1385 (vs), 1329 (m), 1282 (m), 1173 (s), 1124 (m), 1092 (m), 1041 (m), 1005 (m), 966 (m), 908 (m), 760 (m), 685 (m), 638 (s), 617 (s), 598 cm^{-1} (s). Yield: 2.2 g (99.1%). GT. (onset) -52.7 °C; (peak) -52.7 °C (DSC).

3.2 Synthesis of various hydrogels

Gelation of Ca-alginate

Sodium alginate sol was prepared as following: 3 g of sodium alginate were dissolved in about 90 g de-ionized water at 70 °C while stirring according to instruction manual (Ph.Eur. 175860, Protanal LF 200 M) and subsequently cooled down to room temperature. After complete dissolution of sodium alginate, de-ionized water was added to the total amount of 100 g (3%, w/w).

To 0.15 g $CaSO_4 \cdot 2H_2O$ 1500 µL de-ionized water were added. The sparingly soluble salt was mixed with a stirring rod. Also, 500 µL of a 10% (w) $Na_3PO_4 \cdot 12H_2O$ solution was added. 16.5 g sol (3%, w) was mixed by a sheet with this fresh calcium containing suspension. The gelation time is 10 to 15 minutes.

Gelation of polyacrylamide (PAAm)

PAAm hydrogels were synthesized by radical polymerization. Rotiphorese® Gel 30 (1245 µL) was added to 3545 µL de-ionized water. Polymerization was initiated with 69 µL fresh APS (10%, w/w) and TEMED (6.9 µL). The solution was mixed for ca. 10 s using a Vortex mixer.

General procedure for syntheses of hydrogels containing IL monomers

IL-based hydrogels (**1a-4a**) were synthesized by radical polymerization (Scheme 4-1). 7.38 mmol of IL monomer (**1-4**) was dissolved in 2335 µL de-ionized water. Rotiphorese® Gel B (985 µL), 150 µL APS (10%, w/w) and 30 µL of TEMED were added. Solution was mixed using a Vortex for about 10 s. After 10 to 120 min the gelation process was completed and transparent hydrogels were obtained. In general, the procedure can be carried out by using different amounts of water as well as IL to cross-linker ratios (see Table 4-2). The reproducibility of the synthesis of hydrogels (**1a-4a**) was proven by repeated synthesis (> 10 times).

3.3 Specimen for mechanical characterization

All hydrogels were prepared in a specified size according to particularly measurement in a casting mold (Figure 3-1). Two different specimens were used to investigate mechanical behavior of synthesized hydrogels. These materials were stressed by compression and stretching. Measurements were performed at 22 ± 2 °C with a single column zwicki-line testing machine Z 2.5 [Zwick/Roell], a 500 N load cell and jaw inserts, while analyzing the data with *testXpert* standard. All measurements were performed as triplicate.

Compression

Hydrogels were prepared as described in the general procedure to obtain cylindrical test specimens with a height of 10.0 mm and a diameter of 10.0 mm (Figure 3-1a). Resulting specimens were subsequently compressed with a speed of 1 mm/min. In this work, various hydrogels (Ca-alginate, PAAm and poly-ionic liquid hydrogels) were examined.

Tensile test

For tensile tests the hydrogels were prepared as shown in Figure 3-1b. Specimens were stretched with a test speed of 5 mm/min until rupture. The point of break must be at the linear part of the specimen.

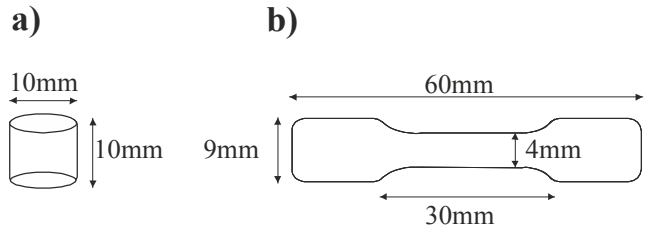

Figure 3-1 Specimen for the mechanical characterization: **a**) specimen for the compression tests, **b**) specimen for the tensile tests

3.4 Thermo gravimetric analysis (TGA)

Thermal stabilities of synthesized hydrogels were assessed by TGA measurements. Mass losses were studied and decomposition temperatures (T_{Dec}) were obtained. All measurements were performed with a Setaram Labsys 1600 TGA-DSC under argon atmosphere (heating rate 5 °K/min). Fresh hydrogels were synthesized and stored in a vial to avoid dehydration. Resulting hydrogels were weighted into an alumina crucible (20-30 mg). After placement on the TGA rod, the furnace was flushed with argon for 30 min. All data were corrected by baseline subtraction and no temperature correction was applied. Revised data were achieved by using Setsoft 2000 software. Thermal stability is depicted as the onset temperature of the corresponding mass loss, achieved by integration of the TG curve derivative (*d*TG).

3.5 Drug-coated balloons – *in-vitro* studies

Synthesis: Ionic liquid (IL) cetylpyridinium salicylate (Cetpyrsal) was synthesized by reaction of cetylpyridinium chloride with sodium salicylate according to published procedures [Bica *et al.* 2010; Petersen *et al.* 2013a]. The resulting IL formed slightly yellow crystals. Structure determination was performed by NMR spectroscopy (^{1}H and ^{13}C in DMSO-d_6 on a Bruker AVANCE 300, 300 MHz, 25 °C).

Materials: Paclitaxel (PTX, ≥ 99.5%) was obtained from Cfm Oscar Tropitzsch e.K, Germany. Cetylpyridinium chloride (Cetpyrsal, ≥ 96%; AppliChem GmbH, Germany) and sodium salicylate (≥ 99.5%; Merck KGaA, Germany) were also used as received. Angioplasty balloon catheters of 4 mm in diameter and 20 or 30 mm length were kindly supplied by Biotronik SE & Co KG, Germany.

Balloon coating: A pipetting technique was used for the coating of the inflated balloon catheter according to Petersen *et al*. [Petersen *et al.* 2013a]. Briefly, PTX and Cetpyrsal were separately dissolved in methanol to yield concentrations of 4.72 mg/mL (both stock solutions). Following this, a Cetpyrsal-PTX solution (50%, w/w) was mixed from both stock solutions. 100 µL of the Cetpyrsal-PTX solution was then slowly pipetted onto each balloon catheter, resulting in a PTX surface load of approx. 3 µg/mm^2, respectively a total of 753.98 µg (20 mm length) or 1130.97 µg (30 mm length). During the pipetting process, the balloon was rotated and evaporation of methanol was ensured by a gentle stream of air. Finally, all balloon catheters were dried at 23±2 °C overnight [Petersen *et al.* 2013a].

Simulated use of DCB in the vessel-simulating flow-through cell in different vessel models

An adapted vessel-simulating flow-through cell was chosen, which is described in detail by Seidlitz *et al*. [Seidlitz *et al.* 2011]. Instead of the acrylic glass disc a metal disc was used. Calcium alginate, PAAm and poly(VEImBr) hydrogels were inserted as hydrogel compartments. The DCB was placed in the simulated vessel wall and dilated for 60 s with a nominal pressure of 7 bar. The flow-through cell with the inflated balloon catheter is shown in Figure 3-2 with PAAm hydrogel as the vessel model. After expansion, the balloon was removed and isotonic sodium chloride (NaCl, 0.9%) as a perfusion medium was circulated along the simulated vessel wall for a duration of 1 min at a flow rate of 35 mL/min. Pumping of medium was managed with a gear pump (Ismatec MCP-Z ISM 405A, pump head model 186-000, Germany; Tygon® tube R 3607, 3.17 mm ID, VWR International GmbH, Germany) and the set flow rate was adjusted to the blood flow velocity in coronaries [Dimario *et al.* 1993]. The isotonic solution was collected in a falcon vessel and the PTX concentrations were measured by HPLC (see HPLC parameters).

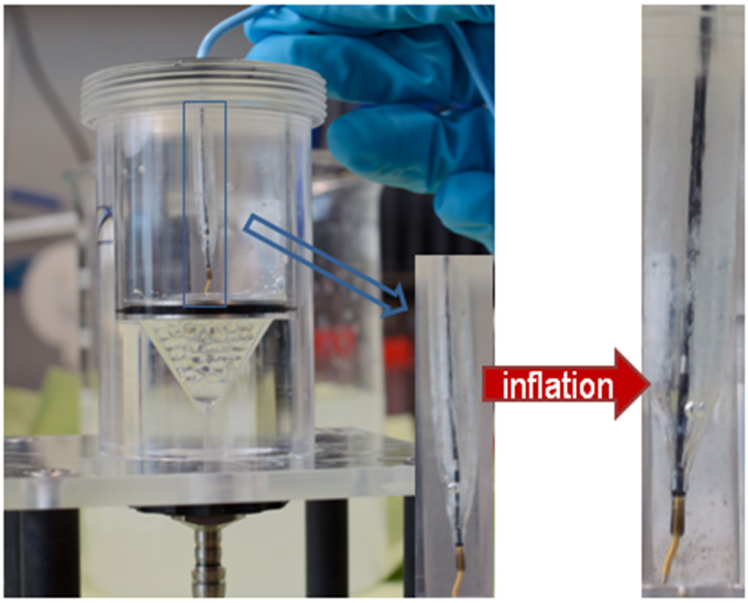

Figure 3-2 Representative picture of the implantation process, vessel model PAAm, *left*: after insertion of the coated balloon catheter, *right*: expansion of the balloon in the vessel wall

The process of balloon angioplasty was simulated applying an *in-vitro* model, consisting of a guiding catheter (Cordis® Vista Brite Tip®; 6F; 1.75 mm ID; 90 cm) with a guide wire (Biotronik SE & Co KG, Galeo M 014) and a flow-through cell with different hydrogel compartments at the end of the test path, representing the vessel wall. Experiments were also performed with a silicone tube (3.0 mm ID) as the vessel model to compare the results. Paclitaxel transfer into different simulated vessel walls was measured. Before balloon dilation, the guiding catheter and vessel model were flushed with 20 mL NaCl-solution (0.9%). PTX-coated balloon catheters using Cetpyrsal additive were inserted into the guiding catheter and via a guide wire, the balloon catheter was placed in the simulated vessel wall. After balloon deflation, the pump was started (flow rate 35 mL/min). The PTX concentration simulating drug wash-off (release) from the vessel model (2b) within the first crucial minute was determined by HPLC measurements. The guiding catheter was then flushed with 20 mL methanol to determine the PTX loss during insertion (1). The balloon catheter was extracted in 10 mL methanol for 30 min at 23±2 °C and then the residue on the balloon was analyzed (3). The used hydrogel after cutting into small pieces was also extracted with methanol (20 mL) for 30 min at 23±2 °C to detect the amount of transferred drug into the vessel model (2a). The entire guiding catheter was then flushed with 20 mL of 0.9% NaCl-solution in preparation of the next experiment.

In summary, the total drug load was composed of (1) PTX loss during insertion, (2) total PTX delivery upon dilation and (3) residual PTX load on the balloon. The total PTX delivery upon dilation composed of drug transfer into the hydrogel (2a) and drug wash-off (release) from the hydrogel compartment (2b) after 1 min by a simulated blood stream. The values of 1-3 should sum up to the full mass (3 µg/mm^2). For all balloon dilations the mass balance was determined. All samples were quantified by means of HPLC after a 1:2 dilution with methanol.

For poly(VEImBr) hydrogels a large amount of the methanol used for extraction was absorbed by the hydrogel compartment. Therefore reproducibility of the PTX extraction was reduced and the mass balance could not be closed in all cases.

Simulated use of DCB in the vessel-simulating flow-through cell after passage through an in-vitro vessel model according to ASTM F2394-07

A standard anatomic model adapted from ASTM F2394-07, recently described in the literature as a standard procedure, was applied to simulate the implantation process of DCB [Schmidt *et al.* 2013]. The model consisted of polymethacrylate plates forming a simulated course of a coronary artery. The used guiding catheter (Cordis® Vista Brite Tip®; 6F; 1.75 mm ID; 90 cm) with a guide wire (Biotronik SE & Co KG, Galeo M 014) and the tortuous path equipped with a PTFE tube was placed in a 37 ± 2 °C heated water bath (Figure 4-17). The model was flushed with 30 mL 0.9% NaCl-solution (before use). A DCB was introduced into the guiding catheter of the model and initially placed at the end of the PTFE tube. The guiding catheter was then flushed with 30 mL 0.9% NaCl-solution to recover particles and PTX released during tracking (after introduction of the balloon, 1a). At the distal end of the test path, a hydrogel vessel model (calcium alginate or PAAm) was placed and the balloon was dilated to 7 bar and held for 1 min. The balloon was removed after deflation and extracted in 20 mL methanol for 10 min (residual PTX load on the balloon, 3) at 23±2 °C. The pump was then started (flow rate 35 mL/min) and the PTX concentration simulating the drug release in the first crucial minute was determined (drug wash-off from the vessel model, 2b). Then the used hydrogel after cutting was also extracted with methanol (20 mL) for 30 min at 23±2 °C (drug transfer into the vessel model, 2a). After balloon extraction (10 min) in methanol, the balloon was removed and the entire pathway was then finally flushed with 30 mL methanol to detect residual PTX concentration released during tracking (after removal of the balloon, 1b). Subsequently, the test path was flushed with 0.9% NaCl-solution in preparation of the next balloon dilation.

In summary, the total drug load was composed of (1) PTX loss during insertion, (2) total PTX delivery upon dilation and (3) residual PTX load on the balloon surface. The PTX loss during insertion composed of after introduction of the balloon (1a) and after removal of the balloon (1b) out of the system. The total PTX delivery upon dilation composed of drug transfer into the hydrogel (2a) and drug wash-off from the hydrogel compartment (2b) after 1 min by a simulated blood stream. The values of 1-3 should sum up to the full mass (3 µg/mm^2). For all balloon dilations the mass balance was determined. All samples were quantified by means of HPLC after a 1:2 dilution with methanol.

HPLC analysis [Petersen et al. 2013a]

Column Eurospher C18, 120 x 4 mm ID; Knauer, Germany, column temperature 23 °C, isocratic eluent PBS (5 mM, pH 3.5) – acetonitril 50-50% (v/v), flow rate 1.0 mL/min, sample volume 20 µL and UV detection at 230 nm with calibrated measurement range (0.5-20.0 mg/L).

Particle quantification

Sub visible particles (>10 µm and >25 µm) were quantified according to USP 788, Eur. Pharmacopeia via the particle counter HIAC ROYCO 9703 device (sensor model HRDL400, HACH, Loveland, Colorado, USA).

4. Results and discussion

The synthesis of novel hydrogels based on polymerized ionic liquids are described and discussed in the following section. These novel hydrogels are characterized in respect to mechanical as well as thermal properties and compared to commonly used hydrogel materials like calcium alginate and polyacrylamide. Also, an application of hydrogels as a vessel model for *in-vitro* studies of drug-coated balloons is presented.

4.1 Synthesis of novel hydrogels

In recent years, biocompatible polymers are widely used in pharmaceutical and medical applications as tissue engineering [Kuo *et al.* 2001; Lee *et al.* 2001; Dalmoro *et al.* 2012]. Hydrogels are three-dimensional cross-linked polymeric structures, which can imbibe a high amount of water of up to 90% or more [Calvert 2009; Peppas *et al.* 2012]. A range of natural and synthetic derived polymers can be used to form hydrogels for tissue engineering scaffolds. For example, alginate, agarose, chitosan, collagen, fibrin, hyaluronic acid and gelatin were selected representative natural polymers, and poly(ethylene oxide) (PEO), poly(vinyl alcohol) (PVA) and poly(acrylic acid) (PAA) are representatives of synthetic materials [Lee *et al.* 2001; Drury *et al.* 2003].

Based on the insufficient long-term stability of calcium alginate [Draget *et al.* 2005] novel hydrogel compartments were successfully synthesized by polymerization of imidazolium-based ionic liquids bearing a vinyl group with the cross-linker *N,N´*-methylenbisacrylamide (Scheme 4-1) [Bandomir *et al.* 2014].

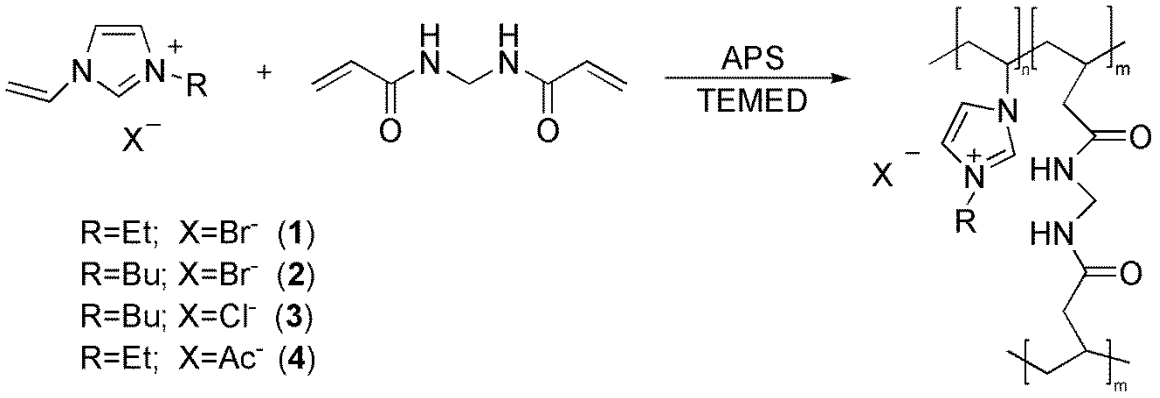

Scheme 4-1 Synthesis of polymerized ionic liquids as hydrogel materials

In a first step, the polymerization of various imidazolium-based ionic liquids [VRIm][X] was studied and the influence of alkyl chain length R and anion X^- on the gelation process was investigated. With alkyl chain length R = ethyl and anion X^- = Br, I, NO_3, BF_4, PF_6, acetate, lactate; with R = *n*-butyl and X^- = Cl, Br, I, NO_3, BF_4, PF_6, NTf_2, acetate, lactate and R = *n*-octyl and X^- = Cl, Br the possible gelation was investigated. Both anion and alkyl chain length were found to have an effect on the gelation process. In all cases iodide-, lactate- and nitrate-containing imidazolium ILs resulted in no gelation. Imidazolium ILs with $[BF_4]^-$ and $[PF_6]^-$ anions are practically insoluble in water, consequently no polymerization took place. ILs 1-4 resulted in hydrogels (1a-4a) by polymerization and they were optically transparent. The gelation time was found to be dependent on alkyl chain length ([VEIm][Br] < [VBIm][Br]) and anion size ([VEIm][Br] < [VEIm][Ac] and [VBIm][Cl] < [VEIm][Br]). Longer alkyl chain lengths had a similar effect on the polymerization process. For example, the polymerization of [VBIm][Ac] in aqueous media could not be achieved in contrast to [VEIm][Ac]. No hydrogels were obtained with octyl group due to its higher hydrophobicity. In addition to vinyl bearing imidazolium ILs we tried to generate hydrogels by polymerization of allyl-functionalized ILs (*e.g.* 1-allyl-3-methyl-imidazolium chloride, 1-allyl-3-propionnitrile-imidazolium bromide and 1-allyl-3-methyl-imidazolium dicyanamide) without success. Important properties like elasticity of the obtained hydrogels could be also influenced by varying IL to cross-linker ratio as well as water content.

4.2 Mechanical characterization

The mechanical characterization of hydrogel materials are investigated by tensile and compression tests [Bandomir *et al.* 2014]. Different parameters like cross-linker content, water content, dried and fresh hydrogels as well as storage effects in organic solvents were varied to investigate the influence on the mechanical properties.

4.2.1 Tensile tests of various fresh hydrogels

Stress-strain curves are widely used in technical studies to specify mechanical behavior like elasticity or stiffness for a range of polymers. The resulting elastic (E) modulus describes the tendency of a material to be deformed elastically when a force is applied. In general, the lower the E-modulus is, the higher the flexibility of the specimen. The stress-strain curves for PAAm and poly(VEImBr) hydrogels follow a similar trend (Figure 4-1). In contrast, alginate hydrogels demonstrate an intensive increase of stress at lower strain compared to PAAm and poly(VEImBr) hydrogels. Tested Ca-alginate hydrogels ruptured at an elongation of 53.2 ± 2.5% of their original length. The E-modulus is 1060.2 ± 167.1 Pa, which is in the range of 1 to 10 kPa, as described in literature [Pajic-Lijakovic *et al.* 2010].

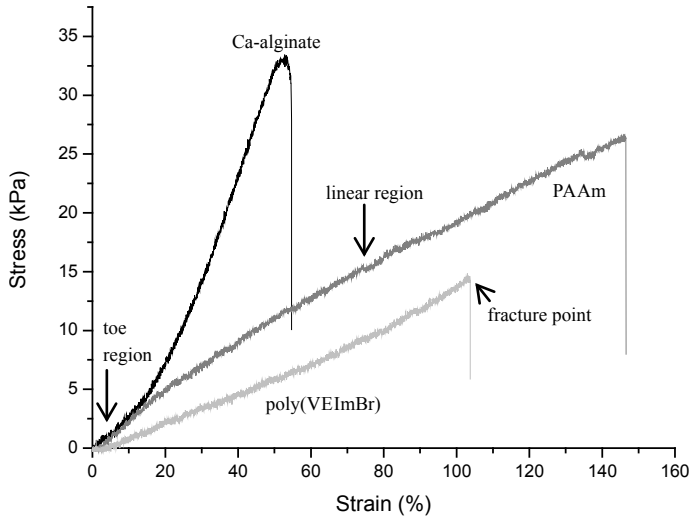

Figure 4-1 Tensile tests of various hydrogels at 22 ± 2 °C (n ≥ 3)

Brachkova *et al*. described tensile strength values for lactobacilli-loaded alginate films ranging from 23-42 kPa (E=8-23 kPa), whereas blank films exhibited smaller variations of tensile strength (44-48kPa, E=18-24 kPa) [Brachkova *et al.* 2012]. The covalently cross-linked networks showed lower E-modulus than ionically cross-linked alginate. However, the elasticity of these hydrogels showed opposite tendency. Achieved E-modulus for PAAm

(182.7 ± 8.2 Pa) and poly(VEImBr) hydrogel (132.0 ± 9.9 Pa) correspond to reported values in a range of 0.01 to 10 kPa regarding hydrogels synthesized by radical polymerization [Okay 2010; Li *et al.* 2011a; Oyen 2014]. An acrylamide concentration of 10% with bisacrylamide variations of 0.03-0.6% resulted in values for the E-modulus ranging from 4.4 to 99.7 kPa [Hazeltine *et al.* 2012]. Thus, the E-modul depends linearly on bisacrylamide concentration [Hazeltine *et al.* 2012; Oyen 2014]. The PIL hydrogel poly(VEImBr) broke at an elongation of 80.4 ± 16.7%. PAAm networks were even more elastic, stretching to 1.5 times their initial length till rupturing (136 ±10%). Despite, the maximum elongation length of poly(VEImBr) hydrogel was shorter than that of PAAm hydrogel, the E-modulus of the poly(VEImBr) hydrogel was almost the same value of the PAAm hydrogel. These results suggest that prepared PIL hydrogels are able to replace PAAm-type hydrogels.

In summary, stiffness of the prepared hydrogels were in following order: Ca-alginate > PAAm > poly(VEImBr). E-modulus as well as strain values from the investigated hydrogels based on polymerized ionic liquids are summarized in Table 4-1 (stress-strain curve only shown for poly(VEImBr)).

The synthesized hydrogel based on poly(VEImBr) showed the superior elongation compared to other PIL hydrogels. The lower the E-modulus is, the higher the flexibility of the specimen. The lowest E-modul was obtained for poly(VEImAc) hydrogels.

Table 4-1 Elastic (E) modulus, stress and strain values from different PIL hydrogels (n ≥ 3)

Hydrogel	E-modul [Pa]	Stress-at-break [kPa]	Strain-at-break [%]
Poly(VEImBr)	132.0 ± 9.9	14.6	80.4 ± 16.7
Poly(VBImBr)	64.6 ± 2.4	6.03	62.2 ± 18.4
Poly(VBImCl)	49.4 ± 6.8	4.14	65.7 ± 3.5
Poly(VEImAc)	20.3 ± 1.6	1.54	54.9 ± 14.1

4.2.2 Compression behavior of various fresh hydrogels

Compression tests were performed to complete the investigation of the mechanical behavior of synthesized hydrogels. Deformation can be used to fully characterize the mechanical stability of a material and is essential for the use in biomedical applications *e.g.* as artificial tissue. The stress-compression curves for PAAm and poly(VEImBr) hydrogels were similar. However, covalently cross-linked PAAm networks could be compressed up to 82.4 ± 1.2% (277.6 kPa), whereas with PIL based hydrogels compressions of up to 75.3 ± 0.8% were possible and stress values of 51.5 kPa were recorded (Figure 4-2).

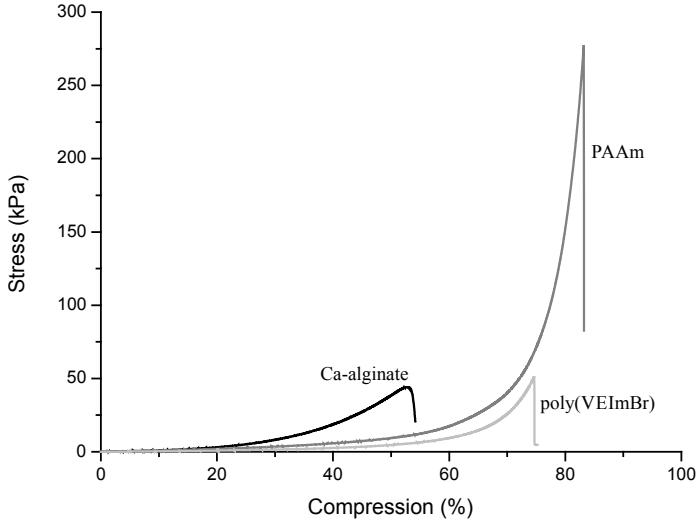

Figure 4-2 Compression curves of Ca-alginate, PAAm and poly(VEImBr) hydrogels at 22 ± 2 °C (n ≥ 3)

Literature data for the compression of PAAm hydrogels range from 300 - 1.4 MPa [Li *et al.* 2011a]. The stress value of synthesized PAAm hydrogel (8% gel concentration with 0.8% cross-linker content) was a little bit lower than the one given in literature with different gel composition [Li *et al.* 2011a]. In the initial linear region of the curve the materials follow Hooke´s law, where they deform elastically and return to their initial length when the stress is removed. The slope of this linear segment correlates to the elastic modulus [Callister *et al.* 2007]. Above a specified point the specimen will not return to its original length (rupture-fracture point). Treated Ca-alginate hydrogels were compressible up to 52.9 ± 2.3%; the half of their initial height. The stress value of Ca-alginate hydrogels was 42.5 kPa, thus lower than poly(VEImBr) hydrogels. In literature the compression modulus of alginate hydrogels ranges from less than 1 kPa to greater than 1000 kPa [Drury *et al.* 2004; Pajic-Lijakovic *et al.* 2010]. Poly(VEImBr) hydrogel was broken like the Ca-alginate hydrogel by stress values higher than

50 kPa. In summary, ionically cross-linked networks were not as compressible as covalently cross-linked networks. The compression value of poly(VEImBr) hydrogel was almost the same as PAAm hydrogel. The very favorable compressibility of PIL hydrogels is shown in Figure 4-3. As Figure 4-3c clearly shows, poly(VEImBr) gel did not break for strains up to 70% (c).

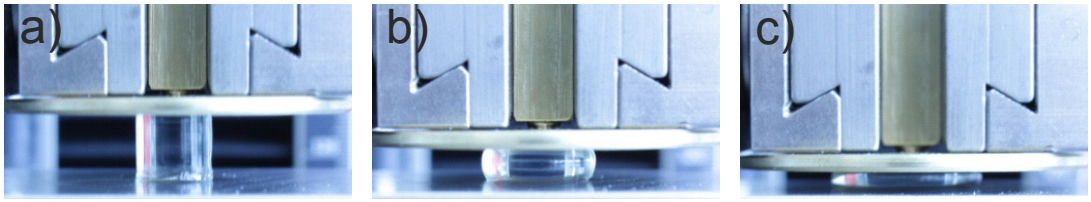

Figure 4-3 Representative picture: compression of poly(VEImBr) hydrogel: a) 0%, b) 40% and c) 70% at 22 ± 2 °C

For compression, the size of the anion as well as alkyl chain length had a noticeable influence shown in Figure 4-4a. A butyl-group resulted in similar compressibility until rupture compared to the ethyl-group with bromide as anion. Stress values showed a larger difference (poly(VBImBr): 32.9 kPa vs. poly(VEImBr) 51.5 kPa). Compared to the longer alkyl chain length on the imidazole cation, the anion is more important for the compressibility. Poly(VBImCl) (74.3 ± 1.5%) was softer then poly(VBImBr) (65.8 ± 2.0%) but the stress value differed about 1.2 kPa. Mechanical strength could be tailored by varying the content of cross-linking agent (Figure 4-4b), *e.g.* poly(VBImBr) with 0.6 mol% cross-linker (instead of 1.7 mol%) resulted in a softer hydrogel (max. stress value: 49.8 kPa, compression up to 75%) and poly(VBImCl) with lower cross-linking content (1.6 mol%) resulted in a stiffer material (max. stress value: 30.8 kPa, compression up to 68%).

Poly(VEImAc) shown a similar compression value (74.8 ± 1.8%) to poly(VEImBr) and poly(VBImCl), but the stress value was only 20.1 kPa. The mechanical behavior of poly(VEImBr) and poly(VEImAc) hydrogels was considerably different by examination of the exposed stress (*e.g.* 70% compression: 26 kPa vs. 6.7 kPa). In comparison to all synthesized PIL hydrogels poly(VEImAc) was the softest material. Size of the anion seemed to be essential for mechanical properties of hydrogels. Of equal importance for the hydrogel properties are the ratio of ionic liquid to cross-linker as well as water content. The resulting mechanical properties for poly(VEImBr) hydrogels with varying composition are summarized in Table 4-2.

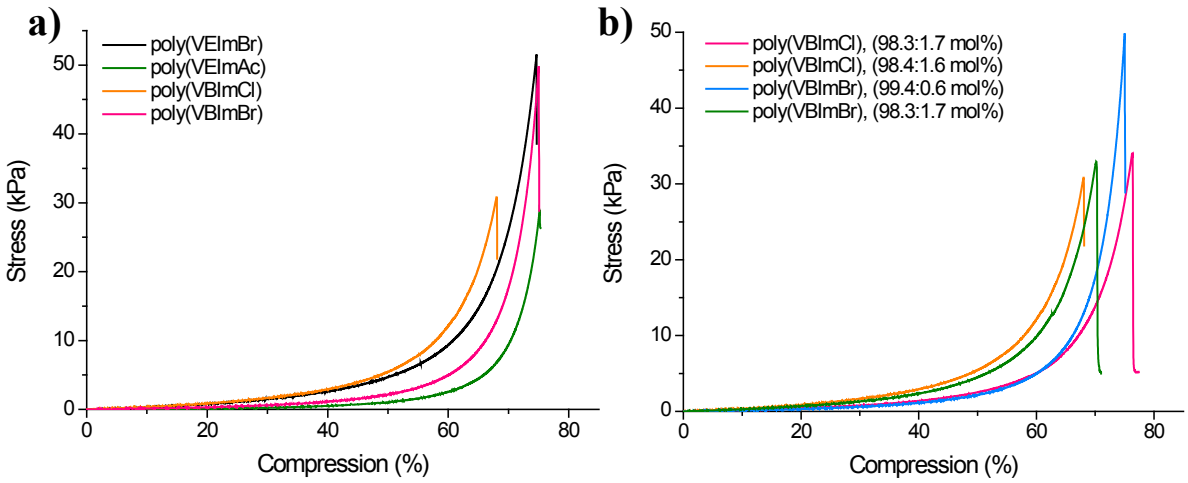

Figure 4-4 Compression curves of (**a**) various polymerized ionic liquid hydrogels; (**b**) with different IL to cross-linker ratios for poly(VBImBr) and poly(VBImCl) hydrogels at 22 ± 2 °C (n ≥ 3)

Table 4-2 Influence of water content and cross-linker (CL) ratio on mechanical behavior (compression) of poly(VEImBr) hydrogels (with composition of the hydrogels)

WC [vol%]	CL content [mol%]	V_{Water} [µL]	V_{CL} [µL]	Stress-at-break [kPa]	Strain-at-break [%]
64	1.7	1450	985	23.5	63.5 ± 2.1
69	1.7	2335	985	51.5	75.3 ± 0.8
74	1.7	3335	985	50.4	69.2 ± 4.8
69	1.4	2335	800	21.9	69.4 ± 2.1
69	1.7	2335	985	51.5	75.3 ± 0.8
69	2.1	2335	1200	33.0	63.9 ± 4.1

WC: water content; CL: cross-linker

More water in the polymer network resulted in softer hydrogels with a lower cross-linker density. Therefore, increasing water content causes less stiffness of the specimen. Lower water content resulted in rupture at a lower compression of only 65%. The higher the cross-linker ratio was, the higher the fragility of the hydrogels as they become more brittle (Figure 4-6). A bisacrylamide content of 1.7 mol% resulted in the highest compression (~75%) and stress value (52 kPa) compared to other tested cross-linker contents. In summary, all synthesized PIL hydrogels could be compressed more than 60%, more than half of their initial length. This value was much smaller for Ca-alginate hydrogels. On the other hand, for PAAm hydrogels compression up to 83% and higher stress values were achieved.

In conclusion, mechanical properties of the obtained hydrogels could be influenced by varying IL to cross-linker ratio. Commonly, an increase of the cross-link density results in stiffer hydrogel materials [Kong *et al.* 2003; Hao *et al.* 2013]. Synthesized hydrogels based on polymeric ionic liquids provide favorable flexibility, controllable by variation of the cross-linker content. Covalently cross-linked networks were more stretchable (about 80-130% of their initial length) than calcium alginate hydrogel materials (about 50%) as ionic-type network. In addition, all novel hydrogels based on polymerized ionic liquids were compressible more than 60-75%, pressing half of their initial length compared to calcium alginate hydrogels (about 50%, 42.5 kPa). However, PAAm hydrogels presented the best compression up to 83% with the highest stress value (277.6 kPa). The mechanical properties of the hydrogel materials, particularly with regard to elastic modulus, depend on the cross-linker ratio, the water content, the gelling and the storage environment, as well as the charge densities of the polymer network [Okay 2010; Pajic-Lijakovic *et al.* 2010].

The intention was to design materials that can replace hydrogels such as calcium alginate which is lack of long-term stability. The development of PILs as novel hydrogel compartments with advantageous mechanical performance should enable these materials for biomedical *in-vitro* applications. These hydrogels are able to incorporate and deliver drugs like paclitaxel or triamteren. According to this, they can be used as tissue model materials to create artificial vessel walls and as hydrogel compartments within a vessel-simulating flow-through cell for *in-vitro* study of drug release and distribution of coated medical devices such as stents or balloon catheters. For direct *in-vivo* applications such as tissue engineering scaffolds or as drug-delivery vehicles their biocompatibility has to be investigated. First, only mechanical properties were studied to evaluate these novel materials as hydrogel compartments. Thus, the biocompatibility of these materials was not important. For hydrogels, the key for their successful use in tissue engineering is the sophisticated control of the mechanical properties [Lee *et al.* 2001; Kong *et al.* 2003; Oyen 2014].

4.2.3 Drying and storage effects in different solvents on mechanical behavior of poly(VEImBr) hydrogels

Since the pioneering work of Wichterle and Lim [Wichterle *et al.* 1960], hydrogels have received tremendous interest for a wide range of applications in biomedical, pharmaceutical and related fields such as wound dressings with chitosan-based antibacterial hydrogels, as well as materials for contact lenses, drug-delivery systems and tissue engineering scaffolds [Hoffman 2001; Lee *et al.* 2001; Drury *et al.* 2003; Langer *et al.* 2003; Lu *et al.* 2014]. Often the range of application is limited by their mechanical properties [Tanaka *et al.* 2005; Varghese *et al.* 2006].

As already mentioned, mechanical characteristics depend on the gelling and storage environment, the cross-linker density, the water content as well as the charge densities of the polymer network [Tanaka *et al.* 2005; Pajic-Lijakovic *et al.* 2010; Wang *et al.* 2011]. Therefore, a couple of research groups published different techniques to enhance the mechanical properties of hydrogel materials [Li *et al.* 2013; Liu *et al.* 2013; Takemoto *et al.* 2014]. For a suited application of hydrogels the characteristics of swelling, shrinking and drying kinetics are very important. In this work, the impact of drying processes and storage effects in different solvents on the mechanical properties of poly(VEImBr) hydrogels were investigated. The importance of dehydration on the mechanical strength of poly(VEImBr) was determined using different conditions and periods of time, shown in Figure 4-5.

Three types of water have been classified in hydrophilic polymer gels: bound water (non-freezing), intermediate water (freezing interfacial) and free water [Hatakeyama *et al.* 1998]. First, due to the free water evaporation the polymer network shrinks, followed by intermediate and bound water. Here, poly(VEImBr) hydrogels showed a favorable, uniform shrinking behavior with a loss of up to 40% (after drying: 6 mm x 6 mm, see Figure 4-7) according to their initial size. The dried hydrogels exhibited an improved compressibility. While fresh poly(VEImBr) hydrogels were compressible up to 75.3 ± 0.8% (stress value: 51.5 kPa), 1-day dried hydrogels showed a higher compression (82.6 ± 2.3%) at a stress value of 200 kPa. After 4-day drying in air still no rupture was observed during compression experiments. Thus, controlled dehydration processes resulted in strengthened hydrogels with high compressibility (Table 4-3).

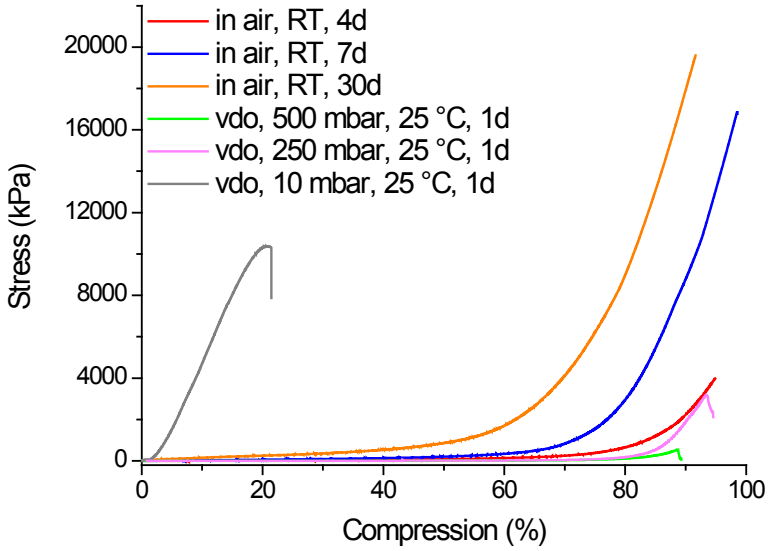

Figure 4-5 Stress-compression curves of poly(VEImBr) hydrogels dried in air at 22 ± 2 °C for various days and dried in a vacuum drying oven (VDO) at 25 °C for one day at different pressures (n = 3)

Table 4-3 Poly(VEImBr) hydrogels after drying in air at 22 ± 2 °C for several days (1, 4, 7 and 30 days) and dried in a vacuum oven at 25 °C at various pressures (10, 250 and 500 mbar)

Conditions	Rupture	Stress-at-break [MPa]	Compression-at-break [%]	Stress-at-80% compression [MPa]
1 day	Yes	0.20	82.6 ± 2.3	0.09 ± 0.003
4 days	No	-	-	0.65 ± 0.01
7 days	No	-	-	3.05 ± 0.34
30 days	No	-	-	8.63 ± 0.69
500bar	Yes	0.54	77.0 ± 12.1	-
250 mbar	Yes	4.44	94.4 ± 2.2	0.18 ± 0.02
10 mbar	Yes	10.4	15.7 ± 5.0	-

Moreover, compressed hydrogels possess beneficial elasticity and hence return to its initial shape within a few minutes (Hooke´s law). Further drying to 7 and 30 days increased the stress-at-80%-compression to 3.05 ± 0.34 MPa and 8.63 ± 0.69 MPa, respectively. 7-day-dried poly(VEImBr) hydrogels were compressible to 2% of its initial height (98%) with a tremendous stress values of 16.4 ± 0.1 MPa. These results correspond with state of the art-hydrogels used in cartilage treatment (compression stress 0.5 to 10 MPa) [Park *et al.* 2008]. In addition, poly(VEImBr) hydrogels, which were dried in a vacuum oven, showed different mechanical properties in response to various pressures (Figure 4-5). Hydrogels dried at 10 mbar were only compressible up to 15.7 ± 5.0% (stress value: 10.4 MPa), whereas a

pressure of 250 mbar facilitated the best compression of 94.4 ± 2.2% by a stress value of 4.44 MPa. Interestingly, the lowest stress value exhibit poly(VEImBr) hydrogels dried at 500 mbar (0.54 MPa), which indicates a direct relationship between applied pressure and mechanical properties. Finally, all hydrogels were ruptured and compared to hydrogels dried in air for 1-day (stress value: 200 kPa) exhibit these hydrogels higher stress values (0.54 - 10.4 MPa). The conditions during the dehydration of the hydrogel materials were crucial for the mechanical properties. The higher the surrounding humidity, the lower is the dehydration rate due to lower concentration gradients (Figure 4-5).

In analogy to poly(VEImBr) further polymerized ionic liquid hydrogels (poly(VBImBr) and poly(VBImCl)) were investigated. The hydrogels were dried in air (7-days) and compressed for mechanical stability-characterization (Figure 4-6). Without considerable differences in shrinking rates of (1) poly(VEImBr), (2) poly(VBImBr) and (3) poly(VBImCl) hydrogels (see Figure 4-7) showed no rupture due to compressive load and the stress-compression curves for (1) and (2) hydrogels are similar. However, dried hydrogels of (3) were softer and possess less mechanical strength (7.8 ± 0.9 MPa by 98% compression) compared to (1) with a stress value of 16.4 ± 0.1 MPa and to (2) with 14.1 ± 1.0 MPa (compressed both 98%).

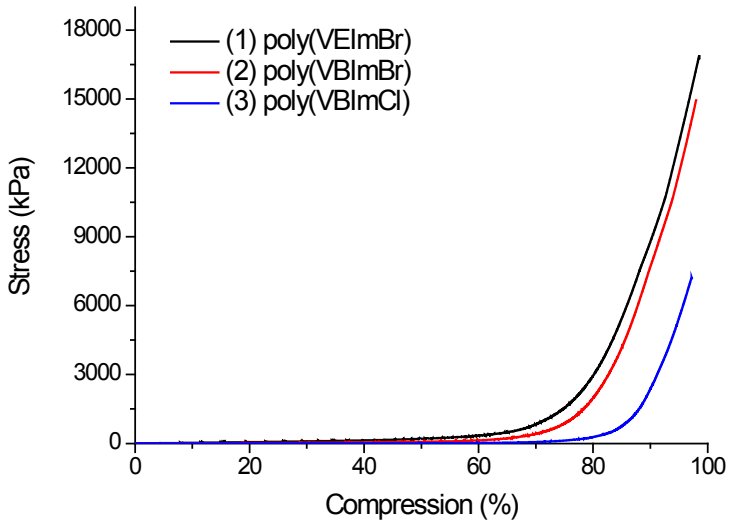

Figure 4-6 Stress-compression curves of different hydrogels based on polymerized ionic liquids (poly(VEImBr), poly(VBImBr) and poly(VBImCl)) dried in air at 22 ± 2 °C for 7 d (n = 3)

Luong *et al*. reported drying effects of poly(ethylene glycol) hydrogels on the mechanical properties (compression and tensile tests) [Luong *et al.* 2013]. Considerable changes in the compression values only occurred for selected processed hydrogels of PEG, thus no selected trend were achieved.

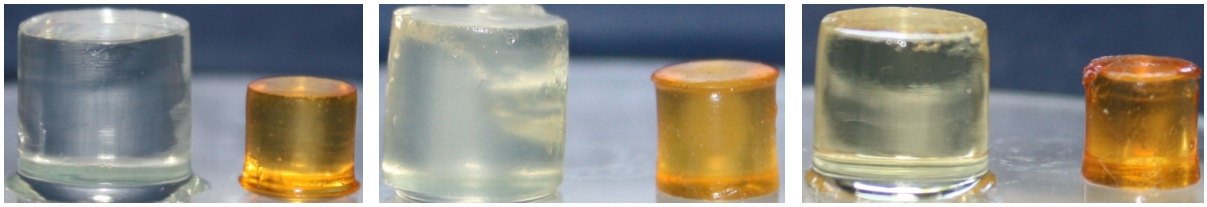

Poly(VEImBr) Poly(VBImBr) Poly(VBImCl)

Figure 4-7 Representative pictures of fresh and shrunken hydrogels of polymerized ionic liquids (poly(VEImBr), poly(VBImBr) and poly(VBImCl); hydrogels *left* – fresh, hydrogel *right* – dried (96 h)

A further improvement of the mechanical properties is possible with the addition of a copolymer [Qiu *et al.* 2003; Way *et al.* 2014]. In case of poly(VEImBr), the influence of a further component, other ILs, was evaluated by exchange of water before gelling. Compared to (1) hydrogels without IL addition (stress value: 51.5 kPa, compressible up to 75.3 ± 0.8%) stiffer gels were achieved when water is replaced by the IL 1-ethyl-3-methyl-imidazolium acetate (26.1 kPa, 56.1 ± 8.0%). The IL AMMOENG™ 110 resulted on the other hand in softer gels (79.1 ± 0.2%, 49.6 kPa).

The dried PIL hydrogels show another color than the fresh ones in contrast to PAAm hydrogels (Figure 4-7). They are in fresh and dried condition a colorless material. The Ca-alginate hydrogels are also darker when they are dried (yellow to brown).

Focussing on the mechanical properties of hydrogels, the storage effects in different solvents were investigated. Here, poly(VEImBr) hydrogels were dried in air (9-days), stored in various solvents (1-day) and subsequently characterized by compression (Figure 4-8, Table 4-4).

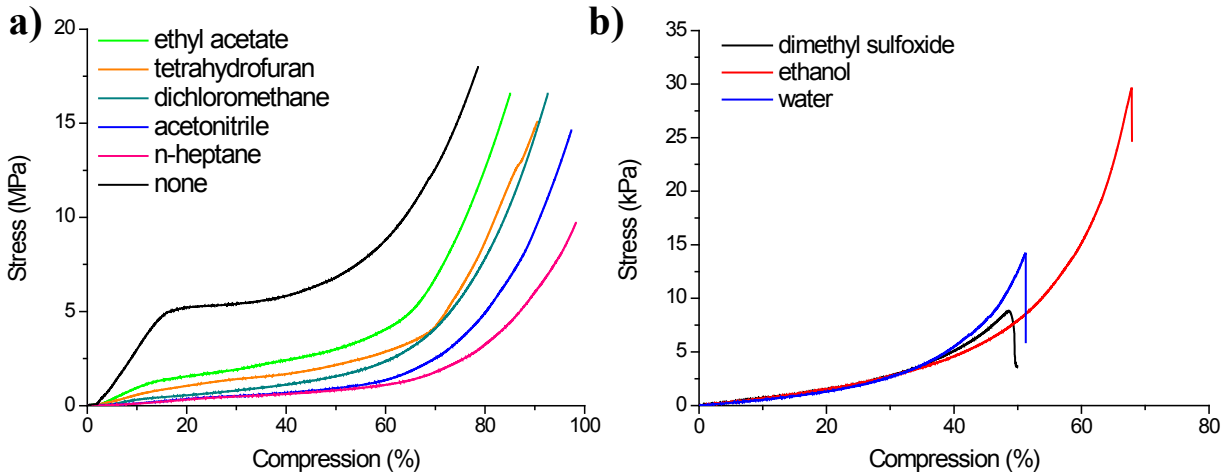

Figure 4-8 Stress-compression curves of poly(VEImBr) hydrogels: **a**) dried in air at 22 ± 2 °C for 9-days and subsequently stored in the respective solvent for 1-day (stress in MPa); **b**) dried in air at 22 ± 2 °C for 9-days and subsequently stored in the respective solvent for 1-day (stress in kPa) (n = 3)

Table 4-4 Storage of dried poly(VEImBr) hydrogels (9-days) in different solvents for 1-day

Solvent	Mass dried hydrogel (9-days) [g]	Mass after storage (1-day) [g]	Height [mm]	Diameter [mm]
water	0.308	5.953	16	16
dimethyl sulfoxide	0.311	n. d.	n. d.	n. d.
dichloromethane	0.317	0.317	6	6
n-heptane	0.307	0.307	6	6
ethyl acetate	0.308	0.294	6	6
tetrahydrofuran	0.316	0.303	6	6
ethanol	0.306	0.764	7	7
acetonitrile	0.314	0.305	6	6

n. d.: not determinable

In general, the transport of solutes through hydrogels and into surrounded media is based on diffusion, as long as the hydrogel is in an equilibrium swelling state [Peppas *et al.* 2012]. In contrast to this, the diffusion through a pure polymer network is influenced by various parameters, including solute size and shape, free volume in the polymer matrix and general polymer properties, *e.g.* stiffness, polarity and morphology. The cross-linking ratio, the polymer-solvent compatibility and the chemical structure of the polymer are other important factors that affect the swelling ratio of such compounds [Peppas *et al.* 2012; Thakur *et al.*

2012]. Macroscopically, the Fick´s first and second law describe the solute diffusion [Peppas *et al.* 2000; Peppas *et al.* 2012]. Dried hydrogels exhibit no noticeable swelling due to the storage in (non-) polar aprotic solvents such as ethyl acetate, tetrahydrofuran, acetonitrile or n-heptane. However, all treated poly(VEImBr) hydrogels were compressible above 80% at very high stress values (Figure 4-8a in MPa). Only the swelling in water after drying of the hydrogel resulted in a rupture at a compression of only 47.5 ± 4.8% at a stress value of 14.2 kPa. Interestingly, water swollen poly(VEImBr) hydrogels (swell up to 132% of their initial shape after drying) show less mechanical properties. In accordance with literature, the mechanical strength decrease with an increased swelling of the hydrogel [Gupta *et al.* 2012]. Considerable swelling of dehydrated poly(VEImBr) hydrogels were also achieved by addition of polar solvents such as ethanol (swell + 56%, compression: 65.9 ± 2.0%, stress value: 29.6 kPa) and dimethyl sulfoxide (swell + 66%, compression: 41.0 ±6.6%, stress value: 8.8 kPa). Thus, the swelling ratio is clearly correlated to polarity and also viscosity of the applied solvent, as shown by Baumberger *et al*. [Baumberger *et al.* 2006]. The used organic solvents show differences according to re-swelling with respect to the mechanical stability (Figure 4-8).

The dried hydrogels, which were stored in dimethyl sulfoxide were broken (Table 4-4). Swelling of the hydrogels was too high and these hydrogels were not stable. After 6 months of drying a reversible swelling in water is possible. Dried hydrogels swell in ethanol and show no change in solvents like dichloromethane, n-heptane, ethyl acetate, tetrahydrofuran as well as acetonitrile.

Moreover, freshly synthesized poly(VEImBr) hydrogels were stored in the same solvents (1-day) and subsequently characterized by compression to compare their swelling behavior to those of previously dried ones (Figure 4-9, Table 4-4).

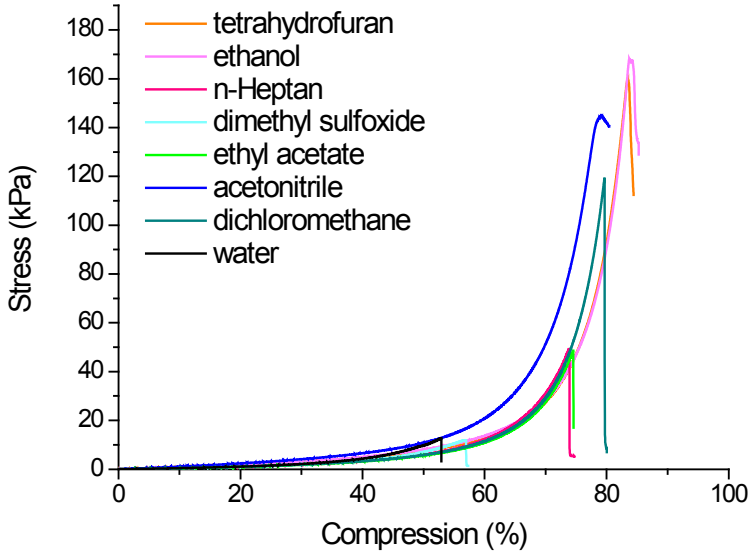

Figure 4-9 Stress-compression curves of fresh poly(VEImBr) hydrogels stored in different solvents for 1-day (n = 3)

Compared to the obtained values of previously dried poly(VEImBr) hydrogels, less swelling occurred using fresh hydrogels because of the higher initial water content of 69%. As Figure 4-9 clearly shows that fresh poly(VEImBr) hydrogels become stiffer in different solvents at considerably lower stress values compared to originally dried hydrogels. However poly(VEImBr) hydrogels stored in acetonitrile and tetrahydrofuran exhibit high stress values (above 140 kPa), while a storage in ethyl acetate and n-heptane facilitated similar compression and stress values. Furthermore, the incorporation of high loadings of water or dimethyl sulfoxide resulted in hydrogels with lower stiffness compared to fresh poly(VEImBr) hydrogels. However, the storage in immiscible or hardly water-miscible solvents such as n-heptane or ethyl acetate resulted in similar stress-compression curves in comparison with untreated, fresh poly(VEImBr) hydrogels including corresponding points of rupture.

Important characteristics like viscosity and density of the used solvents are listed in Table 4-5.

Table 4-5 Mechanical characteristics of fresh poly(VEImBr) hydrogels stored in different solvents for 1-day (n = 3)

Solvent	M_w [g/mol]	Viscosity [mPa s]	Density [g/cm^{-3}]	Dielectric constant	Miscibility in water [%]	Mass fresh gel [g]	Mass after storage [g]	Height, Diameter [mm]	Stress-at-break [kPa]	Compression-at-break [%]
None	n.a.	n.a.	n.a.	n.a.	n.a.	0.863	-	10, 10	51.5	75.3 ± 0.8
water	18.0	1.00	1.00	80	100	0.866	4.456	16, 16	12.7	50.8 ± 1.9
DMSO	78.1	2.24	1.10	47	100	0.847	2.961	15, 15	11.9	51.2 ± 6.2
DCM	84.9	0.43	1.33	9.1	1.60	0.864	0.708	8, 9	119	67.8 ± 13.6
n-Heptane	100	0.42	0.68	1.8	$3 \cdot 10^{-4}$	0.864	0.838	9.5, 9.5	49.7	67.6 ± 6.2
EtOAc	88.1	0.46	0.90	6.0	8.70	0.874	0.501	7, 7	17.0	66.6 ± 7.4
THF	72.1	0.55	0.89	7.5	100	0.831	0.409	7, 7	112	82.2 ± 2.2
ethanol	46.1	1.21	0.82	30	100	0.866	0.449	8, 8	141	84.7 ± 1.8
ACN	41.1	0.37	0.79	37	100	0.888	0.233	6, 6	145	79.1 ± 0.7

M_w: molecular weight; n. a.: not available; DMSO: dimethyl sulfoxide; DCM: dichloromethane; EtOAc: ethyl acetate; THF: tetrahydrofuran; ACN: acetonitrile

Hence, in contrast to dried hydrogels non-polar solvents cause no remarkable effects on the mechanical properties of fresh poly(VEImBr) hydrogels and qualify them as a potential media for the storage of fresh poly(VEImBr) hydrogels. Fresh hydrogels also slightly shrunk in n-heptane and ethyl acetate, −1.8% and −5.3%, respectively. During the storage of freshly gelled poly(VEImBr) hydrogels in tetrahydrofuran, acetonitrile or ethanol larger hydrogel shrinkage (−30%) associated with higher stress values and improved compressibility were achieved. A major exception is water since no significant difference was found (first dried and stored in water vs. freshly stored in water).

In conclusion, dried hydrogels showed no obvious swelling due to the addition of (non-)polar aprotic solvents such as ethyl acetate, tetrahydrofuran, dichloromethane, acetonitrile and n-heptane. However, all treated poly(VEImBr) hydrogels can become softer after solvent exchange or feasible mixing, and no crack was formed (stress value in the level of MPa). Noticeable swelling of dehydrated poly(VEImBr) hydrogels can be obtained by adding polar solvents like ethanol, dimethyl sulfoxide or water. Thus, the hydrogels were compressible in the range of 50-66% at stress values lower than 35 kPa. According to published reports the mechanical strength decreases with a rise in swelling [Butler *et al.* 2006; Gupta *et al.* 2012]. Lizawa *et al*. reported that the swelling rate became higher with increasing cross-linker content in case of poly(*N*-isopropylacrylamide) gel beads [Lizawa *et al.* 2007]. Thus, there exists a dependency between the cross-linker content and swelling behavior of the hydrogels [Okay 2010].

The absorption of high amounts of water or dimethyl sulfoxide resulted in hydrogels with lower compressibility. However, the addition of solvents such as dichloromethane, ethyl acetate or n-heptane to the fresh hydrogels resulted in similar stress-compression curves. Thus, non-polar solvents do not affect the mechanical properties and are suitable for hydrogel storage. On the other hand, fresh hydrogels in tetrahydrofuran, ethanol or acetonitrile showed greater hydrogel shrinkage related with higher stress values (2 to 3-fold) and enhanced compressibility (about 80%). This study enables a design and control of the mechanical characteristics of the hydrogels based on PILs which are important for biomedical applications.

4.3 Water exchange of fresh poly(VEImBr) hydrogels in different solvents

Next to mechanical investigations of fresh poly(VEImBr) hydrogels stored in different solvents Karl-Fischer-titrations were performed. The water exchange of poly(VEImBr) hydrogels in different organic solvents was investigated. Fresh poly(VEImBr) hydrogels (10 x 10 mm) were stored in different solvents (7 mL) and after certain times (up to 24 h), the water content in the solution was analyzed ($n \geq 3$). The results for five various solvents are shown in Figure 4-10. The water content of the respective solvent was taken as a reference.

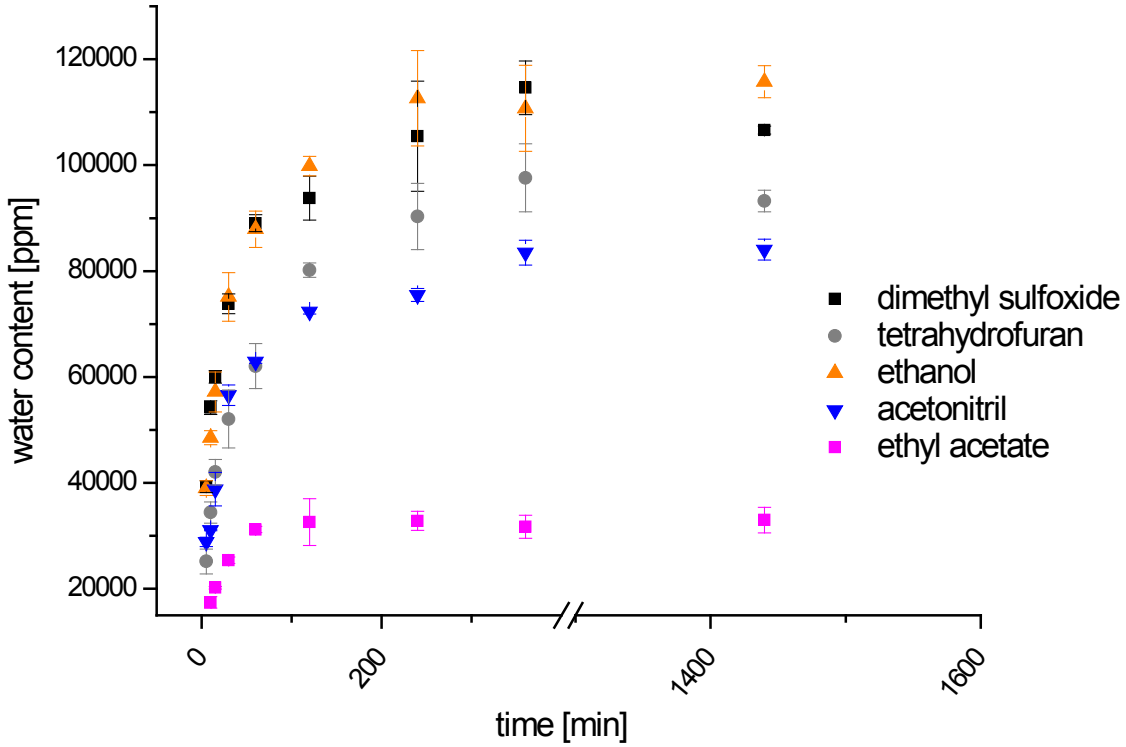

Figure 4-10 Water exchange of poly(VEImBr) hydrogels in different solvents measured with Karl-Fischer at 22 ± 2 °C

A storage of the hydrogels in ethanol and dimethyl sulfoxide resulted in the highest water content (> 100000 ppm). Thus, more water diffuses in the organic phase (solvent) compared to n-heptane (< 50 ppm) or ethyl acetate. The solvent n-heptane could be used as a storage media for the hydrogels because of the low mass loss as well as the kept size of the hydrogel during the storage. All curves show the same trend; after an increase of the water content in the organic solvent is reached an equilibrium.

The miscibility of water with n-heptane is the reason for the observed values. Water and n-heptane forms a two-phase system and because of that only a very low diffusion of water into the solvent are observed. Non-polar solvents like n-hexane or n-heptane are perfect storage media for the hydrogels. Failing this, the hydrogels are drying.

When the water content with the compression-at-break value was compared, there seems to be no direct correlation. Fresh poly(VEImBr) hydrogels stored in solvents like tetrahydrofuran or ethanol shown similar water contents (0.09 vs. 0.11%) and similar compression values (see Table 4-5, > 80%). The storage of fresh hydrogel in dimethyl sulfoxide resulted in a high water content (> 0.1%). However, these hydrogels were only compressible up to 50%. Solvents like ethyl acetate and n-heptane shown similar compression values after storage for 1-day but the water contents in the organic solvent is quite different.

4.4 Thermal characterization of hydrogels

Thermo gravimetry is commonly used to determine thermal properties of materials. Mass loss, decomposition, oxidation or loss of volatiles can be investigated [Coats *et al.* 1963]. Within this study the weight loss of different hydrogels as a function of increasing temperature was studied to evaluate the thermal stability of different hydrogel materials (Figure 4-11).

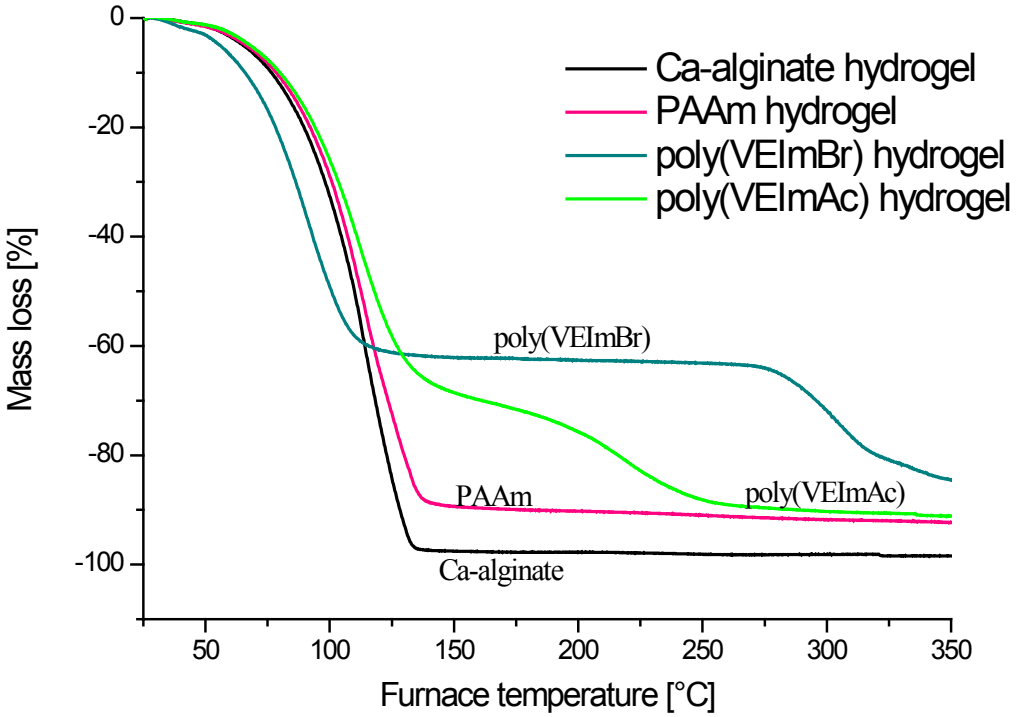

Figure 4-11 TG curves of different hydrogels: Temperature program 25 to 800 °C (heating rate 5 K·min^{-1}, furnace temperature 25 to 350 °C shown), measured under argon atmosphere

Ca-alginate hydrogel was characterized by a first mass loss of about 97%, which corresponds to a complete loss of water from the material (Table 4-6). In contrast, PAAm and IL-based hydrogels were characterized by lower initial contents of water and therefore a decreased first mass loss. Ca-alginate hydrogel fully decomposed above 120-130 °C, when water was no longer present in the network. Therefore, Ca-alginate as an ionically cross-linked network with the highest water amount had the lowest thermal stability of all hydrogels. Covalently cross-linked networks exhibited higher thermal resistance. Different to Ca-alginate hydrogels TG curves for PAAm and IL-based hydrogels showed additional mass losses. Decomposition of covalently cross-linked networks began above 190 °C. Poly(VEImAc) hydrogel had the lowest decomposition temperature (195 °C) compared to other IL- based hydrogels. TG

curves for poly(VBImBr) and poly(VBImCl) hydrogels (not shown in Figure 4-11) were similar to the depicted poly(VEImBr) hydrogel (see Table 4-6). Water losses were slightly different and indicated inferior thermal stability to the poly(VEImBr) hydrogel. Thermal suitability of PIL hydrogels seemed to be dependent on anion size ($T_{(Dec)}$: poly(VEImBr) > poly(VEImAc); $T_{(Dec)}$: poly(VBImBr) > poly(VBImCl)) as well as alkyl chain length at the imidazole cation ($T_{(Dec)}$: poly(VEImBr) > poly(VBImBr)). Due to the lower water content, polymerized IL hydrogels exhibited higher stabilities concerning thermal treatment compared to Ca-alginate hydrogels. Obtained results for the mass loss of water correspond to the initial amount of water within the polymer network. Small variances in results were caused by the fast dehydration of the hydrogel matrices.

Table 4-6 Onset points (decomposition) and peaks of various hydrogels plus first mass loss

Hydrogel	Mass loss water [%]	$T_{(Dec)}$ [°C]	Peak [°C]
Ca-alginate	97.5	n. d.	n. d.
PAAm	89.8	375	378
poly(VEImBr)	62.2	275	302
poly(VEImAc)	70.4	195	221
poly(VBImBr)	64.8	261	299
poly(VBImCl)	68.5	246	295

n. d.: not determinable

Decomposition temperatures of the polymerized ionic liquid hydrogels (**1a-4a**) were in the same order of magnitude as for ILs (**1-4**) used as starting material. Similar to the mechanical properties alkyl chain length and anion had some influence on the thermal properties, but was less pronounced. The water content had no significant effect on the decomposition temperature of the hydrogel (Figure 4-12a). Only the first mass loss for water was different in the TG curves. However, the highest thermal stability was achieved with the lowest amount of cross-linker ($T_{Dec,\ 1.4mol\%}$: 322 °C and $T_{Dec,\ 2.1mol\%}$: 273 °C, shown in Figure 4-12b).

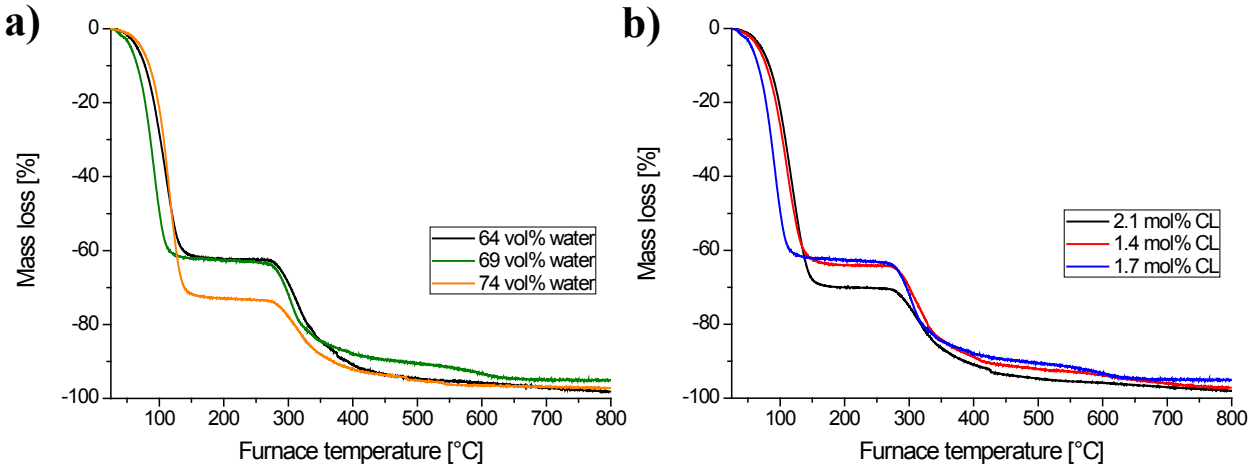

Figure 4-12 TG curves of poly(VEImBr) hydrogels with (**a**) different water content and (**b**) different cross-linker content. Temperature program 25 to 800 °C (heating rate 5 $K \cdot min^{-1}$), measured under argon atmosphere

4.5 *In-vitro* studies of drug-coated balloon catheters

In 1978 the pioneering work performed by Grüntzig introduced the percutaneous transluminal coronary angioplasty (PTCA) [Gruntzig 1978]. At a later time, the inception of stents permitted the control of elastic recoil and flow-limiting dissection [Sigwart *et al.* 1987; Kleber *et al.* 2013]. The balloon angioplasty revolutionized the coronary revascularization. However, restenosis caused by cellular proliferation and elastic recoil are disadvantages of angioplasty [Waksman *et al.* 2009]. In recent years, the paclitaxel drug-coated balloon (DCB) has been shown to be an effective technique in the prevention of restenosis in coronary and peripheral artery diseases [Scheller *et al.* 2006; Afari *et al.* 2012; Kleber *et al.* 2013].

Until now, there are only a few *in-vitro* studies presented, characterizing and describing the simulated use of drug coated balloon catheters in an *in-vitro* vessel model [Petersen *et al.* 2013a; Petersen *et al.* 2013b; Seidlitz *et al.* 2013]. In addition to pure paclitaxel (PTX) balloon catheters, different PTX formulations with additives such as urea, butyryl-tri-hexyl citrate (BTHC), iopromide and Shellac (aleuritic and shellolic acid) are commercially available. Thus, different balloon coating technologies are described in literatures [Kelsch *et al.* 2011; Loh *et al.* 2012; Krokidis *et al.* 2013]. The presence of a drug carrier plays an important role in the transfer of paclitaxel into the vessel wall from the balloon catheter [Afari *et al.* 2012]. In these *in-vitro* studies, the total drug deliveries of paclitaxel in different hydrogel compartments, acting as an artificial vessel wall, were investigated. The previously used models are far from physiological properties of the material, *e.g.* a silicone tube acts like an artery. Polymerized ionic liquids (PILs) were synthesized which are able to form hydrogels. Depending on the type of ionic liquid and degree of cross-linking the mechanical properties can be modified. In the presented study, these hydrogels were evaluated to act as vessel model and compared to known hydrogels. Next to calcium alginate as a natural hydrogel, synthetic polymers with good mechanical and long-term stability were also used.

The drug transfer into the vessel wall as well as the wash-off from the vessel model after a simulated blood stream (for one minute) was determined in a vessel-simulating flow-through cell. An adapted vessel-simulating flow-through cell of Seidlitz *et al.* was used for the *in-vitro* study of DCBs [Seidlitz *et al.* 2011]. The obtained results were compared to a silicone tube as vessel model and different hydrogel characteristics were emphasized. The aim of the work was to find out the influence of the hydrogel compartments with regard to drug transfer. The

applied balloon catheters were coated with paclitaxel using the ionic liquid cetylpyridinium salicylate (Cetpyrsal) as a novel carrier [Petersen *et al.* 2013a]. A pipetting technique was used for the coating of the balloons, resulting in a drug surface load of approx. 3 µg/mm^2. For an assessment of this study, the following values were analyzed by HPLC measurements: drug loss during insertion, total drug delivery upon dilatation (transfer into the hydrogel and wash-off from the hydrogel compartment by a simulated blood stream) and the residual load on the balloon catheter surface.

4.5.1 Balloon coating

Coating the balloon with a mixture of paclitaxel and IL can be prepared by different methods - pipetting, dip-coating and spray-coating process. Recently, light yellow Cetpyrsal crystals were applied as pharmaceutically active ionic liquid for coating of implant material [Bica *et al.* 2010; Stein *et al.* 2012]. The pipetting process with 50 wt.% PTX resulted in the most promising coatings as drug load (Figure 4-13a). These novel paclitaxel-coated balloon catheters based on Cetpyrsal were engineered by Petersen *et al*. in 2013 [Petersen *et al.* 2013a]. Representative photographs and electron micrographs of coated balloon catheters (Cetpyrsal containing 50 wt.%, PTX) are shown in Figure 4-14. At higher PTX concentrations drug crystallization occurs (Figure 4-13c).

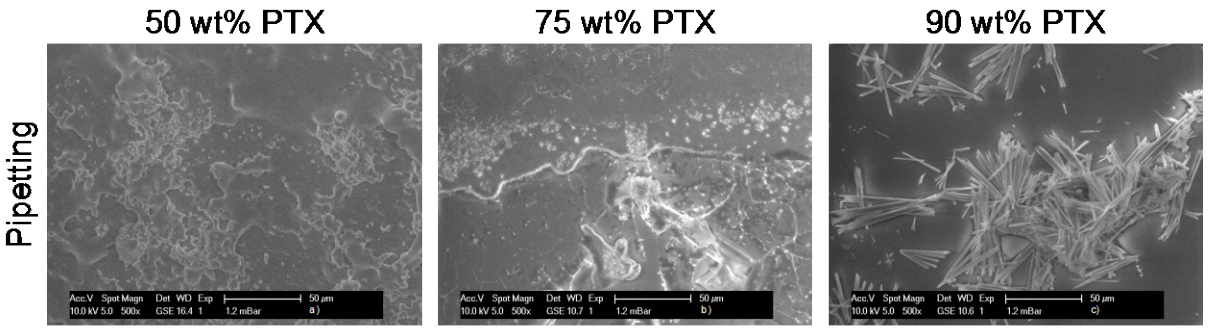

Figure 4-13 Representative ESEM micrographs of pipetted-coated Cetpyrsal on PEBAX containing 50 (**a**), 75 (**b**) and 90 wt.% (**c**) PTX each at a target drug load of 3 µg/mm^2

Coated balloon catheters in expanded and folded condition are shown in Figure 4-14 (a-d). Homogeneous coating can be applied on the balloon catheter (Figure 4-14b). The applicability of Cetpyrsal was investigated as a novel matrix for PTX-coated balloon catheter.

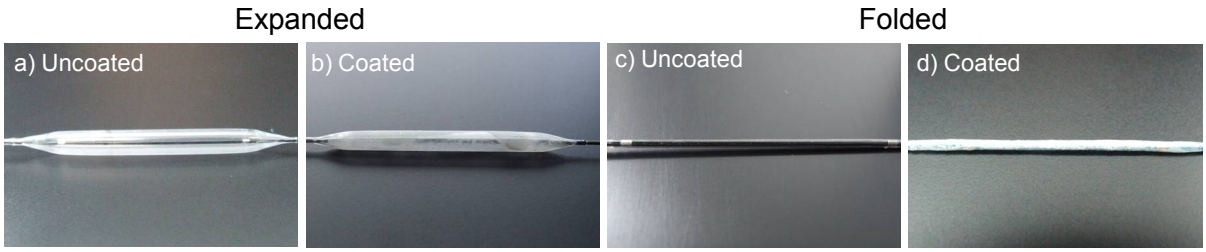

Figure 4-14 Representative photograph pictures (**a-d**) of uncoated and via pipetted coated (Cetpyrsal containing 50 wt.% PTX in a drug load of 3 µg/mm^2) balloon catheters in expanded or folded conditions

These balloon catheters were used for the *in-vitro* studies. After balloon inflation, a residual coating was still evident on the surface of the balloon. The entire load could not be transferred during balloon expansion. The residual loadings on the balloon surface were determined using HPLC measurements.

4.5.2 Comparison of different hydrogels in a flow-through cell

The first set of experiments of DCB compared different hydrogels as tissue models to evaluate drug release of PTX. Drug transfer, the retention of PTX into three different hydrogels as tissue models respectively vessel walls as well as the wash-off (release) from the hydrogel compartment within a vessel-simulating flow-through cell were investigated during balloon dilation. A PTX transfer should be examined by using different hydrogel compartments to determine the influence of the tissue model relating to the PTX transfer upon dilation. Certain properties of the used hydrogels to simulate a vessel wall such as permeability, flexibility and long-term stability of synthetic polymers (poly(VEImBr) and PAAm) are of particular importance. Calcium alginate as a natural polymer is easily accessible but has limited long-term stability. Monovalent cations such as Na^+ dissolve the network within short time. In addition, alginate hydrogels are prone to microbial contamination.

Results for various vessel models are depicted in Figure 4-15. The total drug concentration was composed of (1) PTX loss during insertion (not depicted in Figure 4-15), (2) total PTX delivery upon dilation and (3) residual load of PTX on the balloon catheter surface. The total PTX delivery upon dilation composed of drug transfer into the hydrogel (2a) and drug wash-off from the hydrogel compartment (2b) after 1 min by a simulated blood stream. In the following the results from the balloon dilations will be discussed.

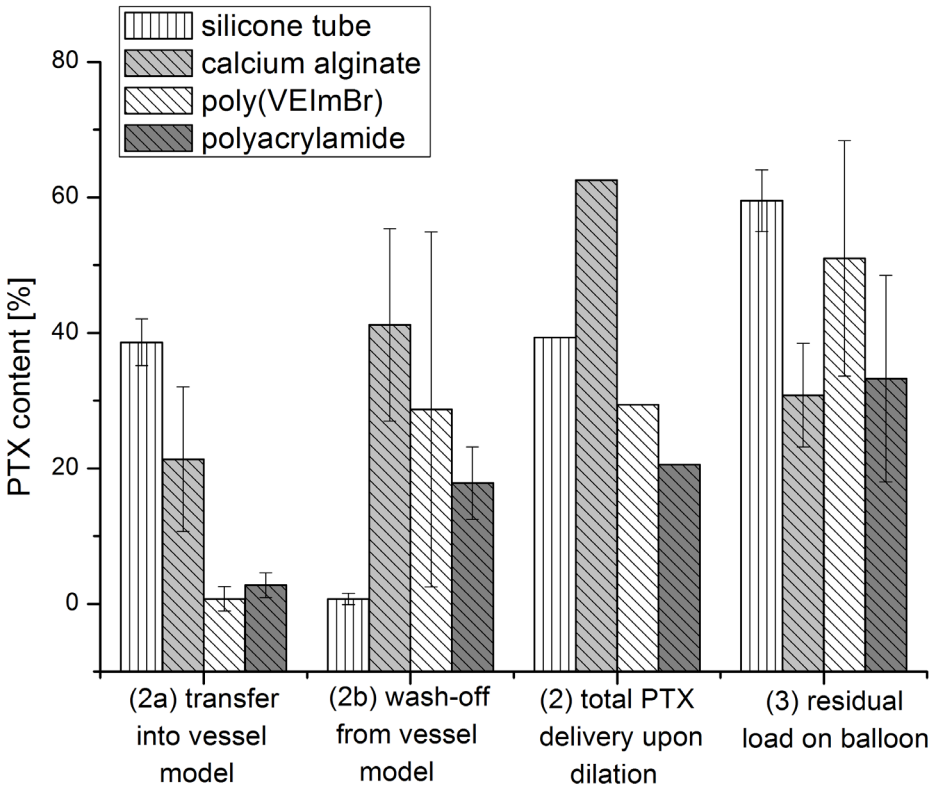

Figure 4-15 Drug transfer rates of paclitaxel for different *in-vitro* vessel models

Drug loss during insertion (1): The guiding catheter and the balloon catheters were reused several times. Also balloons of different length and thus other total load on the surface were used for the experiments. After the first six balloon dilations, the PTX loss in the guiding catheter was only 6.6 ± 3.8%. Nevertheless, the PTX loss during insertion in the last test series of the first *in-vitro* study was very high with two different guiding catheters (46.2 ± 11.6%, 1.0 ± 0.2 µg/mm^2). The reason remains unclear.

Drug transfer into the vessel model (Figure 4-15, entry 2a): The PTX transfer into the vessel models are listed in Table 4-6. Drug delivered in the silicone tube was extracted with methanol (38.6 ± 3.4%, 1.02 ± 0.03 µg/mm^2). Considerably lower PTX was delivered into

hydrogel-based vessel models. In the case of calcium alginate as the vessel wall, a PTX content in the hydrogel of 21.4 ± 10.7% (0.53 ± 0.23 µg/mm^2) was detected. Alternatively, with PAAm as the vessel wall, only 2.8 ± 1.8% (< 0.1 µg/mm^2) of PTX was transferred into the hydrogel. There are different possibilities for interpretation of the observed results. Drug transfer from coated balloons to the simulated vessel wall could occur in different ways. Paclitaxel may dissolve on contact with the hydrogel compartment and diffuse into the gel. Thus, solubility is very important for drug release and delivery. Dissolution depends on solubility of the used drug in 0.9% NaCl-solution. Liggins *et al*. published a maximum solubility of anhydrous PTX 3.59 ± 0.41 µg/mL in water after 3 h at 37 °C [Liggins *et al.* 1997]. Another report described a solubility of <0.1 µg/mL in aqueous medium, which is quite low [Konno *et al.* 2003]. Water solubility could be increased by synthesis of derivatives, under the risk of changing pharmaceutical characteristics [Khmelnitsky *et al.* 1997]. Due to very poor solubility of PTX in water, transport via dissolution and diffusion into the hydrogel is not responsible for the main transfer. Another drug transfer pathway may occur by particle transfer of PTX due to prevailing mechanical forces during balloon expansion onto the vessel wall. Over a period of one minute, a contact between the expanded balloon and simulated vessel wall is established, thus allowing transfer of PTX particles. The contact time was consistent in every case, but the inner diameter of the silicone tube (3.0 mm) was different in comparison to the artificial vessel walls (3.14 mm). Hence, the prevailing mechanical forces during balloon expansion in the silicone tube were stronger and more PTX could be transferred. To conclude, the main PTX transfer during balloon expansion occurred due to prevailing mechanical forces. Furthermore, the hydrogel characteristics were important for PTX transfer and diffusion into hydrogels [Peppas *et al.* 2012]. PAAm and poly(VEImBr) were synthetic polymers with a specific cross-linker content (poly(VEImBr): 1.7% to PAAm: 0.8% cross-linker content). On the contrary, the calcium alginate hydrogel is a natural polymer with variability in its properties. In addition to mechanical properties (flexibility) of the vessel models, different adhesion properties were present. This corresponds to different amounts of PTX wash-off from the vessel models after 1 min by a simulated blood stream (see Table 4-6 or Figure 4-16). Moreover, the diffusion of PTX into the vessel wall occurs at various rates, which may be related with the cross-linker content. This leads to PTX diffusion into synthetic polymers < 5% (poly(VEImBr) and PAAm) compared to the natural polymer of 21.4 ± 10.7%.

Drug wash-off (release) from various vessel models after 1 min (Figure 4-15, entry 2b): A drug release time of only one minute was chosen to simulate a very fast PTX transfer and wash-off. The silicone tube is a hydrophobic material and showed the least amount of wash-off (drug release) (< 1%) from the vessel model (see Table 4-7). Silicone tubes as a vessel model were not very suitable because they are not similar to physiological uptake behavior. A hydrogel is a network of polymer chains that are hydrophilic and should be more appropriate [Kim *et al.* 2014a; Kim *et al.* 2014b].

Table 4-7 Total PTX delivery upon dilation in different vessel models after simulated use in an *in-vitro* model

	Silicone tube	**Calcium alginate**	**Poly(VEImBr)**	**PAAm**
wash-off after 1 min	< 1%	41.2 ± 14.2%	28.7 ± 26.2%	17.8 ± 5.3%
transfer into vessel model	38.6 ± 3.4%	21.4 ± 10.7%	< 2%	2.8 ± 1.8%
total PTX delivery upon dilation	about 40%	about 60%	n. a.	about 20%

n. a.: not available

With a hydrogel compartment as a vessel wall, the PAAm was able to achieve the lowest wash-off quantities (17.8 ± 5.3%, 0.40 ± 0.14 µg/mm^2), compared to poly(VEImBr) (28.7 ± 26.2%) and calcium alginate (41.2 ± 14.2%, 1.15 ± 0.58 µg/mm^2). Thus, the highest drug wash-off after 1 min was achieved in case of calcium alginate as the vessel model. The simulated vessel models chosen were important for an effective drug transfer. Thus, the drug delivery characteristic is dependent on the hydrogel compartment. With poly(VEImBr) as the hydrogel compartment, some analytical problems occurred. Thus, their potential could not be fully explored. The poly(VEImBr) hydrogel show strong swelling behavior in methanol which was used to extract the drug from the hydrogel. Most of the solvent diffused into the polymer and thus the hydrogel rapidly swells. In addition, the high salinity compromised the HPLC analysis of PTX (value for drug wash-off (2b) see Table 4-6) and therefore elongated peaks in the chromatogram were difficult to integrate together with a low interpretable reproducibility of the data. This could be overcome by using other drug candidates or models showing, for example, fluorescence. In summary, the hydrogel material was crucial for the total drug delivery upon dilation (Figure 4-16). Extraction of the vessel model to analyze PTX content was done only once. Since the drug is poorly soluble in water and because of binding to tissue structures, the PTX may persist longer in the vessel wall. Calculated curves for PTX

tissue concentration as function of time are provided in the literature. Within the first hour, the concentration decreases dramatically [Ruebben *et al.* 2010].

Drug residue on the balloon (Figure 4-15, entry 3): The residual loads of PTX on the balloon catheter (3) were also determined. Extraction of the balloon in methanol resulted in the highest PTX concentration for the silicone tube (59.5 ± 4.6%, 1.6 ± 0.2 µg/mm^2) as the vessel model, meaning most of the PTX remained on the balloon surface. Only 40% of the drug could be transferred during balloon dilation. However, considerably less drug on the balloon catheter surface were analyzed in the cases of dilation in calcium alginate (30.8 ± 7.6%, 0.8 ± 0.2 µg/mm^2) and PAAm (33.2 ± 15.3%, 0.8 ± 0.4 µg/mm^2) as vessel models. Consequently, in both cases about 70% of the drug is removed from the balloon catheter.

As already mentioned, PTX is characterized by its very low solubility. The balloon catheters used here exhibit homogeneous coating due to the use of an IL as a novel additive (Cetpyrsal/PTX, 50/50, w/w). There are no needle-like crystals present on the balloon surface. Previous experiments showed that the novel additive reduced the drug loss compared to a commercially available DCB with urea-based coating [Petersen *et al.* 2013a]. For this reason, there is the possibility to deliver (transfer) more PTX during the balloon expansion and therefore we concentrated on this novel DCB. The degree of crystallization is important; Afari *et al*. published that more crystalline coatings yield higher tissue levels and biological efficacy [Afari *et al.* 2012]. In contrast, less crystalline coatings resulted in improved uniformity and less particle formation [Afari *et al.* 2012]. Heilmann *et al*. had found (via an *in-vivo* study) that the advantageous effect of a hydrophilic additive such as using iopromide for higher tissue concentrations was antagonized by increased amounts of wash-off of used coatings [Heilmann *et al.* 2010]. Drug loss is a process constituted of mechanical loss by sheath passage and collisions with the vessel wall and dissolution of the coating in the blood stream [Heilmann *et al.* 2010]. This process will be simulated using a standard anatomic model adapted from ASTM F2394-07 (described in next section). Drug adherence and loss on the way to the vessel was tested *in-vitro* by Kelsch *et al* [Kelsch et al. 2011]. Drug loss upon passage through a blood-filled hemostatic valve and guiding catheter for one minute in stirred blood at 37 °C was investigated. Urea-based DCB lost 26 ± 3% and iopromide-based DCB lost 36 ± 11% of the total amount on the balloon [Kelsch *et al.* 2011].

In conclusion for the simulated use of DCB, the total drug delivery upon dilation is different for the used hydrogels simulating the vessel wall. Calcium alginate hydrogel as the vessel model showed the highest PTX delivery upon dilation. The wash-off from the alginate hydrogel was high (drug release after 1 min by a simulated blood stream: 41.2 ± 14.2%). However, 21.4 ± 10.7% of the drug diffused into the hydrogel. The silicone tube showed the least amount of wash-off (< 1%) from the vessel model after 1 min, but it is quite different to natural vessels. Poly(VEImBr) hydrogels as vessel models were difficult to analyze. In the case of PAAm as the vessel model, only 20% of PTX could be delivered upon dilation. In summary, the mass balance for PTX with HPLC measurements was determined: silicone tube 2.65 ± 0.19 µg/mm^2; calcium alginate 2.65 ± 0.55 µg/mm^2 and PAAm 2.28 ± 0.36 µg/mm^2. These results show a recovery rate of up to 89% for calcium alginate as well as the silicone tube and 76% for PAAm of the actual initial load (3 µg/mm^2).

4.5.3 Simulated use of DCB in the vessel-simulating flow-through cell after passage through an *in-vitro* vessel model according to ASTM F2394-07

In order to simulate the implantation process, the vessel-simulating flow-through cell was combined with a model coronary artery pathway to estimate drug loss and transfer as well as particle release (Figure 4-16). Cetpyrsal-based DCBs were manually advanced through a tortuous vessel path, consisting of a guiding catheter with a guide wire. Calcium alginate and polyacrylamide hydrogels were used as tissue models for the simulated use in an *in-vitro* model (Figure 4-17). The obtained results can be compared with the data from Petersen *et al*. [Petersen *et al.* 2013a]. In their study, they also used the anatomic model according to ASTM F2394-07 with a silicone tube as the vessel model. Furthermore, Weitschies and co-workers used the anatomic model with a commercially available balloon catheter (pure PTX-coated balloon) [Seidlitz *et al.* 2013].

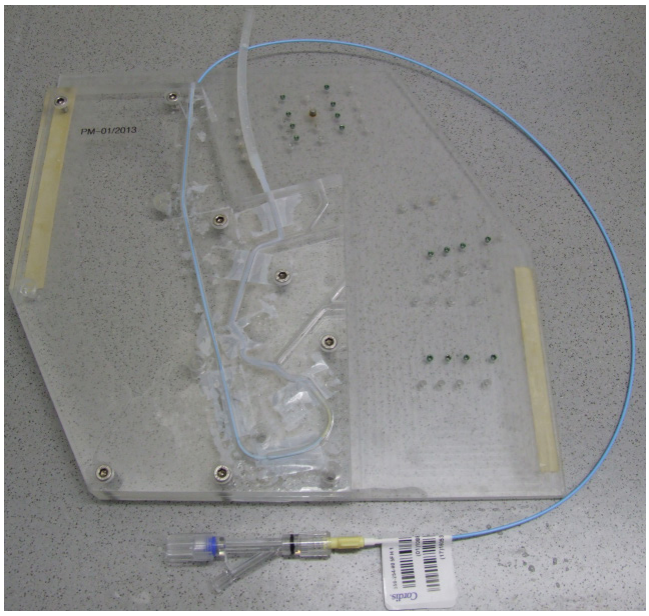

Figure 4-16 Photograph of the model coronary artery pathway

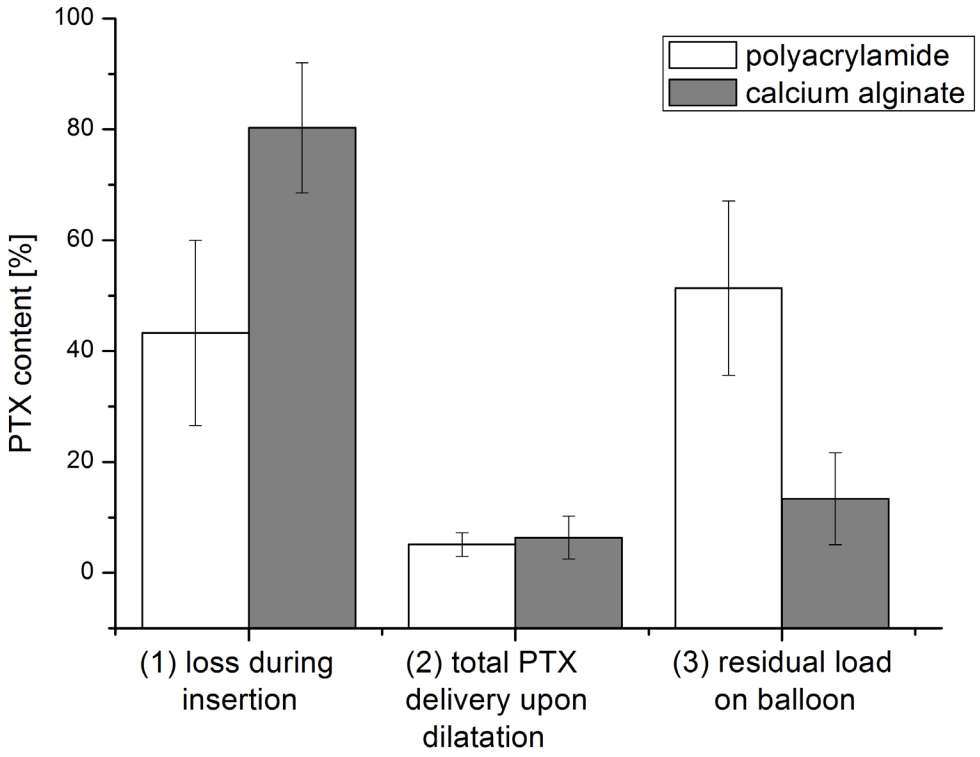

Figure 4-17 Drug loss and transfer rates after simulated anatomic passage

Drug loss during insertion (Figure 4-17, entry 1): The results show that large amounts of the coated drug (in total) were lost during the simulated artery pathway. In the case of PAAm as the vessel model (first test series), a PTX loss during insertion (1) of 43.3 ± 16.7% (1.2 ± 0.4 µg/mm^2) was determined (Figure 4-17). Considerably higher loss was ascertained in the second test series with calcium alginate as the vessel model (1.8 ± 0.7 µg/mm^2). This corresponds to a PTX loss of 80.3 ± 11.7%. The guiding catheter as well as the balloons was used several times. Also different balloon sizes were applied for the experiments. In contrast to the *in-vitro* study without an artery pathway considerably more drug was lost. Higher loss was to be expected because of simulation of the anatomic implantation process. Petersen *et al*. have published somewhat lower losses of PTX during the track of an average 30 – 40% [Petersen *et al.* 2013a]. In their *in-vitro* study they compared DCB coated in expanded and folded condition, but a other guiding (Cordis® Vista Brite Tip®; 5F; 1.4 mm ID; 100 cm) catheter as well as PEBAX balloons were used. Therefore, different conditions may be the reason for the observed difference.

Total PTX delivery upon dilation (Figure 4-17, entry 2): Only small transferred fractions were observed for both vessel models after passage of the balloon catheter through a simulated anatomic model. In the case of PAAm, a total PTX delivery upon dilation of 5.1 ± 2.1% (0.14 ±0.06 µg/mm^2) was achieved. Similar transfer rates for PTX upon dilation were detected with calcium alginate as the vessel model (6.4 ± 3.8%, (0.13 ±0.07 µg/mm^2). As before, a short wash-off time (drug release after one minute) was chosen to simulate the drug behavior after pass through the tracking model. With PAAm as the vessel model, a PTX content of 1.7 ± 0.7% could be detected in the wash-off solution. A similar value for calcium alginate as the vessel model was found (PTX content of 2.0 ± 1.1%) as wash-off from the hydrogel in the first minute. The PTX transfer into the hydrogel compartment was slightly higher (PAAm: of 3.4 ± 1.9%; calcium alginate: of 4.3 ± 2.8%). Thus, the drug diffused into the vessel model or adhered on the vessel wall and was not released in one minute into the medium. However, the total PTX delivery upon dilation was similar for two different vessel models after the simulated implantation process. Petersen *et al*. transferred more PTX in the silicone tube (up to 40%) with a PTX-Cetpyrsal balloon catheter (50:50, w/w) coated in a folded condition. With the balloon coated in an expanded condition, the PTX transfer in the silicone tube was lower (5-15%) [Petersen *et al.* 2013a]. Here, the used balloon catheters were coated in an expanded condition. Seidlitz *et al*. used pure PTX-coated balloons and showed PTX transfer rates to gel below 1% (calcium alginate as vessel model) [Seidlitz *et al.* 2013]. In their study, they also used a model of a coronary artery pathway to investigate drug loss and drug transfer to the gel. However, in our study with the novel DCB coating more PTX was delivered upon dilation (calcium alginate: 6.4 ± 3.8% compared to below 1%). In conclusion, the PTX transfer upon dilation depends on the coating of the balloon and the used vessel model simulating the vessel wall.

Drug residue on the balloon (Figure 4-17, entry 3): Extraction of the balloon catheter in methanol resulted in a PTX content of 1.38 ± 0.46 µg/mm^2 with PAAm as the vessel model (Figure 4-18). Consequently, there was still 51.4 ± 15.7% PTX remaining on the balloon surface and about 50% of the drug is removed from the balloon catheter. However, expansion of the balloon in calcium alginate yielded only 0.27 ± 0.14 µg/mm^2 PTX residue on the balloon (13.3 ± 8.3%). The balloon was almost completely unloaded. From the total loading (approx. 3 µg/mm^2), the following values were recovered to evaluate the mass balance of PTX: using PAAm as the vessel model, 2.67 ± 0.06 µg/mm^2 (89%), and with calcium

alginate, 2.23 ± 0.49 µg/mm^2 (74%). Also here, the mass balance shows reproducible values for PTX.

Particle quantification: In addition to drug loss and transfer, particle measurements (>10 µm, >25 µm) were performed after track and dilation of the balloon (Table 4-8). These size limits (>10 µm, >25 µm) are assumed from the evaluation of surface and coating damage of stent delivery catheter. The estimated mechanism from DCB involves the delivery of particles to the inner lumen of coronary arteries, the release of particles or coating fragments in the coronary arteries. Complications are occlusions of small vessels or capillaries [Cortese *et al.* 2012; Schmidt *et al.* 2013].

Table 4-8 Particle quantification

	PAAm >10 µm	**PAAm >25 µm**	**Calcium alginate >10 µm**	**Calcium alginate >25 µm**
after track	230 ± 126	33 ± 16	580 ± 308	56 ± 27
after expansion	4 ± 1	1 ± 1	9 ± 1	1 ± 1
sum	234 ± 127	34 ± 17	589 ± 309	57 ± 28

Quantified particles are mainly PTX particles because Cetpyrsal does not form any ascertainable particles in aqueous solution under used conditions. The number of particles correlates with drug losses during track. Using calcium alginate as the vessel model, a PTX loss of approx. 80% was determined and at total of 589 ± 309 particles (>10 µm) per mm^2 were generated. Contained particles >25 µm per mm^2 were detected in a ratio of 1:10 (57 ± 28). In contrast to lower loss of PTX in the track model, the expected sum of particles was decreased (234 ± 127 (>10 µm) per mm^2, 34 ± 7 (>25 µm) per mm^2 balloon surface). Petersen *et al*. described that DCB based on Cetpyrsal generated a lower quantity of particles (expanded condition: 280 ± 91 particles (>10 µm) per mm^2 balloon surface) compared to commercially available DCB using a urea-based coating (329 ± 161 particles (>10 µm) per mm^2 balloon surface) [Petersen *et al.* 2013a]. Amounts of particles generated from the PTCA balloon catheters by comparing two modified lubricous polymeric hydrogel coatings used at various thicknesses were demonstrated by Babcock *et al*. [Babcock *et al.* 2013]. [Babcock *et al.* 2013] In their study, a submicron coating (dry thickness of 0.5 µm) generates far fewer particulates than the micron coating (dry thickness of 2 µm) on the same substrate in a standard anatomic model adapted from ASTM F2394-07 [Babcock *et al.* 2013].

In conclusion, drug-coated balloon catheters are an alternative for coronary and peripheral artery disease. Based on the limited number of published results of *in-vitro* characterization of drug coated balloons, there is a need for further research. Novel PTX-coated balloons using ionic liquid Cetpyrsal as an additive for the *in-vitro* study were applied. Drug delivery upon dilation in different tissue models (calcium alginate, poly(VEImBr) and PAAm) using a vessel-simulating flow-through cell was investigated and compared to a silicone tube as the tissue model. The highest PTX delivery upon dilation was achieved with calcium alginate as the vessel model (about 60%). However, a total PTX delivery upon dilation of 20% was determined with polyacrylamide as vessel model. The used vessel models showed seemingly various adhesion properties, thus the PTX wash-off quantities during simulated blood flow were different. The silicone tube showed the lowest amount of wash-off (< 1%) from the vessel model after 1 min simulated blood stream. The highest drug wash-off (release) was achieved with calcium alginate as vessel model. Moreover, the diffusion of PTX into the vessel wall occurs at various rates, which may be related to the cross-linker content of the hydrogels. In addition to solubility and thus diffusion of PTX, the hydrogel material as well as the coating was crucial for drug transfer from the balloon into the vessel wall when compared to reported data. Furthermore, the vessel-simulating flow-through cell was combined with a model coronary artery pathway to estimate drug loss during an anatomic implantation process. Vast amounts of the coated drug were lost during a simulated artery pathway. Only a small fraction of the total loads of PTX were delivered upon dilation. Similar transfer rates for PTX upon dilation were achieved with calcium alginate and PAAm as vessel models. The crucial drug delivery (transfer) upon dilation was examined with the aid of different hydrogel materials to evaluate the *in-vitro* research. These are important data for the *in-vivo* application.

5. Summary

Four novel hydrogel materials based on polymerized ionic liquids were synthesized. These new hydrogels were characterized in respect to thermal and mechanical properties. The mechanical characterization was investigated by tensile and compression tests. All results were compared with commonly used hydrogels like calcium alginate as ionic-type network and polyacrylamide as cross-linked network. The mechanical and thermal properties of the obtained hydrogels could be influenced by varying IL to cross-linker ratio as well as water content. The synthesized novel hydrogels provide favorable flexibility, controllable by variation of the cross-linker content. Ca-alginate as ionic-type network with the highest water amount had the lowest thermal stability of all hydrogels. Covalently cross-linked networks exhibited higher thermal resistance. Furthermore, the impact of drying processes and storage effects in different solvents on the mechanical properties of poly(VEImBr) hydrogels were investigated. A gentle drying procedure of these hydrogels allows the preparation of strengthened materials with extremely high flexibility and compressibility without crack formation. Moreover, compressed hydrogels possess beneficial elasticity and hence return to its initial shape within a few minutes. Dried hydrogels exhibit no noticeable swelling due to the storage in (non-) polar aprotic solvents. Hence, in contrast to dried hydrogels non-polar solvents cause no remarkable effects on the mechanical properties of fresh poly(VEImBr) hydrogels and qualify them as a potential media for the storage of fresh poly(VEImBr) hydrogels. A major exception for the mechanical stability of poly(VEImBr) hydrogels is water since no significant difference was found (first dried and stored in water vs. freshly stored in water). The development of PILs with advantageous mechanical performance should enable these materials for biomedical *in-vitro* applications. In two *in-vitro* studies of DCBs, the drug deliveries of paclitaxel in different hydrogel compartments were investigated. The drug transfer into the vessel wall as well as the wash-off from the vessel model after a simulated blood stream was determined in a vessel-simulating flow-through cell. The hydrogel as well as the balloon coating was crucial for drug transfer from the balloon catheter into the vessel wall. The vessel-simulating flow-through cell was combined with a model coronary artery pathway to estimate drug loss during an anatomic implantation process. Vast amounts of the coated drug were lost during a simulated artery pathway. Only a small fraction of the total loads of PTX were delivered upon dilation.

6. Conclusion and outlook

Novel hydrogel materials were successfully synthesized by radical polymerization of imidazolium-based ionic liquids. The polymerization of different imidazolium-based ionic liquids [VRIm][X] was studied, and the influence of alkyl chain length R and anion X on the gelation was investigated. Also, the water and the cross-linker content were examined. Moreover, mechanical and thermal properties of these novel hydrogels based on PILs were investigated in comparison to calcium alginate as ionically and polyacrylamide as covalently cross-linked networks. Thermal stabilities of all synthesized hydrogels were proved using thermal gravimetric analysis. Covalently cross-linked hydrogels showed higher thermal stability than calcium alginate networks. The mechanical properties were studied with tensile and compression tests. Also here, the covalently cross-linked networks were more stretchable than ionically cross-linked hydrogels (calcium alginate). All novel PIL-hydrogels were compressible more than 60%. PAAm networks exhibited the best compression values (83%). In summary, mechanical characteristics of the hydrogel materials could be regulated by the cross-linker content, the gelling and the storage environment, characteristics of the polymer, as well as the water content. These new PIL-hydrogels with advantageous mechanical performance should enable these materials for biomedical *in-vitro* applications such as tissue models.

These novel hydrogels were used as tissue model to determine the drug transfer and release of drug-coated balloons. In this study, three different hydrogel compartments (calcium alginate, poly(VEImBr) and polyacrylamide) and a silicone tube as tissue models were investigated for DCB. The drug wash-off from the hydrogel compartment and the transfer into the material were analyzed using a vessel-simulating flow-through cell under a simulated blood flow. Novel paclitaxel-coated balloon catheters using ionic liquid cetylpyridinium salicylate as an additive for the *in-vitro* study were applied. The study resulted in the highest drug delivery upon dilatation with calcium alginate as the vessel model (about 60%). In case of polyacrylamide, a total drug delivery upon dilatation of 20% was analyzed. The silicone tube as a hydrophobic material exhibited the lowest amount of drug wash-off (< 1%) from the vessel model. The inserted vessel models showed various adhesion properties and consequently the paclitaxel wash-off quantities from the vessel wall were different. Furthermore, the diffusion of the used drug into the vessel wall occurs at various rates, which may be related to the cross-linker content of the hydrogel compartment. With the PIL-

hydrogel as tissue model some analytical problems occurred and thus their potential could not be fully ascertained. The hydrogels based on polymerized ionic liquids exhibited strong swelling behavior. Moreover, the high salinity impeded the HPLC analysis and no reproducibility of the data was achieved. One possibility is to use other drug candidates or models showing, for example, fluorescence. Possible drug alternatives for the *in-vitro* study are fluorescein sodium, dexamethasone, rhodamin B and triamterene. It should be noted that in addition to the solubility and thus diffusion of the drug, the hydrogel material as well as the balloon coating are crucial for the paclitaxel transfer from the balloon into the vessel wall. Further measurements could be carried out under *in-vivo* conditions (*e.g*. pig or rabbit artery) with a simulated blood flow.

Moreover, additional characterizations of the PIL-hydrogels were conducted. The drying and storage effects in different solvents on the mechanical properties of PIL hydrogel materials were investigated. Controlled dehydration processes resulted in strengthened hydrogels with extremely high compressibility without crack formation (stress values above 10 MPa). Subsequently, the hydrogels returned to the initial shape after unloading. Different drying procedures and drying times could be a suitable tool for the tune ability of mechanical strength of the PIL hydrogels. Focusing on the mechanical properties of hydrogels, the storage effects in different solvents were investigated. PILs were dried for 9-days in air, stored in various organic solvents (1-day), and subsequently loaded by compression. Moreover, freshly synthesized PILs were stored in the same solvents and loaded by compression to compare their behaviors to those of previously dried ones. Fresh PIL hydrogels became stiffer in different solvents at considerably higher stress values compared to originally dried ones. Non-polar solvents such as n-heptane caused no remarkable effects on the mechanical properties, so they can be qualified as a potential media for the storage of fresh hydrogels. During the storage in ethanol or acetonitrile, an improved compressibility was achieved. A major exception was water since no significant difference was found (first dried and stored in water vs. freshly stored in water). There existed various factors to influence the swelling, and thereby the mechanical behaviors of the used hydrogels next to the cross-linker content, *e.g*. the polarity as well as the aprotic/protic nature of the solvent, the density, the viscosity, the molecular weight and the water miscibility.

Furthermore, these novel PIL hydrogels could be used for other applications, *e.g*. enzyme immobilization, catalyst immobilization or as membranes in thin layers. The application possibilities can offer a broad potential for research in the future. Moreover, the biocompatibility of the PIL-based hydrogels must be investigated. For *in-vivo* applications, such as contact lenses, the biocompatibility is very important. Another possibility is the use of PIL hydrogels as separating gel for the gel electrophoresis. These novel hydrogels can be suitable for the separation of proteins.

Further new PILs as hydrogels can be synthesized by using other cations (1), *e.g*. vinyl-triazolium monomers, vinyl-benzyl-ammonium monomers or vinyl-methacrylate monomers, polymerization of zwitterionic-type ILs (2) or use of polymerizable anionic-type IL monomers (3). In addition, different cross-linkers can provide special properties and are worth future study, *e.g*. acrylic acid, polyethylene glycol diacrylate or (ethylene glycol) divinyl ether.

7. References

[Adzima *et al.* 2014] Adzima, B. J., Taylor, S. C., He, H., Luebke, D. R., Matyjaszewski, K. and Nulwala, H. B. (2014). Vinyl-triazolium monomers: Versatile and new class of radically polymerizable ionic monomers. *J. Polym. Sci. Part A: Polym. Chem.* 52(3): 417-423.

[Afari *et al.* 2012] Afari, M. and Granada, J. (2012). Mechanisms of action in drug-coated Balloons. *Endovascular Today August*: 53-58.

[Ahmed 2013] Ahmed, E. M. (2013). Hydrogel: Preparation, characterization, and applications. *J. Adv. Res.*(0).

[Andersen *et al.* 2012] Andersen, T., Strand, B. L., Formo, K., Alsberg, E. and Christensen, B. E. (2012). Alginates as biomaterials in tissue engineering. Carbohydrate Chemistry: Volume 37**:** 227-258.

[Babcock *et al.* 2013] Babcock, D. E., Hergenrother, R. W., Craig, D. A., Kolodgie, F. D. and Virmani, R. (2013). In vivo distribution of particulate matter from coated angioplasty balloon catheters. *Biomaterials* 34(13): 3196-3205.

[Bait *et al.* 2013] Bait, N., Grassl, B., Benaboura, A. and Derail, C. (2013). Tailoring the adhesion properties of polyacrylamide-based hydrogels. Application for skin contact. *J. Adhes. Sci.Technol.* 27(9): 1032-1047.

[Bajpai *et al.* 1991] Bajpai, U. D. N. and Bajpai, A. K. (1991). Determination of cohesive energy density of polyacrylamide by swelling measurements. *J. Appl. Polym. Sci.* 43(12): 2279-2281.

[Bandomir *et al.* 2014] Bandomir, J., Schulz, A., Taguchi, S., Schmitt, L., Ohno, H., Sternberg, K., Schmitz, K.-P. and Kragl, U. (2014). Synthesis and Characterization of Polymerized Ionic Liquids: Mechanical and Thermal Properties of a Novel Type of Hydrogels. *Macromol. Chem. Phys.* 215(8): 716-724.

[Bara *et al.* 2008a] Bara, J. E., Gabriel, C. J., Hatakeyama, E. S., Carlisle, T. K., Lessmann, S., Noble, R. D. and Gin, D. L. (2008a). Improving CO2 selectivity in polymerized room-temperature ionic liquid gas separation membranes through incorporation of polar substituents. *J. Membr. Sci.* 321(1): 3-7.

[Bara *et al.* 2008b] Bara, J. E., Hatakeyama, E. S., Gin, D. L. and Noble, R. D. (2008b). Improving CO2 permeability in polymerized room-temperature ionic liquid gas separation membranes through the formation of a solid composite with a room-temperature ionic liquid. *Polym. Adv. Technol.* 19(10): 1415-1420.

[Baumberger *et al.* 2006] Baumberger, T., Caroli, C. and Martina, D. (2006). Solvent control of crack dynamics in a reversible hydrogel. *Nat. Mater.* 5(7): 552-555.

[Becker *et al.* 2001] Becker, T. A., Kipke, D. R. and Brandon, T. (2001). Calcium alginate gel: A biocompatible and mechanically stable polymer for endovascular embolization. *J. Biomed. Materials Res.* 54(1): 76-86.

[Belkacemi *et al.* 2011] Belkacemi, A., Agostoni, P., Voskuil, M., Doevendans, P. and Stella, P. (2011). Drug-eluting Balloons in Coronary Artery Disease - Current and Future Perspectives. *Interv. Cardiol.* 6: 157-160.

[Bica *et al.* 2010] Bica, K., Rijksen, C., Nieuwenhuyzen, M. and Rogers, R. D. (2010). In search of pure liquid salt forms of aspirin: ionic liquid approaches with acetylsalicylic acid and salicylic acid. *Phys. Chem. Chem. Phys.* 12(8): 2011-2017.

[Bindu *et al.* 2012] Bindu, S. M., V, A. and chatterjee, A. (2012). As A Review on Hydrogels as Drug Delivery in the Pharmaceutical Field. *Int. J. Pharm. and Chem. Sci.* 1(2): 642-661.

[Brachkova *et al.* 2012] Brachkova, M. I., Duarte, A. and Pinto, J. F. (2012). Alginate Films Containing Viable Lactobacillus Plantarum: Preparation and In Vitro Evaluation. *AAPS PharmSciTech* 13(2): 357-363.

[Butler *et al.* 2006] Butler, M. F., Clark, A. H. and Adams, S. (2006). Swelling and Mechanical Properties of Biopolymer Hydrogels Containing Chitosan and Bovine Serum Albumin. *Biomacromolecules* 7(11): 2961-2970.

[Callister *et al.* 2007] Callister, W. D. and Rethwisch, D. G. (2007). Materials Science and Engineering: an Introduction. NJ, John Wiley & Sons.

[Calvert 2009] Calvert, P. (2009). Hydrogels for Soft Machines. *Adv. Mater.* 21(7): 743-756.

[Cardiano *et al.* 2008] Cardiano, P., Mineo, P. G., Neri, F., Lo Schiavo, S. and Piraino, P. (2008). A new application of ionic liquids: hydrophobic properties of tetraalkylammonium-based poly(ionic liquid)s. *J. Mater. Chem.* 18(11): 1253-1260.

[Carrasco *et al.* 2011] Carrasco, P. M., Ruiz de Luzuriaga, A., Constantinou, M., Georgopanos, P., Rangou, S., Avgeropoulos, A., Zafeiropoulos, N. E., Grande, H.-J., CabanÌ*f*ero, G. n., Mecerreyes, D. and Garcia, I. (2011). Influence of Anion Exchange in Self-Assembling of Polymeric Ionic Liquid Block Copolymers. *Macromolecules* 44(12): 4936-4941.

[Chan *et al.* 2012] Chan, B. K., Wippich, C. C., Wu, C.-J., Sivasankar, P. M. and Schmidt, G. (2012). Robust and Semi-Interpenetrating Hydrogels from Poly(ethylene glycol) and Collagen for Elastomeric Tissue Scaffolds. *Macromol. Biosci.* 12(11): 1490-1501.

[Chen *et al.* 2009] Chen, H., Choi, J.-H., Salas-de la Cruz, D., Winey, K. I. and Elabd, Y. A. (2009). Polymerized Ionic Liquids: The Effect of Random Copolymer Composition on Ion Conduction. *Macromolecules* 42(13): 4809-4816.

[Choi *et al.* 2013] Choi, U. H., Mittal, A., Price, T. L., Gibson, H. W., Runt, J. and Colby, R. H. (2013). Polymerized Ionic Liquids with Enhanced Static Dielectric Constants. *Macromolecules* 46(3): 1175-1186.

[Christensen *et al.* 2003] Christensen, L. H., Breiting, V. B., Aasted, A., Jorgensen, A. and Kebuladze, I. (2003). Long-term effects of polyacrylamide hydrogel on human breast tissue. *Plast. Reconstr. Surg.* 111(6): 1883-1890.

[Coats *et al.* 1963] Coats, A. W. and Redfern, J. P. (1963). Thermogravimetric analysis. A review. *Analyst* 88(1053): 906-924.

[Cortese *et al.* 2012] Cortese, B. and Bertoletti, A. (2012). Paclitaxel coated balloons for coronary artery interventions: A comprehensive review of preclinical and clinical data. *Int. J. Cardiol.* 161(1): 4-12.

[Dalmoro *et al.* 2012] Dalmoro, A., Barba, A. A., Lamberti, G., Grassi, M. and d'Amore, M. (2012). Pharmaceutical applications of biocompatible polymer blends containing sodium alginate. *Adv. Polym. Technol.* 31(3): 219-230.

[Darnell *et al.* 2013] Darnell, M. C., Sun, J. Y., Mehta, M., Johnson, C., Arany, P. R., Suo, Z. G. and Mooney, D. J. (2013). Performance and biocompatibility of extremely tough alginate/polyacrylamide hydrogels. *Biomaterials* 34(33): 8042-8048.

[Das 2013] Das, N. (2013). Preparation methods and properties of hydrogel: A review. *Int. J. Pharm. Pharmaceutical Sci.* 5(3): 112-117.

[Dimario *et al.* 1993] Dimario, C., Meneveau, N., Gil, R., Dejaegere, P., Defeyter, P. J., Slager, C. J., Roelandt, J. and Serruys, P. W. (1993). Maximal blood-flow velocity in severe coronary stenoses measured with a Doppler guidewire - limitations for the application of the continuity equation in the assessment of stenosis severity. *Am. J. Cardiol.* 71(14): D54-D61.

[Dinu *et al.* 2013] Dinu, M., Cazacu, M. and Dragan, E. S. (2013). Mechanical, thermal and surface properties of polyacrylamide/dextran semi-interpenetrating network hydrogels tuned by the synthesis temperature. *Cent. Eur. J. Chem.* 11(2): 248-258.

[Dinu *et al.* 2007] Dinu, M. V., Ozmen, M. M., Dragan, E. S. and Okay, O. (2007). Freezing as a path to build macroporous structures: Superfast responsive polyacrylamide hydrogels. *Polymer* 48(1): 195-204.

[Doebbelin *et al.* 2011] Doebbelin, M., Jovanovski, V., Llarena, I., Claros Marfil, L. J., Cabanero, G., Rodriguez, J. and Mecerreyes, D. (2011). Synthesis of paramagnetic polymers using ionic liquid chemistry. *Polym. Chem.* 2(6): 1275-1278.

[Donati *et al.* 2005] Donati, I., Holtan, S., Morch, Y. A., Borgogna, M. and Dentini, M. (2005). New Hypothesis on the Role of Alternating Sequences in Calcium-Alginate Gels. *Biomacromolecules* 6(2): 1031-1040.

[Draget *et al.* 2005] Draget, K. I., Smidsrød, O. and Skjåk-Bræk, G. (2005). Alginates from Algae. Biopolymers Online, Wiley-VCH Verlag GmbH & Co. KGaA.

[Drury *et al.* 2004] Drury, J. L., Dennis, R. G. and Mooney, D. J. (2004). The tensile properties of alginate hydrogels. *Biomaterials* 25(16): 3187-3199.

[Drury *et al.* 2003] Drury, J. L. and Mooney, D. J. (2003). Hydrogels for tissue engineering: scaffold design variables and applications. *Biomaterials* 24(24): 4337-4351.

[Exon 2006] Exon, J. H. (2006). A Review of the Toxicology of Acrylamide. *J.Toxicol. Environ. Health, Part B* 9(5): 397-412.

[Feng *et al.* 1988] Feng, X. D., Guo, X. Q. and Qiu, K. Y. (1988). Study of the initiation mechanism of the vinyl polymerization with the system persulfate/N,N,N′,N′-tetramethylethylenediamine. *Makromol. Chem.* 189(1): 77-83.

[Frank-Finney *et al.* 2013] Frank-Finney, R. J., Bradley, L. C. and Gupta, M. (2013). Formation of polymer-ionic liquid gels using vapor phase precursors. *Macromolecules* 46(17): 6852-6857.

[Gallagher *et al.* 2014] Gallagher, S., Florea, L., Fraser, K. J. and Diamond, D. (2014). Swelling and Shrinking Properties of Thermo-Responsive Polymeric Ionic Liquid Hydrogels with Embedded Linear pNIPAAM. *Int. J. Mol. Sci.* 15(4): 5337-5349.

[Ganji *et al.* 2010] Ganji, F., Vasheghani-Farahani, S. and Vasheghani-Farahani, E. (2010). Theoretical Description of Hydrogel Swelling: A Review. *Iran. Polym. J.* 19(5): 375-398.

[Ghazali-Esfahani *et al.* 2013] Ghazali-Esfahani, S., Song, H., Paunescu, E., Bobbink, F. D., Liu, H., Fei, Z., Laurenczy, G., Bagherzadeh, M., Yan, N. and Dyson, P. J. (2013). Cycloaddition of CO2 to epoxides catalyzed by imidazolium-based polymeric ionic liquids. *Green Chem.* 15(6): 1584-1589.

[Gibas *et al.* 2010] Gibas, I. and Janik, H. (2010). Review: synthetic polymer hydrogels for biomedical applications. *Chem. Chem. Technol.* 4(4): 297-304.

[Gin *et al.* 1990] Gin, H., Dupuy, B., Bonnemaison-Bourignon, D., Bordenave, L., Bareille, R., Latapie, M., Baquey, C., Bezian, J. and Ducassou, D. (1990). Biocompatibility of polyacrylamide microcapsules implanted in peritoneal cavity or spleen of the rat. Effect on various inflammatory reactions in vitro. *Artificial Cells, Blood Substitutes and Biotechnology* 18(1): 25-42.

[Gombotz *et al.* 1998] Gombotz, W. R. and Wee, S. (1998). Protein release from alginate matrices. *Adv. Drug Deliv. Rev.* 31(3): 267-285.

[Gonzalez-Alvarez *et al.* 2012] Gonzalez-Alvarez, J., Blanco-Gomis, D., Arias-Abrodo, P., Diaz-Llorente, D., Rios-Lombardia, N. s., Busto, E., Gotor-Fernandez, V. and Guteirrez-Alvarez, M. D. (2012). Polymeric imidazolium ionic liquids as valuable stationary phases in gas chromatography: Chemical synthesis and full characterization. *Anal. Chim. Acta* 721(0): 173-181.

[Grasselli *et al.* 1993] Grasselli, M., Diaz, L. E. and Cascone, O. (1993). Beaded matrices from cross-linked alginate for affinity and ion exchange chromatography of proteins. *Biotechnol. Tech.* 7(10): 707-712.

[Green *et al.* 2009a] Green, M. D. and Long, T. E. (2009a). Designing Imidazole-Based Ionic Liquids and Ionic Liquid Monomers for Emerging Technologies. *Polym. Rev.* 49(4): 291-314.

[Green *et al.* 2011] Green, M. D., Salas-de la Cruz, D., Ye, Y., Layman, J. M., Elabd, Y. A., Winey, K. I. and Long, T. E. (2011). Alkyl-Substituted N-Vinylimidazolium Polymerized Ionic Liquids: Thermal Properties and Ionic Conductivities. *Macromol. Chem. Phys.* 212(23): 2522-2528.

[Green *et al.* 2009b] Green, O., Grubjesic, S., Lee, S. W. and Firestone, M. A. (2009b). The Design of Polymeric Ionic Liquids for the Preparation of Functional Materials. *Polym. Rev.* 49(4): 339-360.

[Grubjesic *et al.* 2009] Grubjesic, S., Seifert, S. and Firestone, M. A. (2009). Cytoskeleton Mimetic Reinforcement of a Self-Assembled N,N′-Dialkylimidazolium Ionic Liquid Monomer by Copolymerization. *Macromolecules* 42(15): 5461-5470.

[Gruntzig 1978] Gruntzig, A. (1978). Trans-luminal dilatation of coronary-artery stenosis. *Lancet* 1(8058): 263-263.

[Gu *et al.* 2011] Gu, Y. and Lodge, T. P. (2011). Synthesis and Gas Separation Performance of Triblock Copolymer Ion Gels with a Polymerized Ionic Liquid Mid-Block. *Macromolecules* 44(7): 1732-1736.

[Gulrez *et al.* 2011] Gulrez, S. K., Al-Assaf, S. and Phillips, G. O. (2011). Hydrogels: methods of preparation, characterisation and applications. *Progress in molecular and environmental bioengineering - from analysis and modeling to technology applications. InTech, Winchester*: 117-150.

[Gupta *et al.* 2012] Gupta, N. V. and Shivakumar, H. G. (2012). Investigation of Swelling Behavior and Mechanical Properties of a pH-Sensitive Superporous Hydrogel Composite. *Iran. J. Pharm. Res.* 11(2): 481-493.

[Hao *et al.* 2013] Hao, J. and Weiss, R. A. (2013). Mechanical behavior of hybrid hydrogels composed of a physical and a chemical network. *Polymer* 54(8): 2174-2182.

[Harjani *et al.* 2009] Harjani, J. R., Farrell, J., Garcia, M. T., Singer, R. D. and Scammells, P. J. (2009). Further investigation of the biodegradability of imidazolium ionic liquids. *Green Chem.* 11(6): 821-829.

[Hatakeyama *et al.* 1998] Hatakeyama, H. and Hatakeyama, T. (1998). Interaction between water and hydrophilic polymers. *Thermochim. Acta* 308(1-2): 3-22.

[Hazeltine *et al.* 2012] Hazeltine, L. B., Simmons, C. S., Salick, M. R., Lian, X., Badur, M. G., Han, W., Delgado, S. M., Wakatsuki, T., Crone, W. C., Pruitt, B. L. and Palecek, S. P. (2012). Effects of substrate mechanics on contractility of cardiomyocytes generated from human pluripotent stem cells. *Int. J. Cell Biol.* 2012: 508294-508294.

[Heilmann *et al.* 2010] Heilmann, T., Richter, C., Noack, H., Post, S., Mahnkopf, D., Mittag, A., Thiele, H. and Figulla, H.-R. (2010). Drug release profiles of different drug-coated balloon platforms. *European Cardiology Review* 6: 40-44

[Hennink *et al.* 2012] Hennink, W. E. and van Nostrum, C. F. (2012). Novel crosslinking methods to design hydrogels. *Adv. Drug Deliv. Rev.* 64, Supplement(0): 223-236.

[Ho *et al.* 2013] Ho, T. D., Zhang, C., Hantao, L. W. and Anderson, J. L. (2013). Ionic Liquids in Analytical Chemistry: Fundamentals, Advances, and Perspectives. *Anal. Chem.* 86(1): 262-285.

[Hoffman 2001] Hoffman, A. S. (2001). Hydrogels for biomedical applications. Bioartificial Organs Iii: Tissue Sourcing, Immunoisolation, and Clinical Trials. Hunkeler, D., Cherrington, A., Prokop, A. and Rajotte, R. New York, New York Acad Sciences. 944**:** 62-73.

[Hoffman 2002] Hoffman, A. S. (2002). Hydrogels for biomedical applications. *Adv. Drug Deliv. Rev.* 54(1): 3-12.

[Hoover 1970] Hoover, M. F. (1970). Cationic Quaternary Polyelectrolytes - A Literature Review. *J. Macromol. Sci. Part A: Chem.* 4(6): 1327-1418.

[Hsieh *et al.* 2007] Hsieh, Y.-N., Ho, W.-Y., Horng, R., Huang, P.-C., Hsu, C.-Y., Huang, H.-H. and Kuei, C.-H. (2007). Study of Anion Effects on Separation Phenomenon for the Vinyloctylimidazolium Based Ionic Liquid Polymer Stationary Phases in GC. *Chromatographia* 66(7-8): 607-611.

[Hsieh *et al.* 2008] Hsieh, Y.-N., Horng, R., Ho, W.-Y., Huang, P.-C., Hsu, C.-Y., Whang, T.-J. and Kuei, C.-H. (2008). Characterizations for Vinylimidazolium Based Ionic Liquid Polymer Stationary Phases for Capillary Gas Chromatography. *Chromatographia* 67(5-6): 413-420.

[Hu *et al.* 2010] Hu, B., Wu, T., Ding, K., Zhou, X., Jiang, T. and Han, B. (2010). Seeding Growth of Pd/Au Bimetallic Nanoparticles on Highly Cross-Linked Polymer Microspheres with Ionic Liquid and Solvent-Free Hydrogenation. *J. Phys. Chem. C* 114(8): 3396-3400.

[Huang *et al.* 2010] Huang, J., Tao, C.-a., An, Q., Zhang, W., Wu, Y., Li, X., Shen, D. and Li, G. (2010). 3D-ordered macroporous poly(ionic liquid) films as multifunctional materials. *Chem. Commun.* 46(6): 967-969.

[Jeon *et al.* 2009] Jeon, O., Bouhadir, K. H., Mansour, J. M. and Alsberg, E. (2009). Photocrosslinked alginate hydrogels with tunable biodegradation rates and mechanical properties. *Biomaterials* 30(14): 2724-2734.

[Jeon *et al.* 2010] Jeon, O., Powell, C., Ahmed, S. M. and Alsberg, E. (2010). Biodegradable, Photocrosslinked Alginate Hydrogels with Independently Tailorable Physical Properties and Cell Adhesivity. *Tissue Eng. Part A* 16(9): 2915-2925.

[Jeremias *et al.* 2013] Jeremias, S., Kunze, M., Passerini, S. and Schönhoff, M. (2013). Polymerizable Ionic Liquid with State of the Art Transport Properties. *J. Phys. Chem. B* 117(36): 10596-10602.

[Kadokawa] Kadokawa, J.-i. Polymerizable ionic liquids: Development to photo functional poly (ionic liquid) materials. TCIMAIL No. 159: 2-6.

[Kadokawa *et al.* 2008] Kadokawa, J.-i., Murakami, M.-a. and Kaneko, Y. (2008). A facile method for preparation of composites composed of cellulose and a polystyrene-type polymeric ionic liquid using a polymerizable ionic liquid. *Compos. Sci. Technol.* 68(2): 493-498.

[Kasahara *et al.* 2014] Kasahara, S., Kamio, E., Yoshizumi, A. and Matsuyama, H. (2014). Polymeric ion-gels containing an amino acid ionic liquid for facilitated CO2 transport media. *Chem. Commun.* 50(23): 2996-2999.

[Kelsch *et al.* 2011] Kelsch, B., Scheller, B., Biedermann, M., Clever, Y. P., Schaffner, S., Mahnkopf, D., Speck, U. and Cremers, B. (2011). Dose Response to Paclitaxel-Coated Balloon Catheters in the Porcine Coronary Overstretch and Stent Implantation Model. *Invest. Radiol.* 46(4): 255-263.

[Khmelnitsky *et al.* 1997] Khmelnitsky, Y. L., Budde, C., Arnold, J. M., Usyatinsky, A., Clark, D. S. and Dordick, J. S. (1997). Synthesis of water-soluble paclitaxel derivatives by enzymatic acylation. *J. Am. Chem. Soc.* 119(47): 11554-11555.

[Kim *et al.* 2014a] Kim, J. K., Kim, H. J., Chung, J. Y., Lee, J. H., Young, S. B. and Kim, Y. H. (2014a). Natural and synthetic biomaterials for controlled drug delivery. *Arch. Pharmacal. Res.* 37(1): 60-68.

[Kim *et al.* 2010] Kim, T. Y., Lee, H. W., Stoller, M., Dreyer, D. R., Bielawski, C. W., Ruoff, R. S. and Suh, K. S. (2010). High-Performance Supercapacitors Based on Poly(ionic liquid)-Modified Graphene Electrodes. *ACS Nano* 5(1): 436-442.

[Kim *et al.* 2014b] Kim, Y. G., Lee, C. H. and Bae, Y. C. (2014b). Hydrophilic-hydrophobic copolymer nano-sized particle gels: Swelling behavior and dependence on crosslinker chain length. *Fluid Phase Equilib.* 361: 200-207.

[Kiviranta *et al.* 2008] Kiviranta, P., Lammentausta, E., Töyräs, J., Kiviranta, I. and Jurvelin, J. S. (2008). Indentation diagnostics of cartilage degeneration. *Osteoarthr. Cartilage* 16(7): 796-804.

[Kleber *et al.* 2013] Kleber, F. X., Rittger, H., Bonaventura, K., Zeymer, U., Wohrle, J., Jeger, R., Levenson, B., Mobius-Winkler, S., Bruch, L., Fischer, D., Hengstenberg, C., Porner, T., Mathey, D. and Scheller, B. (2013). Drug-coated balloons for treatment of

coronary artery disease: updated recommendations from a consensus group. *Clin. Res. Cardiol.* 102(11): 785-797.

[Kleemann *et al.* 2005] Kleemann, R. U., Krocker, D., Cedraro, A., Tuischer, J. and Duda, G. N. (2005). Altered cartilage mechanics and histology in knee osteoarthritis: relation to clinical assessment (ICRS Grade). *Osteoarthr. Cartilage* 13(11): 958-963.

[Kong *et al.* 2003] Kong, H. J., Wong, E. and Mooney, D. J. (2003). Independent control of rigidity and toughness of polymeric hydrogels. *Macromolecules* 36(12): 4582-4588.

[Konno *et al.* 2003] Konno, T., Watanabe, J. and Ishihara, K. (2003). Enhanced solubility of paclitaxel using water-soluble and biocompatible 2-methacryloyloxyethyl phosphorylcholine polymers. *J. Biomed. Mater. Res. A* 65A(2): 209-214.

[Kopecek *et al.* 2012] Kopecek, J. and Yang, J. (2012). "Intelligente" Biomaterialien durch Selbstorganisation von Hybridhydrogelen. *Angew. Chem.* 124(30): 7512-7535.

[Kopecek *et al.* 2007] Kopecek, J. and Yang, J. Y. (2007). Review - Hydrogels as smart biomaterials. *Polym. Int.* 56(9): 1078-1098.

[Krebs *et al.* 2009] Krebs, M. D., Jeon, O. and Alsberg, E. (2009). Localized and Sustained Delivery of Silencing RNA from Macroscopic Biopolymer Hydrogels. *J. Am. Chem. Soc.* 131(26): 9204-9206.

[Krokidis *et al.* 2013] Krokidis, M., Spiliopoulos, S., Katsanos, K. and Sabharwal, T. (2013). Peripheral Applications of Drug-Coated Balloons: Past, Present and Future. *Cardiovasc. Inter. Rad.* 36(2): 281-291.

[Kuo *et al.* 2001] Kuo, C. K. and Ma, P. X. (2001). Ionically crosslinked alginate hydrogels as scaffolds for tissue engineering: Part 1. Structure, gelation rate and mechanical properties. *Biomaterials* 22(6): 511-521.

[Langer *et al.* 2003] Langer, R. and Peppas, N. A. (2003). Advances in biomaterials, drug delivery, and bionanotechnology. *AIChE J.* 49(12): 2990-3006.

[Lee *et al.* 2000] Lee, K. Y., Bouhadir, K. H. and Mooney, D. J. (2000). Degradation behavior of covalently cross-linked poly(aldehyde guluronate) hydrogels. *Macromolecules* 33(1): 97-101.

[Lee *et al.* 2004] Lee, K. Y., Bouhadir, K. H. and Mooney, D. J. (2004). Controlled degradation of hydrogels using multi-functional cross-linking molecules. *Biomaterials* 25(13): 2461-2466.

[Lee *et al.* 2001] Lee, K. Y. and Mooney, D. J. (2001). Hydrogels for tissue engineering. *Chem. Rev.* 101(7): 1869-1879.

[Lee *et al.* 2012] Lee, K. Y. and Mooney, D. J. (2012). Alginate: Properties and biomedical applications. *Prog. Polym. Sci.* 37(1): 106-126.

[Li *et al.* 2011a] Li, C., Allen, J., Alliston, T. and Pruitt, L. A. (2011a). The use of polyacrylamide gels for mechanical calibration of cartilage - A combined nanoindentation and unconfined compression study. *J. Mech. Behav. Biomed.* 4(7): 1540-1547.

[Li *et al.* 2010] Li, J., Han, H., Wang, Q., Liu, X. and Jiang, S. (2010). Polymeric ionic liquid as a dynamic coating additive for separation of basic proteins by capillary electrophoresis. *Anal. Chim. Acta* 674(2): 243-248.

[Li *et al.* 2011b] Li, J., Han, H., Wang, Q., Liu, X. and Jiang, S. (2011b). Polymeric ionic liquid-coated capillary for capillary electrophoresis. *J. Sep. Sci.* 34(13): 1555-1560.

[Li *et al.* 2011c] Li, L., Jiang, X., Guan, H. and Wang, P. (2011c). Preparation, purification and characterization of alginate oligosaccharides degraded by alginate lyase from Pseudomonas sp. HZJ 216. *Carbohydr. Res.* 346(6): 794-800.

[Li *et al.* 2014] Li, M., Wang, L., Yang, B., Du, T. and Zhang, Y. (2014). Facile preparation of polymer electrolytes based on the polymerized ionic liquid poly((4-vinylbenzyl)trimethylammonium bis(trifluoromethanesulfonylimide)) for lithium secondary batteries. *Electrochim. Acta* 123(0): 296-302.

[Li *et al.* 2013] Li, Y., Ding, Y., Qin, M., Cao, Y. and Wang, W. (2013). An enzyme-assisted nanoparticle crosslinking approach to enhance the mechanical strength of peptide-based supramolecular hydrogels. *Chem. Commun.* 49(77): 8653-8655.

[Li *et al.* 2011d] Li, Z. and Guan, J. (2011d). Hydrogels for cardiac tissue engineering. *Polymers* 3(2): 740-761.

[Liggins *et al.* 1997] Liggins, R. T., Hunter, W. L. and Burt, H. M. (1997). Solid-state characterization of paclitaxel. *J. Pharm. Sci.* 86(12): 1458-1463.

[Lin *et al.* 2010] Lin, B., Qiu, L., Lu, J. and Yan, F. (2010). Cross-Linked Alkaline Ionic Liquid-Based Polymer Electrolytes for Alkaline Fuel Cell Applications. *Chem. Mater.* 22(24): 6718-6725.

[Lira *et al.* 2009] Lira, L. M., Martins, K. A. and Torresi, S. I. C. r. d. (2009). Structural parameters of polyacrylamide hydrogels obtained by the Equilibrium Swelling Theory. *Eur. Polym. J.* 45(4): 1232-1238.

[Liu *et al.* 2012] Liu, F., Wang, L., Sun, Q., Zhu, L., Meng, X. and Xiao, F.-S. (2012). Transesterification Catalyzed by Ionic Liquids on Superhydrophobic Mesoporous Polymers: Heterogeneous Catalysts That Are Faster than Homogeneous Catalysts. *J. Am. Chem. Soc.* 134(41): 16948-16950.

[Liu *et al.* 2013] Liu, Z. Q., Lu, A. G., Yang, Z. P. and Luo, Y. L. (2013). Enhanced Swelling and Mechanical Properties of P(AM-co-SMA) Semi-IPN Composite Hydrogels by Impregnation with PANI and MWNTs-COOH. *Macromol. Res.* 21(4): 376-384.

[Lizawa *et al.* 2007] Lizawa, T., Taketa, H., Maruta, M., Ishido, T., Gotoh, T. and Sakohara, S. (2007). Synthesis of porous poly(N-isopropylacrylamide) gel beads by sedimentation polymerization and their morphology. *J. Appl. Polym. Sci.* 104(2): 842-850.

[Loh *et al.* 2012] Loh, J. P. and Waksman, R. (2012). Paclitaxel Drug-Coated Balloons A Review of Current Status and Emerging Applications in Native Coronary Artery De Novo Lesions. *JACC Cardiovasc. Interv.* 5(10): 1001-1012.

[Lopez *et al.* 2006] Lopez, M. S.-P., Mecerreyes, D., Lopez-Cabarcos, E. and Lopez-Ruiz, B. (2006). Amperometric glucose biosensor based on polymerized ionic liquid microparticles. *Biosens. Bioelectron.* 21(12): 2320-2328.

[Lu *et al.* 2014] Lu, C. C., Wang, X. J., Wu, G. L., Wang, J. J., Wang, Y. N., Gao, H. and Ma, J. B. (2014). An injectable and biodegradable hydrogel based on poly(alpha,beta-aspartic acid) derivatives for localized drug delivery. *J. Biomed. Materials Res. Part A* 102(3): 628-638.

[Lu *et al.* 2009] Lu, J. M., Yan, F. and Texter, J. (2009). Advanced applications of ionic liquids in polymer science. *Prog. Polym. Sci.* 34(5): 431-448.

[Luong *et al.* 2013] Luong, P. T., Browning, M. B., Bixler, R. S. and Cosgriff-Hernandez, E. (2013). Drying and storage effects on poly(ethylene glycol) hydrogel mechanical properties and bioactivity. *J. Biomed. Mater. Res. A*.

[Lupi *et al.* 2013] Lupi, A., Rognoni, A., Secco, G. G., Porto, I., Nardi, F., Lazzero, M., Rossi, L., Parisi, R., Fattori, R., Genoni, G., Rosso, R., Stella, P. R., Sheiban, I., Bolognese, L., Liistro, F., Bongo, A. S. and Agostoni, P. (2013). Drug eluting balloon versus drug eluting stent in percutaneous coronary interventions: Insights from a meta-analysis of 1462 patients. *Int. J. Cardiol.* 168(5): 4608-4616.

[Malana *et al.* 2014] Malana, M. A., Bukhari, J. U. D. and Zohra, R. (2014). Synthesis, swelling behavior, and network parameters of novel chemically crosslinked poly (acrylamide-co-methacrylate-co-acrylic acid) hydrogels. *Des. Monomers Polym.* 17(3): 266-274.

[Marcilla *et al.* 2006a] Marcilla, R., Alcaide, F., Sardon, H., Pomposo, J. A., Pozo-Gonzalo, C. and Mecerreyes, D. (2006a). Tailor-made polymer electrolytes based upon ionic liquids and their application in all-plastic electrochromic devices. *Electrochem. Commun.* 8(3): 482-488.

[Marcilla *et al.* 2004] Marcilla, R., Blazquez, J. A., Rodriguez, J., Pomposo, J. A. and Mecerreyes, D. (2004). Tuning the solubility of polymerized ionic liquids by simple anion-exchange reactions. *J. Polym. Sci., Part A: Polym. Chem.* 42(1): 208-212.

[Marcilla *et al.* 2006b] Marcilla, R., Sanchez-Paniagua, M., Lopez-Ruiz, B., Lopez-Cabarcos, E., Ochoteco, E., Grande, H. and Mecerreyes, D. (2006b). Synthesis and characterization of new polymeric ionic liquid microgels. *J. Polym. Sci. Part A: Polym. Chem.* 44(13): 3958-3965.

[Matricardi *et al.* 2013] Matricardi, P., Di Meo, C., Coviello, T., Hennink, W. E. and Alhaique, F. (2013). Interpenetrating Polymer Networks polysaccharide hydrogels for drug delivery and tissue engineering. *Adv. Drug Deliv. Rev.* 65(9): 1172-1187.

[Mazur *et al.* 2014] Mazur, K., Buchner, R., Bonn, M. and Hunger, J. (2014). Hydration of Sodium Alginate in Aqueous Solution. *Macromolecules* 47(2): 771-776.

[Mecerreyes 2011] Mecerreyes, D. (2011). Polymeric ionic liquids: Broadening the properties and applications of polyelectrolytes. *Prog. Polym. Sci.* 36(12): 1629-1648.

[Meng *et al.* 2011] Meng, Y., Pino, V. n. and Anderson, J. L. (2011). Role of counteranions in polymeric ionic liquid-based solid-phase microextraction coatings for the selective extraction of polar compounds. *Anal. Chim. Acta* 687(2): 141-149.

[Merle *et al.* 2013] Merle, G., Chairuna, A., Ven, E. V. d. and Nijmeijer, K. (2013). An easy method for the preparation of anion exchange membranes: Graft-polymerization of ionic liquids in porous supports. *J. Appl. Polym. Sci.* 129(3): 1143-1150.

[Morch *et al.* 2006] Morch, Y. A., Donati, I., Strand, B. L. and Skjåk-Bræk, G. (2006). Effect of Ca2+, Ba2+, and Sr2+ on Alginate Microbeads. *Biomacromolecules* 7(5): 1471-1480.

[Moreno *et al.* 2012] Moreno, M., Aboudzadeh, M. A., Barandiaran, M. J. and Mecerreyes, D. (2012). Facile incorporation of natural carboxylic acids into polymers via

polymerization of protic ionic liquids. *J. Polym. Sci. Part A: Polym. Chem.* 50(6): 1049-1053.

[Mori *et al.* 2009] Mori, H., Yahagi, M. and Endo, T. (2009). RAFT Polymerization of N-Vinylimidazolium Salts and Synthesis of Thermoresponsive Ionic Liquid Block Copolymers. *Macromolecules* 42(21): 8082-8092.

[Mu *et al.* 2005] Mu, X.-d., Meng, J.-q., Li, Z.-C. and Kou, Y. (2005). Rhodium Nanoparticles Stabilized by Ionic Copolymers in Ionic Liquids: Long Lifetime Nanocluster Catalysts for Benzene Hydrogenation. *J. Am. Chem. Soc.* 127(27): 9694-9695.

[Naficy *et al.* 2013] Naficy, S., Kawakami, S., Sadegholvaad, S., Wakisaka, M. and Spinks, G. M. (2013). Mechanical properties of interpenetrating polymer network hydrogels based on hybrid ionically and covalently crosslinked networks. *J. Appl. Polym. Sci.* 130(4): 2504-2513.

[Nakashima *et al.* 2009] Nakashima, K., Kamiya, N., Koda, D., Maruyama, T. and Goto, M. (2009). Enzyme encapsulation in microparticles composed of polymerized ionic liquids for highly active and reusable biocatalysts. *Org. Biomol. Chem.* 7(11): 2353-2358.

[Narbute *et al.* 2011] Narbute, I., Jegere, S., Kumsars, I., Mintale, I., Zakke, I., Bumeistere, K., Sondore, D., Grave, A. and Erglis, A. (2011). Are paclitaxel-eluting stents better in unprotected left main coronary artery disease? Three-year clinical and intravascular imaging results from a randomized study. *Medicina (Kaunas)* 47(10): 536-543.

[Neubert *et al.* 2008] Neubert, A., Sternberg, K., Nagel, S., Harder, C., Schmitz, K. P., Kroemer, H. K. and Weitschies, W. (2008). Development of a vessel-simulating flow-through cell method for the in vitro evaluation of release and distribution from drug-eluting stents. *J. Control. Release* 130(1): 2-8.

[Ohno *et al.* 1998] Ohno, H. and Ito, K. (1998). Room-temperature molten salt polymers as a matrix for fast ion conduction. *Chem. Lett.*(8): 751-752.

[Ohno *et al.* 2004] Ohno, H., Yoshizawa, M. and Ogihara, W. (2004). Development of new class of ion conductive polymers based on ionic liquids. *Electrochim. Acta* 50(2-3): 255-261.

[Okay 2010] Okay, O. (2010). General properties of hydrogels. Hydrogel Sensors and Actuators. Gerald Gerlach and Arndt, K.-F. Berlin Heidelberg, Springer. 6**:** 1-14.

[Omidian *et al.* 2008] Omidian, H. and Park, K. (2008). Swelling agents and devices in oral drug delivery. *J. Drug Del. Sci. Tech.* 18(2): 83.

[Ottenbrite *et al.* 2010] Ottenbrite, R. M., Park, K., Okano, T. and Peppas, N. A. (2010). Biomedical applications of hydrogels handbook, Springer New York Dordrecht Heidelberg London.

[Oyen 2014] Oyen, M. L. (2014). Mechanical characterisation of hydrogel materials. *Int. Mater. Rev.* 59(1): 44-59.

[Page *et al.* 2007] Page, P. M., McCarty, T. A., Baker, G. A., Baker, S. N. and Bright, F. V. (2007). Comparison of dansylated aminopropyl controlled pore glass solvated by molecular and ionic liquids. *Langmuir* 23(2): 843-849.

[Pajic-Lijakovic *et al.* 2010] Pajic-Lijakovic, I., Plavsic, M., Nedovic, V. and Bugarski, B. (2010). Ca-alginate hydrogel rheological changes caused by yeast cell growth dynamics. *Microbiology Book Series*(2): 1486-1493.

[Pandey *et al.* 2012] Pandey, G. P. and Rastogi, A. C. (2012). Graphene-Based All-Solid-State Supercapacitor with Ionic Liquid Gel Polymer Electrolyte. *MRS Online Proceedings Library* 1440.

[Park *et al.* 2013] Park, M. J., Choi, I., Hong, J. and Kim, O. (2013). Polymer electrolytes integrated with ionic liquids for future electrochemical devices. *J. Appl. Polym. Sci.* 129(5): 2363-2376.

[Park *et al.* 2008] Park, S., Nicoll, S. B., Mauck, R. L. and Ateshian, G. A. (2008). Cartilage mechanical response under dynamic compression at physiological stress levels following collagenase digestion. *Ann. Biomed. Eng.* 36(3): 425-434.

[Patel *et al.* 2011] Patel, A. and Mequanint, K. (2011). Hydrogel biomaterials. *Biomedical Engineering – Frontiers and Challenges* 275-296.

[Pawar *et al.* 2012] Pawar, S. N. and Edgar, K. J. (2012). Alginate derivatization: A review of chemistry, properties and applications. *Biomaterials* 33(11): 3279-3305.

[Peppas 2004] Peppas, N. A. (2004). 7 Kinetics of Smart Hydrogels. *Reflexive Polymers and Hydrogels: Understanding and Designing Fast Responsive Polymeric Systems*: 99.

[Peppas *et al.* 2000] Peppas, N. A., Bures, P., Leobandung, W. and Ichikawa, H. (2000). Hydrogels in pharmaceutical formulations. *Eur. J. Pharm. Biopharm.* 50(1): 27-46.

[Peppas *et al.* 2006] Peppas, N. A., Hilt, J. Z., Khademhosseini, A. and Langer, R. (2006). Hydrogels in Biology and Medicine: From Molecular Principles to Bionanotechnology. *Adv. Mater.* 18(11): 1345-1360.

[Peppas *et al.* 2012] Peppas, N. A., Slaughter, B. V., Kanzelberger, M. A., Matyjaszewski, K. and Möller, M. (2012). 9.20 - Hydrogels. Polymer Science: A Comprehensive Reference. Amsterdam, Elsevier. 9**:** 385-395.

[Petersen *et al.* 2013a] Petersen, S., Kaule, S., Stein, F., Minrath, I., Schmitz, K. P., Kragl, U. and Sternberg, K. (2013a). Novel paclitaxel-coated angioplasty balloon catheter based on cetylpyridinium salicylate: Preparation, characterization and simulated use in an in vitro vessel model. *Mater. Sci. Eng. C: Mater. Biol. Appl.* 33(7): 4244-4250.

[Petersen *et al.* 2013b] Petersen, S., Minrath, I., Kaule, S., Kocher, J., Schmitz, K. P. and Sternberg, K. (2013b). Development and in Vitro Characterization of Photochemically Crosslinked Polyvinylpyrrolidone Coatings for Drug-Coated Balloons. *Coatings* 3(4): 253-267.

[Pinaud *et al.* 2011] Pinaud, J., Vignolle, J., Gnanou, Y. and Taton, D. (2011). Poly(N-heterocyclic-carbene)s and their CO2 Adducts as Recyclable Polymer-Supported Organocatalysts for Benzoin Condensation and Transesterification Reactions. *Macromolecules* 44(7): 1900-1908.

[Pohako-Esko *et al.* 2013] Pohako-Esko, K., Taaber, T., Saal, K., Lohmus, R., Kink, I. and Mäeorg, U. (2013). New Method for Synthesis of Methacrylate-Type Polymerizable Ionic Liquids. *Synth. Commun.* 43(21): 2846-2852.

[Posa *et al.* 2010] Posa, A., Nyolczas, N., Hemetsberger, R., Pavo, N., Petnehazy, O., Petrasi, Z., Sangiorgi, G. and Gyoengyoesi, M. (2010). Optimization of Drug-Eluting Balloon

Use for Safety and Efficacy: Evaluation of the 2nd Generation Paclitaxel-Eluting DIOR-Balloon in Porcine Coronary Arteries. *Catheter Cardio. Inte.* 76(3): 395-403.

[Pourjavadi *et al.* 2012] Pourjavadi, A., Hosseini, S. H. and Soleyman, R. (2012). Crosslinked poly(ionic liquid) as high loaded dual acidic organocatalyst. *J. Mol. Catal. A: Chem.* 365(0): 55-59.

[Qiu *et al.* 2010] Qiu, H., Takafuji, M., Sawada, T., Liu, X., Jiang, S. and Ihara, H. (2010). New strategy for drastic enhancement of selectivity via chemical modification of counter anions in ionic liquid polymer phase. *Chem. Commun.* 46(46): 8740-8742.

[Qiu *et al.* 2003] Qiu, Y. and Park, K. (2003). Superporous IPN hydrogels having enhanced mechanical properties. *AAPS PharmSciTech* 4(4): 406-412.

[Rahman *et al.* 2013] Rahman, M. T., Barikbin, Z., Badruddoza, A. Z. M., Doyle, P. S. and Khan, S. A. (2013). Monodisperse Polymeric Ionic Liquid Microgel Beads with Multiple Chemically Switchable Functionalities. *Langmuir* 29(30): 9535-9543.

[Rees *et al.* 1977] Rees, D. A. and Welsh, E. J. (1977). Secondary and tertiary structure of polysaccharides in solutions and gels. *Angew. Chem. Int. Edit.* 16(4): 214-223.

[Ruebben *et al.* 2010] Ruebben, A., Boeing, J. and Weiss, N. (2010). Drug-eluting Balloon Analysis. *Interv. Cardiol.* 5: 74-76.

[Salas-de la Cruz *et al.* 2012] Salas-de la Cruz, D., Green, M. D., Ye, Y. S., Elabd, Y. A., Long, T. E. and Winey, K. I. (2012). Correlating backbone-to-backbone distance to ionic conductivity in amorphous polymerized ionic liquids. *J. Polym. Sci. Part B: Polym. Phys.* 50(5): 338-346.

[Schadt *et al.* 2013] Schadt, K., Kerscher, B., Thomann, R. and MÃ¼lhaupt, R. (2013). Structured Semifluorinated Polymer Ionic Liquids for Metal Nanoparticle Preparation and Dispersion in Fluorous Compartments. *Macromolecules* 46(12): 4799-4804.

[Scheller 2011] Scheller, B. (2011). Opportunities and limitations of drug-coated balloons in interventional therapies. *Herz* 36(3): 232-240.

[Scheller *et al.* 2006] Scheller, B., Hehrlein, C., Bocksch, W., Rutsch, W., Haghi, D., Dietz, U., Bohm, M. and Speck, U. (2006). Treatment of coronary in-stent restenosis with a paclitaxel-coated balloon catheter. *N. Engl. J. Med.* 355(20): 2113-2124.

[Scheller *et al.* 2004] Scheller, B., Speck, U., Abramjuk, C., Bernhardt, U., Bohm, M. and Nickenig, G. (2004). Paclitaxel balloon coating, a novel method for prevention and therapy of restenosis. *Circulation* 110(7): 810-814.

[Schmidt *et al.* 2013] Schmidt, W. and Lanzer, P. (2013). Instrumentation. Catheter-Based Cardiovascular Interventions. Lanzer, P., Springer-Verlag Berlin Heidelberg**:** 445-472.

[Seidlitz *et al.* 2013] Seidlitz, A., Kotzan, N., Nagel, S., Reske, T., Grabow, N., Harder, C., Petersen, S., Sternberg, K. and Weitschies, W. (2013). In Vitro Determination of Drug Transfer from Drug-Coated Balloons. *PLoS One* 8(12): e83992.

[Seidlitz *et al.* 2011] Seidlitz, A., Nagel, S., Semmling, B., Grabow, N., Martin, H., Senz, V., Harder, C., Sternberg, K., Schmitz, K.-P., Kroemer, H. K. and Weitschies, W. (2011). Examination of drug release and distribution from drug-eluting stents with a vessel-simulating flow-through cell. *Eur. J. Pharm. Biopharm.* 78(1): 36-48.

[Seiffert *et al.* 2012] Seiffert, S. and Sprakel, J. (2012). Physical chemistry of supramolecular polymer networks. *Chem. Soc. Rev.* 41(2): 909-930.

[Shaplov *et al.* 2009] Shaplov, A. S., Goujon, L., Vidal, F., Lozinskaya, E. I., Meyer, F., Malyshkina, I. A., Chevrot, C., Teyssié, D., Odinets, I. L. and Vygodskii, Y. S. (2009). Ionic IPNs as novel candidates for highly conductive solid polymer electrolytes. *J. Polym. Sci. Part A: Polym. Chem.* 47(17): 4245-4266.

[Shaplov *et al.* 2011a] Shaplov, A. S., Vlasov, P. S., Armand, M., Lozinskaya, E. I., Ponkratov, D. O., Malyshkina, I. A., Vidal, F., Okatova, O. V., Pavlov, G. M., Wandrey, C., Godovikov, I. A. and Vygodskii, Y. S. (2011a). Design and synthesis of new anionic "polymeric ionic liquids" with high charge delocalization. *Polym. Chem.* 2(11): 2609-2618.

[Shaplov *et al.* 2011b] Shaplov, A. S., Vlasov, P. S., Lozinskaya, E. I., Ponkratov, D. O., Malyshkina, I. A., Vidal, F., Okatova, O. V., Pavlov, G. M., Wandrey, C., Bhide, A., Schönhoff, M. and Vygodskii, Y. S. (2011b). Polymeric Ionic Liquids: Comparison of Polycations and Polyanions. *Macromolecules* 44(24): 9792-9803.

[Shaplov *et al.* 2012] Shaplov, A. S., Vlasov, P. S., Lozinskaya, E. I., Shishkan, O. A., Ponkratov, D. O., Malyshkina, I. A., Vidal, F., Wandrey, C., Godovikov, I. A. and Vygodskii, Y. S. (2012). Thiol-Ene Click Chemistry as a Tool for a Novel Family of Polymeric Ionic Liquids. *Macromol. Chem. Phys.* 213(13): 1359-1369.

[Sigwart *et al.* 1987] Sigwart, U., Puel, J., Mirkovitch, V., Joffre, F. and Kappenberger, L. (1987). Intravascular stents to prevent occlusion and restenosis after trans-luminnal angioplasty. *N. Engl. J. Med.* 316(12): 701-706.

[Singh *et al.* 2010] Singh, A., Sharma, P. K., Garg, V. K. and Garg, G. (2010). Hydrogels: A Review. *Int. J. Pharm. Sci. Rev. Res.* 4(2): 97-105.

[Skjåk-Bræk *et al.* 1989] Skjåk-Bræk, G., Grasdalen, H. and Smidsrød, O. (1989). Inhomogeneous polysaccharide ionic gels. *Carbohydr. Polym.* 10(1): 31-54.

[Snedden *et al.* 2003] Snedden, P., Cooper, A. I., Scott, K. and Winterton, N. (2003). Cross-Linked Polymer-Ionic Liquid Composite Materials. *Macromolecules* 36(12): 4549-4556.

[Soll *et al.* 2013] Soll, S., Zhang, P., Zhao, Q., Wang, Y. and Yuan, J. (2013). Mesoporous zwitterionic poly(ionic liquid)s: intrinsic complexation and efficient catalytic fixation of CO2. *Polym. Chem.* 4(19): 5048-5051.

[Stein *et al.* 2012] Stein, F., Kragl, U., Harder, C., Löbler, M., Sternberg, K. and Schmitz, K.-P. (2012). Ballonkatheter mit einer aktiven Beschichtung. Cortronik, G. DE 10 2012 200 077.1.

[Sun *et al.* 2012a] Sun, J. Y., Zhao, X. H., Illeperuma, W. R. K., Chaudhuri, O., Oh, K. H., Mooney, D. J., Vlassak, J. J. and Suo, Z. G. (2012a). Highly stretchable and tough hydrogels. *Nature* 489(7414): 133-136.

[Sun *et al.* 2012b] Sun, S. J., Song, J., Feng, R. X. and Shan, Z. Q. (2012b). Ionic liquid gel electrolytes for quasi-solid-state dye-sensitized solar cells. *Electrochim. Acta* 69: 51-55.

[Sushmitha *et al.* 2010] Sushmitha, S., Joydip, K. and Subhas, C. K. (2010). Biopolymeric nanoparticles. *Sci. Technol. Adv. Mater.* 11(1): 014104.

[Taguchi *et al.* 2012] Taguchi, S., Ichikawa, T., Kato, T. and Ohno, H. (2012). Nano-biphasic ionic liquid systems composed of hydrophobic phosphonium salts and a hydrophilic ammonium salt. *Chem. Commun.* 48(43): 5271-5273.

[Taguchi *et al.* 2011] Taguchi, S., Matsumoto, T., Ichikawa, T., Kato, T. and Ohno, H. (2011). Gelation of an amino acid ionic liquid by the addition of a phosphonium-type zwitterion. *Chem. Commun.* 47(40): 11342-11344.

[Takemoto *et al.* 2014] Takemoto, Y., Ajiro, H. and Akashi, M. (2014). Amphiphilic Poly(N-vinyl acetamide) Gels Strengthened with Swelling Solvent. *Macromol. Chem. Phys.* 215(4): 384-390.

[Tanaka *et al.* 2005] Tanaka, Y., Gong, J. P. and Osada, Y. (2005). Novel hydrogels with excellent mechanical performance. *Prog. Polym. Sci.* 30(1): 1-9.

[Tang *et al.* 2009] Tang, J., Shen, Y., Radosz, M. and Sun, W. (2009). Isothermal Carbon Dioxide Sorption in Poly(ionic liquid)s. *Ind. Eng. Chem. Res.* 48(20): 9113-9118.

[Tang *et al.* 2005a] Tang, J., Tang, H., Sun, W., Plancher, H., Radosz, M. and Shen, Y. (2005a). Poly(ionic liquid)s: a new material with enhanced and fast CO2 absorption. *Chem. Commun.* (26): 3325-3327.

[Tang *et al.* 2005b] Tang, J., Tang, H., Sun, W., Radosz, M. and Shen, Y. (2005b). Poly(ionic liquid)s as new materials for CO2 absorption. *J. Polym. Sci. Part A: Polym. Chem.* 43(22): 5477-5489.

[Tang *et al.* 2014] Tang, S., Liu, S., Guo, Y., Liu, X. and Jiang, S. (2014). Recent advances of ionic liquids and polymeric ionic liquids in capillary electrophoresis and capillary electrochromatography. *J. Chrom. A* in press: DOI 10.1016/j.chroma.2014.04.037.

[Thakur *et al.* 2012] Thakur, A., Wanchoo, R. K. and Singh, P. (2012). Hydrogels of Poly(acrylamide-co-acrylic acid): In-vitro Study on Release of Gentamicin Sulfate. *Chem. Biochem. Eng. Q.* 25(4): 471-482.

[Thu *et al.* 1996] Thu, B., Bruheim, P., Espevik, T., Smidsrød, O., Soon-Shiong, P. and Skjåk-Bræk, G. (1996). Alginate polycation microcapsules: II. Some functional properties. *Biomaterials* 17(11): 1069-1079.

[Torriero *et al.* 2011] Torriero, A. A. and Shiddiky, M. J. (2011). Electrochemical properties and applications of ionic liquids. New York, N.Y., Nova Science Publishers.

[Tse *et al.* 2010] Tse, J. R. and Engler, A. J. (2010). Preparation of hydrogel substrates with tunable mechanical properties. *Current protocols in cell biology*: 10.16. 1-10.16. 16.

[Ueda *et al.* 2011] Ueda, S., Kagimoto, J., Ichikawa, T., Kato, T. and Ohno, H. (2011). Anisotropic Proton-Conductive Materials Formed by the Self-Organization of Phosphonium-Type Zwitterions. *Adv. Mater.* 23(27): 3071-+.

[Van Vlierberghe *et al.* 2011] Van Vlierberghe, S., Dubruel, P. and Schacht, E. (2011). Biopolymer-Based Hydrogels As Scaffolds for Tissue Engineering Applications: A Review. *Biomacromolecules* 12(5): 1387-1408.

[Varghese *et al.* 2006] Varghese, S. and Elisseeff, J. H. (2006). Hydrogels for musculoskeletal tissue engineering. Polymers for Regenerative Medicine. Werner, C., Eisseeff, J. H., Fischbach, C.et al. Berlin, Springer-Verlag Berlin**:** 95-144.

[Vermonden *et al.* 2012] Vermonden, T., Censi, R. and Hennink, W. E. (2012). Hydrogels for Protein Delivery. *Chem. Rev.* 112(5): 2853-2888.

[Vygodskii *et al.* 2007] Vygodskii, Y. S., Mel´nik, O. A., Shaplov, A. S., Lozinskaya, E. I., Malyshkina, I. A. and Gavrilova, N. D. (2007). Synthesis and ionic conductivity of polymer ionic liquids. *Polymer Science Series A* 49(3): 256-261.

[Waksman *et al.* 2009] Waksman, R. and Pakala, R. (2009). Drug-Eluting Balloon The Comeback Kid? *Circ. Cardiovasc. Interv.* 2(4): 352-358.

[Walden 1914] Walden, P. (1914). Molecular magnitude and electrical conductivity of some fused salts. *Bulletin de l'Academie Imperiale des Sciences de St. Petersbourg*(6): 405-422.

[Walker 1996] Walker, J. (1996). SDS Polyacrylamide Gel Electrophoresis of Proteins. The Protein Protocols Handbook, Humana Press**:** 55-61.

[Wang *et al.* 2011] Wang, J. and Li, X. (2011). Enhancing protein resistance of hydrogels based on poly(2-hydroxyethyl methacrylate) and poly(2-methacryloyloxyethyl phosphorylcholine) with interpenetrating network structure. *J. Appl. Polym. Sci.* 121(6): 3347-3352.

[Wanigasekara *et al.* 2010] Wanigasekara, E., Perera, S., Crank, J., Sidisky, L., Shirey, R., Berthod, A. and Armstrong, D. (2010). Bonded ionic liquid polymeric material for solid-phase microextraction GC analysis. *Anal. Bioanal. Chem.* 396(1): 511-524.

[Washiro *et al.* 2004] Washiro, S., Yoshizawa, M., Nakajima, H. and Ohno, H. (2004). Highly ion conductive flexible films composed of network polymers based on polymerizable ionic liquids. *Polymer* 45(5): 1577-1582.

[Way *et al.* 2014] Way, A. E., Korpusik, A. B., Dorsey, T. B., Buerkle, L. E., von Recum, H. A. and Rowan, S. J. (2014). Enhancing the Mechanical Properties of Guanosine-Based Supramolecular Hydrogels with Guanosine-Containing Polymers. *Macromolecules* 47(5): 1810-1818.

[Weber *et al.* 2011] Weber, R. L., Ye, Y. S., Banik, S. M., Elabd, Y. A., Hickner, M. A. and Mahanthappa, M. K. (2011). Thermal and Ion Transport Properties of Hydrophilic and Hydrophobic Polymerized Styrenic Imidazolium Ionic Liquids. *J. Polym. Sci. Part B: Polym.Phys.* 49(18): 1287-1296.

[Wichterle *et al.* 1960] Wichterle, O. and Lim, D. (1960). Hydrophilic Gels for Biological Use. *Nature* 185(4706): 117-118.

[Wong *et al.* 2000] Wong, T. Y., Preston, L. A. and Schiller, N. L. (2000). Alginate lyase: Review of major sources and enzyme characteristics, structure-function analysis, biological roles, and applications. *Annu. Rev. Microbiol.* 54: 289-340.

[Wu *et al.* 2009] Wu, B., Hu, D., Kuang, Y., Liu, B., Zhang, X. and Chen, J. (2009). Functionalization of Carbon Nanotubes by an Ionic-Liquid Polymer: Dispersion of Pt and PtRu Nanoparticles on Carbon Nanotubes and Their Electrocatalytic Oxidation of Methanol. *Angew. Chem. Int. Ed.* 48(26): 4751-4754.

[Wu *et al.* 2013] Wu, M., Ni, C. H., Yao, B. L., Zhu, C. P., Huang, B. and Zhang, L. P. (2013). Covalently cross-linked and hydrophobically modified alginic acid hydrogels and their application as drug carriers. *Polym. Eng. Sci.* 53(8): 1583-1589.

[Xiong *et al.* 2012a] Xiong, Y.-B., Wang, H., Wang, Y.-J. and Wang, R.-M. (2012a). Novel imidazolium-based poly(ionic liquid)s: preparation, characterization, and absorption of CO2. *Polym. Adv. Technol.* 23(5): 835-840.

[Xiong *et al.* 2012b] Xiong, Y., Liu, J., Wang, Y., Wang, H. and Wang, R. (2012b). One-Step Synthesis of Thermosensitive Nanogels Based on Highly Cross-Linked Poly(ionic liquid)s. *Angew. Chem. Int. Ed.* 51(36): 9114-9118.

[Xiong *et al.* 2011] Xiong, Y., Wang, Y., Wang, H. and Wang, R. (2011). A facile one-step synthesis to ionic liquid-based cross-linked polymeric nanoparticles and their application for CO2 fixation. *Polym. Chem.* 2(10): 2306-2315.

[Xu *et al.* 2009] Xu, J., Chen, G., Li, X., Sun, Y., Gao, J. and Liu, B. (2009). Process for preparation of acetate containing ionic liquids. Academy, C. T.**:** 11pp.

[Yan *et al.* 2006] Yan, F. and Texter, J. (2006). Surfactant ionic liquid-based microemulsions for polymerization. *Chem. Commun.* (25): 2696-2698.

[Yan *et al.* 2007] Yan, F. and Texter, J. (2007). Solvent-Reversible Poration in Ionic Liquid Copolymers. *Angew. Chem. Int. Ed.* 46(14): 2440-2443.

[Yang *et al.* 2013] Yang, C. H., Wang, M. X., Haider, H., Yang, J. H., Sun, J.-Y., Chen, Y. M., Zhou, J. and Suo, Z. (2013). Strengthening Alginate/Polyacrylamide Hydrogels Using Various Multivalent Cations. *ACS Appl. Mater. Interfaces* 5(21): 10418-10422.

[Yang *et al.* 2011] Yang, J., Qiu, L., Liu, B., Peng, Y., Yan, F. and Shang, S. (2011). Synthesis of Polymeric Ionic Liquid Microsphere/Pt Nanoparticle Hybrids for Electrocatalytic Oxidation of Methanol and Catalytic Oxidation of Benzyl Alcohol. *J. Polym. Sci. Part A: Polym. Chem.* 49(21): 4531-4538.

[Ye *et al.* 2012] Ye, Y., Choi, J.-H., Winey, K. I. and Elabd, Y. A. (2012). Polymerized Ionic Liquid Block and Random Copolymers: Effect of Weak Microphase Separation on Ion Transport. *Macromolecules* 45(17): 7027-7035.

[Ye *et al.* 2011] Ye, Y. and Elabd, Y. A. (2011). Anion exchanged polymerized ionic liquids: High free volume single ion conductors. *Polymer* 52(5): 1309-1317.

[Ye *et al.* 2013] Ye, Y., Sharick, S., Davis, E. M., Winey, K. I. and Elabd, Y. A. (2013). High Hydroxide Conductivity in Polymerized Ionic Liquid Block Copolymers. *ACS Macro Letters* 2(7): 575-580.

[Yin *et al.* 2014] Yin, K., Zhang, Z., Yang, L. and Hirano, S.-I. (2014). An imidazolium-based polymerized ionic liquid via novel synthetic strategy as polymer electrolytes for lithium ion batteries. *J. Power Sources* 258(0): 150-154.

[Yoshizawa *et al.* 2001] Yoshizawa, M., Hirao, M., Ito-Akita, K. and Ohno, H. (2001). Ion conduction in zwitterionic-type molten salts and their polymers. *J. Mater. Chem.* 11(4): 1057-1062.

[Yoshizawa *et al.* 2002] Yoshizawa, M., Ogihara, W. and Ohno, H. (2002). Novel polymer electrolytes prepared by copolymerization of ionic liquid monomers. *Polym. Adv. Technol.* 13(8): 589-594.

[Yuan *et al.* 2011a] Yuan, J. and Antonietti, M. (2011a). Poly(ionic liquid)s: Polymers expanding classical property profiles. *Polymer* 52(7): 1469-1482.

[Yuan *et al.* 2011b] Yuan, J., Schlaad, H., Giordano, C. and Antonietti, M. (2011b). Double hydrophilic diblock copolymers containing a poly(ionic liquid) segment: Controlled synthesis, solution property, and application as carbon precursor. *Eur. Polym. J.* 47(4): 772-781.

[Yuan *et al.* 2011c] Yuan, J. Y. and Antonietti, M. (2011c). Poly(ionic liquid) Latexes Prepared by Dispersion Polymerization of Ionic Liquid Monomers. *Macromolecules* 44(4): 744-750.

[Yuan *et al.* 2013] Yuan, J. Y., Mecerreyes, D. and Antonietti, M. (2013). Poly(ionic liquid)s: An update. *Prog. Polym. Sci.* 38(7): 1009-1036.

[Zhang *et al.* 2014] Zhang, C. and Anderson, J. L. (2014). Polymeric ionic liquid bucky gels as sorbent coatings for solid-phase microextraction. *J. Chromatogr. A* 1344(0): 15-22.

[Zhang *et al.* 2009] Zhang, G., Liu, X., Li, B. and Bai, Y. (2009). Free-radical solution copolymerization of the ionic liquid monomer 1-vinyl-3-ethylimidazolium bromide with acrylonitrile. *J. Appl. Polym. Sci.* 112(6): 3337-3340.

[Zhang *et al.* 2006] Zhang, Z.-Q., Yu, G.-L., Zhao, X., Wang, Y.-H., Lv, Z.-H. and Guan, S.-H. (2006). Degradation Character of a Alginate Lyase from Vibrio sp. WYA. *Chem. J. Chin. Univ.* 27(1): 71-74.

[Zhao *et al.* 2008] Zhao, F., Meng, Y. and Anderson, J. L. (2008). Polymeric ionic liquids as selective coatings for the extraction of esters using solid-phase microextraction. *J. Chromatogr. A* 1208(1-2): 1-9.

[Zhao *et al.* 2012] Zhao, Q., Zhang, P., Antonietti, M. and Yuan, J. (2012). Poly(ionic liquid) Complex with Spontaneous Micro-/Mesoporosity: Template-Free Synthesis and Application as Catalyst Support. *J. Am. Chem. Soc.* 134(29): 11852-11855.

[Zhao *et al.* 2013] Zhao, W., Jin, X., Cong, Y., Liu, Y. and Fu, J. (2013). Degradable natural polymer hydrogels for articular cartilage tissue engineering. *J. Chem. Technol. Biotechnol.* 88(3): 327-339.

[Zhao *et al.* 2010] Zhao, X., Huebsch, N., Mooney, D. J. and Suo, Z. (2010). Stress-relaxation behavior in gels with ionic and covalent crosslinks. *J. Appl. Phys.* 107(6): 63509.

[Zhou *et al.* 2011] Zhou, Y., Li, J., Han, H., Liu, X. and Jiang, S. (2011). Polymeric ionic liquid as a background electrolyte modifier enhancing the separation of inorganic anions by capillary electrophoresis. *Chem. Pap.* 65(3): 267-272.

[Ziolkowski *et al.* 2013] Ziolkowski, B. and Diamond, D. (2013). Thermoresponsive poly(ionic liquid) hydrogels. *Chem. Commun.* 49(87): 10308-10310.

Doktorandenerklärung

Universität Rostock
Dezernat 1
Referat 1.1

Doktoranden-Erklärung gemäß § 4 Absatz 1 Buchstaben g und h der Promotionsordnung der Mathematisch-Naturwissenschaftlichen Fakultät der Universität Rostock

Name: Jenny Bandomir
Anschrift: Südring 48, 18059 Rostock

Ich habe eine Dissertation zum Thema:

Development and characterization of hydrogels and their use in *in-vitro* studies of drug-coated balloons

an der Mathematisch-Naturwissenschaftlichen Fakultät der Universität Rostock angefertigt. Dabei wurde ich von Herrn Professor Dr. Udo Kragl betreut.

Ich gebe folgende Erklärung ab:

1. Die Gelegenheit zum vorliegenden Promotionsvorhaben ist mir nicht kommerziell vermittelt worden. Insbesondere habe ich keine Organisation eingeschaltet, die gegen Entgelt Betreuerinnen/Betreuer für die Anfertigung von Dissertationen sucht oder die mir obliegenden Pflichten hinsichtlich der Prüfungsleistungen für mich ganz oder teilweise erledigt.
2. Ich versichere hiermit an Eides statt, dass ich die vorliegende Arbeit selbstständig angefertigt und ohne fremde Hilfe verfasst habe. Dazu habe ich keine außer den von mir angegebenen Hilfsmitteln und Quellen verwendet und die den benutzten Werken inhaltlich und wörtlich entnommenen Stellen habe ich als solche kenntlich gemacht.

Rostock, den 23.07.2014 Jenny Bandomir

Curriculum Vitae

Name Jenny Bandomir

Academic Career/Professional Career

Promotion	
since 09/2010	Ph.D. student in the group of Prof. Dr. Udo Kragl, University of Rostock: Development and characterization of hydrogels and their use in *in-vitro* studies of drug-coated balloons
09/2009 – 08/2010	Research assistant in the group of Prof. Dr. Udo Kragl, University of Rostock: Ingredient analysis of potatoes for the identification of pointer substances and development of new methods for the determination of pointer substances (GC/MS, LC/MS)
Study of chemistry	
09/2009	Diploma (Equivalent to Master of Science) Diploma thesis in the group of Prof. Dr. Udo Kragl "Study on resource recovery from process streams in industrial fermentation plants"
10/2004 – 09/2009	Study of chemistry, University of Rostock

Education

06/2004	Abitur (German University Entrance Qualification)
09/1995 – 06/2004	Gerhart-Hauptmann-Gymnasium Wismar
09/1991 – 08/1995	Fritz-Reuter-Grundschule Wismar (Primary school)

Rostock, den 23.07.2014 Jenny Bandomir

Publications

Paper	*Synthesis and characterization of polymerized ionic liquids: mechanical and thermal properties of a novel type of hydrogels* **J. Bandomir**, A. Schulz, S. Taguchi, L. Schmitt, H. Ohno, K. Sternberg, K.-P. Schmitz, U. Kragl, *Macromol. Chem. Phys*. **2014**, 215, 716-724
Poster	*Poly-ionic liquids as new hydrogel materials: Synthesis, characterization and application* **J. Bandomir**, A. Schulz, S. Taguchi, S. Petersen, U. Kragl, H. Ohno, K. Sternberg, BMT **2013** Graz *Cetylpyridinium salicylate for coating of implants: synthesis, characterization and application* **J. Bandomir**, F. Stein, S. Petersen, K. Sternberg, U. Kragl, COIL-5 **2013** Algarve *Ionische Flüssigkeiten als temporäre Implantatbeschichtungen* **J. Bandomir***,* B. Semmling, A. Seidlitz, S. Wenda, W. Weitschies, U. Kragl, Remedis Klausurtagung **2011** *Analysis of plant metabolites – the baseline-treshold principle* K. Neubauer, **J. Bandomir**, A. Grunenberg, A. Müller, U. Kragl, K. Schmidt, PMEM **2010**
Oral Presentations	*Ionische Flüssigkeiten und ihr Potential für medizinische und pharmazeutische Anwendungen* 7. Klausurtagung REMEDIS, Mai **2013** *Polymerisierte ionische Flüssigkeiten als neuartige Hydrogele – chemische und mechanische Charakterisierung* 8. Klausurtagung REMEDIS, November **2013** *Rostocker „PILs" – Wenn das Blut nicht mehr fließt* Rostock´s Eleven, Science & Communication Challenge, Juni **2014**